超臨界流体抽出／超臨界流体クロマトグラフィーと
中真空化学イオン化質量分析法を組み合わせた装置の開発と応用

関西大学大学院　理工学研究科
化学生命工学専攻
化学・物質工学分野
21M6731　太田　千尋

指導教員　青田 浩幸　㊞

論文要旨

超臨界流体抽出／超臨界流体クロマトグラフィーと
中真空化学イオン化質量分析法を組み合わせた装置の開発と応用

21M6731　太田千尋

超臨界流体抽出 (supercritical fluid extraction;SFE) ／超臨界流体クロマトグラフィー (supercritical fluid chromatography;SFC) と，中真空化学イオン化 (medium vacuum chemical ionization;MVCI) 質量分析法 (mass spectrometry;MS) を組み合わせる新しい超高感度脂質測定法を開発し，それについて検討を行った．MVCI と名付けたこのイオン化法は，約 100 Pa の加水した He 雰囲気で放電により水から生じる試薬イオン (H_3O^+, OH^-) を用いて測定対象分子をイオン化する化学イオン化法のひとつである．この手法は，気体中の痕跡程度の揮発性有機物 (VOC) をリアルタイムに定量する手法，プロトン移動反応質量分析法 (PTR-MS) に類似した方法である．PTR-MS の定量下限 (lower limit of quantitation;LLOQ) は，parts-par-trillion (ppt) レベルであることから，超臨界二酸化炭素 ($scCO_2$) に溶解している不揮発性有機物に対しても低い定量下限が得られることが考えられる．また，$scCO_2$ は比較的容易に中真空に接続することができ，分析対象の分子をイオン源空間に円滑に開放することで，効率のよいイオン化を可能とする．

超臨界流体が物質を溶解する現象は 1880 年から知られていたが，SFE あるいは SFC としての応用は，1960 年代にはじまった．二酸化炭素は，臨界温度が 31 °C, 臨界圧力が 7.4 MPa と比較的扱い易く，毒性が低く，安価で調達が容易なことなどから超臨界流体の応用に最もよく用いられている物質である．SFE は，脂質や脂溶性ビタミンなど低極性化合物を食肉などの組織から効率よく定量的に抽出できることが知られている．また SFC は，液体クロマトグラフィー (LC) での分離が困難な低極性化合物を短時間に分析することができる．加えて，低極性化合物は，LC-MS で広く用いられているエレクトロスプレーイオン化法 (ESI) では十分な感度が得られないことが多い．脂質には，細胞膜を構成するリン脂質や，そこから遊離される長鎖脂肪酸など，様々な生命現象や疾病への関与が指摘される化合物が含まれる．それら化合物の組織毎の定量は試みられているものの，個別の細胞内の濃度変化や細胞間の差異を測定するには，多くの場合，検出感度が十分ではない．

本稿では，SFE-MVCI MS を用いることで，遊離脂肪酸 (FFA) について 48 amol から 27 fmol という定量下限を達成できることを明らかにした．これは，文献に示されている FFA 定量下限に比べ 3 桁低い値である．同様に，アセトアミノフェン，カフェイン，ピレン，α-トコフェロール，ビタミン K_1，γ-オリザノール，およびレセルピンについてそれぞれ，4.9 fmol，0.077 fmol，9.5 fmol，4.0 fmol，41.0 fmol，1.6 fmol，8.3 fmol が得られた．

本稿ではさらに，SFE/SFC オンライン接続と MVCI MS とのインターフェースについて検討を行った．その結果，アラキドン酸の定量下限は，SFC 分離を伴わない SFE-MVCI MS 法と比較して一桁低い 1 fmol を達成した．定量下限改善の要因は，SFC と MVCI イオン源インタフェースの最適化により，共存する化合物が明瞭なバンドとして分離してイオン源に到達することで，それぞれの測定対象の分子がより効率よくイオン化されるためと考えられる．また，極性が極端に小さいことから LC-MS では分離・検出が容易ではない α-トコフェロールおよびビタミン K_1 についても，2 分以下の分析時間，41 fmol の定量下限を達成した．α-トコフェロールは室温で保存すると速やかに酸化反応が進行するが，本法をもちいて，酸化の過程とその生成物を分離できることを示した．さらに，本法を用いて，ヒト血漿 0.1 µL 中の脂肪酸を測定できることを示し，標準添加法によってアラキドン酸量 78 fmol という結果を得た．同じ測定において，C12:0 から C24:0 の範囲の 16 種の FFA についてもアラキドン酸量換算として定量しており，定量の繰返し性は 5.7 % から 15 % と良好であった．

単一細胞中の低分子化合物を検出する可能性を調べる目的で，HeLa 1 細胞を用いて SFE-MVCI MS 測定を行った．その結果，細胞由来と考えられる 200 (91) 種類のポジティブ（ネガティブ）イオンを検出することができた．本研究を通じて様々な化合物について MVCI による生成イオンを調べた結果，測定対象分子 M に対して，得られるイオンは，ポジティブイオン: $[M + H]^+$, $[M - H + H]^+$, $[M - H_2O + H]^+$，ネガティブイオン: $[M - H]^+$, [M +

H –H]$^+$, [M + OH]$^-$ のいずれかであった．この結果に基づいて，LipidMaps LMSD データベースに登録されている化合物中，質量 1200 以下の 45932 構造に対して，可能性のあるイオン式を *in silico* 合成し，HeLa 細胞から得られたイオンの *m/z* と比較した結果，11 (10) ポジティブイオン（ネガティブイオン）について組成式を特定できた．しかしながら，得られたほぼすべての組成式に対して異性体が存在することから，構造同定には至っていない．とはいえ，数多くのイオンが HeLa 1 細胞から検出できたことで，この方法がシングルセル解析へ応用できる可能性を示すことができた．

目次

Abbreviations

α-T	α-tocopherol
APCI	atmospheric pressure chemical ionization
APPI	atmospheric pressure photoionization
ESI	electrospray ionization
MS	mass spectrometry
MVCI	medium vacuum chemical ionization
PTR	proton-transfer-reaction
PTR-MS	proton-transfer-reaction mass spectrometry
R.P.	mass resolving power
Rs	resolution (chromatography)
SFC	supercritical fluid chromatography
SFE	supercritical fluid extraction
VOC	volatile organic compounds
VK_1	vitamine K_1
$scCO_2$	supercritical carbon dioxide
k	retention factor
log P	logarithm of octanol-water partition
t_R	retention time

第 1 章

序論

超臨界流体が物質を溶解することは，1880 年に Hannay らによって，“On the Solubility of Solids in Gases”[1)] と題する論文によって示された．その後，約 80 年を経て，1962 年，Klasper ら[2)] によって，”High Pressure Gas Chromatography above Critical Temperatures” と題する最初の超臨界流体クロマトグラフィー (supercritical fluid chromatography; SFC) が実施された．これは，世界初の高速液体クロマトグラフ ALC 100 (Waters Corporation, MA, US)[3)] に数年先立って開発されたものであり，ガスクロマトグラフィー (GC) 技術を用いて不揮発性化合物の分析を可能とした最初の実験である．それとは独立して，1960 年代 Zosel によって一連の超臨界流体抽出法 (supercritical fluid extraction; SFE) に関する特許が出願され[4,5)]，その後，実用化された[6)]．

物質は，それぞれ固有の臨界温度を有し，臨界温度以下では，温度，圧力に応じて気体，液体，固体のいずれかの相をとるが，臨界温度以上では，いくら加圧しても液体になり得ない．同様に，臨界圧力以上ではどんなに温度を上げても気体にはなり得ない．物質がその臨界温度・臨界圧力より高い状態にある場合，その流体を超臨界流体 (supercritical fluid) と呼ぶ[7)]．また，温度，圧力いずれか一方が臨界条件を超えた状態にある物質を亜臨界流体 (subcritical fluid) と呼ぶが，両者を区別せず超臨界流体として扱う場合も少なくない．亜臨界状態を保つ限り，温度あるいは圧力いずれか一方のみを変化させても沸騰や凝固・凝集といった相変化を伴わないため，流体の温度や圧力を連続的に変化させることができ，それによって溶質の溶解度を任意に制御できる点が，応用上，極め

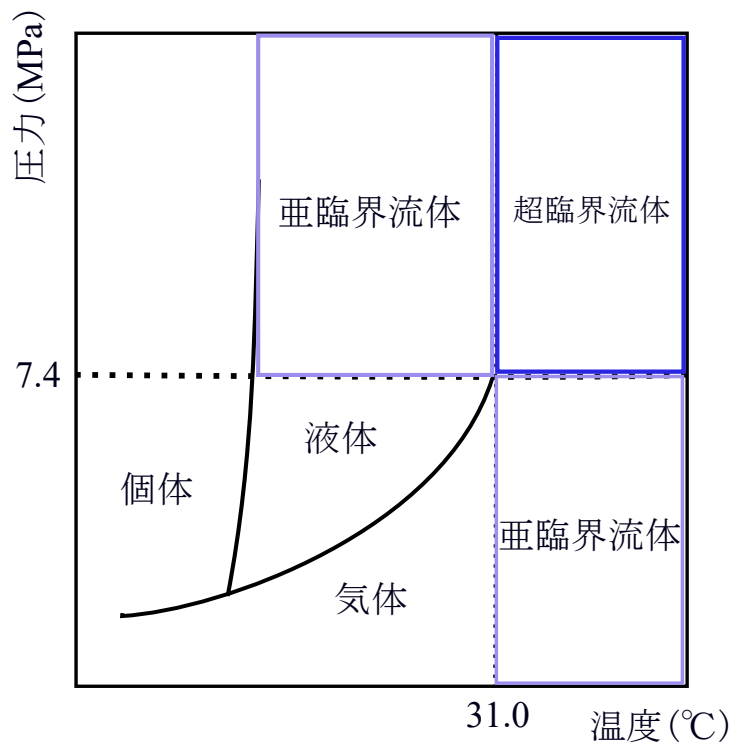

Figure 1.1: CO_2 Phase diagram.

て重要である．

SFE や SFC に用いる流体には，様々な物質を用いることが原理上可能であるが，最も一般的に用いられる物質は CO_2 である．Figure 1.1 に温度，圧力と CO_2 の状態の関係を示す．CO_2 は臨界温度が 30.98 °C，臨界圧力が 7.38 MPa[8] と比較的低く，調達が安価であり，毒性が低いことから広く用いられている．超臨界 CO_2 ($scCO_2$) の極性は一般に n-hexane 相当といわれるが，アルコールなど極性溶媒と混合可能である．近年では，液体クロマトグラフィー (LC) で広く用いられる有機溶媒に比べ，CO_2 の使用は環境負荷が低いことも指摘されている．

超臨界流体の特徴は，液体と同等の密度を有しながら，液体より一桁低い粘性，高い拡散係数を持つことである．とりわけ臨界点付近では温度・圧力に対して大きな密度変化があるため，溶質の溶解度を温度や圧力の制御によって大きく変化させることが可能である．このような大きな溶媒強度（溶質を保持する能力）の変化は気体でも液体でも達成することはできない．また，拡散係数が大きいことにより超臨界流体クロマトグラフィー（SFC）において高いカラム効率が得られ，分離時間を大幅に短縮する効果がある．保持を圧力と温度の操作によって制御できる点も，他のクロマトグラフィーにはない特徴である．SFC では，一連の構造類似性のある化合物の保持係数 (k) の対数（log k）と化合物の octanol-water partion の対数 (log P) および molecular polarizability と高い相関を有する[9,10]．またラセミ化合物では，選択性（２化合物の保持係数の比）は，熱力学により予測可能とされ[11]，分離の最適化が低コストで行えることも利点である．その一方，SFC は圧力と流量を独立して管理する必要があるため，より精密な装置的制御が必要となる．SFC は光学異性体や幾何異性体など，他の方法で分離が難しい化合物分離を可能にするが，そのためには，線流速を正確に制御する必要がある．超臨界流体は，わずかな温度，圧力の変化で密度が大きく変化するため，線速度を安定させるためには，より精度の高い工業技術による装置が必要である．近年，装置設計技術の進歩により，SFC 技術は大きな躍進を遂げた[12]．

1985 年，数ミリリットル以下という小さな SFE 容器と SFC をオンライン接続することで，抽出過程の解析や複雑なサンプルの SFC クロマトグラムを直接フォトダイオードアレイ検出器を用いて紫外吸収スペクトルの時間変化としてモニターする装置が開発された[13–16]．これによりフォトダイオードアレイ検出器が SFC のための主要な検出手段となった．初期の SFC 装置は，GC 技術を基礎とした中空キャピラリーカラムが用いられてきたが，1980 年代中頃には，高速液体クロマトグラフィー（high performance liquid chromatography; HPLC) 用送液ポンプ技術を基礎とした超臨界流体送液システムが用いられるようになった．背景としては，液体状態で CO_2 にモディファイアを混合する技術によって，常に安定した混合比率でモディファイアを加えることができるよう改良された[17] ことが挙げられる．このモディファイアを安定して加える技術により，それまで非極性物質に応用が限定されてきた SFC は，アミノ酸などの極性物質にも応用できるようになり，従来 30 分を要していたアミノ酸の光学異性体分離が 3 分以下で達成できることが明らかとなった[18]．近年では，工業技術のさらなる進歩により，クロマトグラフィー分離時間はさらに短縮され，また，様々な方法での SFE 抽出と超高速 SFC のオンライン接続が考案され[12,19]，より迅速で高い精度での測定が可能となっている．

SFC と質量分析法 (MS) の接続は，2000 年頃から試みられており，中空キャピラリーカラムと 電子イオン化 (EI) を組合せて農薬分析に応用した例[20] などがあるが，実用化された多くは移動相にモディファイアの使用が可能な充填カラムを用い，検出法として，エレクトロスプレーイオン化 (ESI), 大気圧化学イオン化 (APCI), 大気圧光イオン化 (APPI) などを組み合わせたものである[21,22]．

プロトン移動反応イオン化質量分析法 (PTR-MS) は，100 Pa 程度の中真空環境で放電により水から生成するヒドロニウムイオン (H_3O^+) や OH^- と試料分子との間でプロトン移動により生成したイオンを質量分離する手法である．このイオン化法は，後述のプロトン移動反応質量分析法として大気中の揮発性化合物の測定に広く用いられている[23]．プロトン移動反応質量分析法[24–27] (proton-transfer-reaction mass spectrometry;PTR-MS) は，1990 年代後半に Lindinger ら[28,29] によって構築され，気体中の極微量な揮発性有機物の検出および濃度のリアルタイムモニタリングなどに使われてきた．Lindinger らによって構築された PTR-MS の測定の原理は，試薬イオン源で生成した水由来のイオンから，ドリフトチューブを用いて，正イオンのみを取り出したり，あるいは四重極質量分離部を備えることによって高純度の H_3O^+ を取り出して試薬イオンとして用い，測定対象化合物にプロトン付加する化学イオン化である．応用範囲は，大気中の揮発性有機物 (volatile organic compounds; VOC)[27]，火山ガ

スのモニタリング[30] や，森林火災等における大気中の VOC[31,32]，微生物や食品分析への応用[33]，畜産過程での VOC 排出[34]，あるいは呼気による医薬品代謝物の測定[35] など多岐にわたっている．VOC 測定では，測定装置を航空機など移動手段に搭載し，フィールドで測定を行う必要がある場合が多い．また，大気中に存在する VOC は希薄で part per billion (ppb) 以下でしかなく，定量には，ppt レベルの定量下限が要求される．通常，機器分析では標準物質を測定し，得られた結果とサンプルの測定結果を比較することで定量結果を得るが，多成分かつ希薄な VOC を，現場で，一斉に効率よく定量するため，プロトン移動反応の反応速度を計測し，反応定数から定量結果を得る手法が用いられてきている[36]．そのためには，PTR-MS イオン源は理想に近い状態で式 (1.1) の反応を進行させることが必要であり，試薬イオン源で生成するイオンのうち，高純度の H_3O^+ を選択的に取り出す機構が重要である[37,38]．同様に，選択的に OH^- を試薬イオンとして用い，プロトン脱離反応[39] を利用することでネガティブイオンを検出する測定法は proton-extraction reaction MS (PER-MS)[40] として区別されている．

$$H_3O^+ + R \longrightarrow RH^+ + H_2O \tag{1.1}$$

大気の主要成分である O_2, N_2, CO_2, などは，水よりもプロトン親和性が低く PTR-MS ではイオン化されない．このことも，前述の通り PTR-MS において反応速度の計測に基づく低濃度化合物の定量を可能とした[37]．CO_2 がイオン化されないことは，CO_2 を移動相に用いる SFC にとっても，高い検出感度が得られると考えられる．このイオン化は 100 Pa 程度の中真空下で行われるものであるため，10 MPa 以上にある $scCO_2$ をイオン化が行われる中真空に接続することが求められる．先に述べたとおり，超臨界流体は減圧過程で相変化を伴わない．$scCO_2$ が減圧される過程において，臨界温度（31 °C）以上である限り相変化なく，亜臨界状態を経て中真空に到達する．その過程で，流体が保持していた溶質は中真空空間に開放されると考えられる．すなわち，数十メガパスカルの超臨界流体は，簡単な機構の圧力リストリクターを用いて中真空空間に接続でき，SFE 抽出過程のモニターや SFC クロマトグラムが得られると期待される．このような仮定に基づいて，作製したイオン源について基礎的な実験を行い，不揮発性有機物が測定できることはすでに報告した[41]．

本論文では，この方法を発展させ，分子量 1000 以下の不揮発性低分子量化合物，とりわけ様々な疾病との関連が近年明らかにされつつある脂肪酸や脂質の新しい高感度測定法の開発を目的としている．すでに述べたとおり，本研究に用いるイオン源は PTR-MS とは異なるものであるが，本研究の成果のうち、2, 5, 6, 7章については “PTR MS” を略語として論文掲載されていることから，これらの章では “PTR MS” の略語を用いる．それ以外の 3，4，及び 8章については “medium vacuum chemical ionization (MVCI)” を略語として用いる．

2章では試作した SFE-MVCI MS[42] を用いて標準試料を有機溶媒に溶解した液体状態で試料導入する場合，ならびに，標準試料を焼結フィルター（フリット）に浸透させ，有機溶媒を揮発させた状態で試料を導入する方法について検討し，CO_2 送液部および圧力リストリクター部を含む測定流路系におけるピークの拡散，線速度の推定といったクロマトグラフ設計の基本的データを収集する．

3章では，この方法が，どのような化合物の検出に応用できるか未知であることから，広い範囲の化合物について，それぞれポジティブイオンモード・ネガティブイオンモードでの検出可能性について検討する．また，その結果から，質量分析装置の質量キャリブレーションに使える可能性のある化合物を探索する．

4章では，α-tocopherol (α-T) について，ESI と SFE-MVCI MS のポジティブイオンモードでの質量スペクトルの比較を行い，ESI と MVCI それぞれで生成するイオンの違いについて考察する．

5章では，近年まで調べられていなかった α-T の酸化生成物の測定を試みる．α-T は，植物が光合成の際に生じる一重項酸素から自らの細胞を保護するために存在すると考えられているが，その低い極性のため，液体クロマトグラフィー技術では分離が極めて困難であった[43]．α-T の酸化過程は複雑で，かつ反応が迅速であり，さらに酸化生成物の多くが異性体である．植物の光合成過程での細胞保護メカニズムを調べるには，迅速な前処理，高速な異性体分離と高い検出感度が必要である．5章では，α-T 酸化物の迅速一斉分析を可能とするような，オンライン SFE/SFC-MVCI MS について検討を行い，必要な装置構成および問題点を検討する．

6章では，5章で得られた知見に基づいて，理論上 SFC で得られる狭いバンド幅のピークの計測についてシステマティックに検討する．一連の同族化合物であるフタル酸エステル類および保持の大きい VK_1, α-T の保持挙動

について，複数のカラム条件で計測を行い，装置的なピークの広がり要因を特定し，ピーク分離 (resolution) を最適化する．また，SFC を用いた場合の定量下限について，より詳細な検討を行う．得られた結果の実用可能性を調べる目的で，ヒトプール血清中の遊離脂肪酸の一斉測定を試みる．

7章では HeLa シングルセルについて SFE-MVCI MS 測定し，単一細胞中の代謝物の検出とその同定を試みるとともに，問題点について検討する．

8章に本論文全体の結果を概観し，今後の検討事項について述べる．

参考文献

[1] Hannay, J. B.; Hogarth, J.; Stokes, G. G. *Proceedings of the Royal Society of London* 1880, **30**, 178–188.

[2] Klasper, E.; CorwinIber, P. K.; Iber, P. K. *J. Org. Chem.* 1962, **27**, 700–706.

[3] Waters Corporation: Fifty Years of Innovation in Analysis and Purification. 2008; https://www.sciencehistory.org/distillations/waters-corporation-fifty-years-of-innovation-in-analysis-and-purification.

[4] Zosel, K.; DT United States Patent: 3969196 - Process for the separation of mixtures of substances. 1976.

[5] Zosel, K. *Angewandte Chemie International Edition in English* 1978, **17**, 702–709.

[6] Zosel, K. Process for the decaffeination of coffee. 1981.

[7] Ettre, L. S. Nomenclature for chromatography (IUPAC Recommendations 1993). 1993; https://www.degruyter.com/document/doi/10.1351/pac199365040819/html, Publisher: De Gruyter.

[8] Lemmon, E.; Bell, I. H.; Huber, M. L.; McLinden, M. O. NIST Chemistry WebBook, SRD 69. 2022; https://doi.org/10.18434/T4D303, Publisher: National Institute of Standards and Technology.

[9] Jinno, K.; Hoshino, T.; Hondo, T.; Saito, M.; Senda, M. 1986, **58**, 2696–2699.

[10] Fatemi, M. H.; Malekzadeh, H.; Shamseddin, H. 2009, **32**, 653–659.

[11] Stringham, R. W.; Blackwell, J. A. *Anal. Chem.* 1996, **68**, 2179–2185.

[12] Yamamoto, K.; Machida, K.; Kotani, A.; Hakamata, H. *Chemical and Pharmaceutical Bulletin* 2021, **69**, 970–975.

[13] Sugiyama, K.; Saito, M.; Hondo, T.; Senda, M. *Journal of Chromatography A* 1985, **332**, 107–116.

[14] del Carmen Salvatierra-Stamp, V.; Ceballos-Magaña, S. G.; Gonzalez, J.; Ibarra-Galván, V.; Muñiz-Valencia, R. *Anal Bioanal Chem* 2015, **407**, 4219–4226.

[15] Åsberg, D.; Enmark, M.; Samuelsson, J.; Fornstedt, T. *Journal of Chromatography A* 2014, **1374**, 254–260.

[16] Heiland, J. J.; Geissler, D.; Piendl, S. K.; Warias, R.; Belder, D. *Anal. Chem.* 2019, **91**, 6134–6140.

[17] Fields, S. M.; Markides, K. E.; Lee, M. L. *Journal of High Resolution Chromatography* 1988, **11**, 25–29.

[18] Hara, S.; Dobashi, A.; Kinoshita, K.; Hondo, T.; Saito, M.; Senda, M. *Journal of Chromatography A* 1986, **371**, 153–158.

[19] Sakai, M.; Hayakawa, Y.; Funada, Y.; Ando, T.; Fukusaki, E.; Bamba, T. *Journal of Chromatography A* 2019, **1592**, 161–172.

[20] Voorhees, K. J.; Gharaibeh, A. A.; Murugaverl, B. 1998, **46**, 2353–2359.

[21] Gordillo, R. *J. Sep. Sci.* 2021, **44**, 448–463.

[22] Laboureur, L.; Ollero, M.; Touboul, D. *International Journal of Molecular Sciences* 2015, **16**, 13868–13884.

[23] Sato, N.; Sekimoto, K.; Takayama, M. *Mass Spectrometry* 2017, **5**, S0067–S0067.

[24] Akiyama, K. *Bunseki Kagaku* 2013, **62**, 249–252.

[25] Sekimoto, K. *Mass spectroscopy* 2017, **65**, 2–6.

[26] Sekimoto, K.; Li, S.-M.; Yuan, B.; Koss, A.; Coggon, M.; Warneke, C.; de Gouw, J. *International Journal of Mass Spectrometry* 2017, **421**, 71–94.

[27] Yuan, B.; Koss, A. R.; Warneke, C.; Coggon, M.; Sekimoto, K.; de Gouw, J. A. *Chem. Rev.* 2017, **117**, 13187–13229.

[28] Hansel, A.; Jordan, A.; Holzinger, R.; Prazeller, P.; Vogel, W.; Lindinger, W. *International Journal of Mass Spectrometry and Ion Processes* 1995, **149-150**, 609–619.

[29] Lindinger, W.; Jordan, A. *Chem. Soc. Rev.* 1998, **27**, 347.

[30] Diaz, J. A.; Pieri, D.; Arkin, C. R.; Gore, E.; Griffin, T. P.; Fladeland, M.; Bland, G.; Soto, C.; Madrigal, Y.; Castillo, D.; Rojas, E.; Achí, S. *International Journal of Mass Spectrometry* 2010, **295**, 105–112.

[31] Ditto, J. C.; He, M.; Hass-Mitchell, T. N.; Moussa, S. G.; Hayden, K.; Li, S.-M.; Liggio, J.; Leithead, A.; Lee, P.; Wheeler, M. J.; Wentzell, J. J. B.; Gentner, D. R. *Atmospheric Chemistry and Physics* 2021, **21**, 255–267.

[32] Brilli, F.; Gioli, B.; Ciccioli, P.; Zona, D.; Loreto, F.; Janssens, I. A.; Ceulemans, R. *Atmospheric Environment* 2014, **97**, 54–67.

[33] Romano, A.; Capozzi, V.; Spano, G.; Biasioli, F. *Appl Microbiol Biotechnol* 2015, **99**, 3787–3795.

[34] Ni, J.-Q.; Robarge, W. P.; Xiao, C.; Heber, A. J. *Chemosphere* 2012, **89**, 769–788.

[35] Berchtold, C.; Bosilkovska, M.; Daali, Y.; Walder, B.; Zenobi, R. *Mass Spectrometry Reviews* 2014, **33**, 394–413.

[36] Sekimoto, K.; Koss, A. R. *J Mass Spectrom* 2021, **56**.

[37] Blake, R. S.; Monks, P. S.; Ellis, A. M. *Chem. Rev.* 2009, **109**, 861–896.

[38] Zhang, Q.; Bao, X.; Liang, Q.; Sun, Q.; Xu, W.; Zou, X.; Huang, C.; Shen, C.; Chu, Y. 2022, **94**, 7174–7180.

[39] Muller, P. *Pure and Applied Chemistry* 1994, **66**, 1077–1184.

[40] Pan, Y.; Zhang, Q.; Zhou, W.; Zou, X.; Wang, H.; Huang, C.; Shen, C.; Chu, Y. *J. Am. Soc. Mass Spectrom.* 2017, **28**, 873–879.

[41] Hondo, T.; Ota, C.; Miyake, Y.; Furutani, H.; Toyoda, M. *Anal. Chem.* 2021, **93**, 6589–6593.

[42] 太田千尋 超臨界流体抽出/クロマトグラフィ-プロトン移動反応質量分析計（SFE/SFC-PTR-MS) の開発. 卒業論文, 関西大学, 2021.

[43] Tomai, P.; Bosco, C. D.; D'Orazio, G.; Scuto, F. R.; Felli, N.; Gentili, A. *Journal of Chromatography Open* 2022, **2**, 100027.

第 2 章

Analysis of nonvolatile molecules in supercritical carbon dioxide using proton-transfer-reaction ionization time-of-flight mass spectrometry

Proton-transfer-reaction (PTR) mass spectrometry (MS) is capable of detecting trace-level volatile organic compounds (VOCs) in gaseous samples in real time. Therefore, PTR-MS has become a popular method in many different study areas. Most of the currently reported PTR-MS applications are designed to determine volatile compounds. However, the method might be applicable for nonvolatile organic compound detection. Supercritical fluid chromatography (SFC) has been studied in the last five decades. This approach has high separation efficiency and predictable retention behavior, making separation optimization easy. Atmospheric ionization techniques, such as atmospheric chemical ionization (APCI) and electrospray ionization (ESI), are the most studied SFC-MS interfaces. These processes require the addition of make-up solvents to prevent precipitation or crystallization of solute while depressurizing the mobile phase. In contrast, the PTR process is carried out in a vacuum; supercritical carbon dioxide may release solute into the PTR flow tube without a phase transition as long as it is maintained above a critical temperature. Therefore, this might constitute yet another use for the SFC-MS interface. Caffeine and a few other non-polar compounds in supercritical carbon dioxide were successfully detected with time-of-flight MS without adding solvent by using preliminarily assembled supercritical flow injection and supercritical extraction (SFE)-PTR interfaces.

Supercritical fluid chromatography (SFC) has several advantages compared to liquid chromatography (LC) due to its enhanced column efficiency[1–4]. The greater density of supercritical fluids than gases imbues the mobile phase with solvating powers, which can readily be controlled by applying pressure and temperature; in contrast, the mobile phase in GC only acts as a carrier. Historically, the same principle has been applied to industrial-scale supercritical extraction, such as that used in a decaffeinated coffee plant[5]. A significant advantage of SFC is that the behavior of the retention factor (k) is predictable, which allows for a systematic approach for chromatography optimization[6–8]. On the other hand, it requires more precise control for the apparatus to manage pressure and flow rate independently, due to the compressibility of the mobile phase in SFC[1–4]. Small changes in pressure and temperature cause significant

Reprinted with permission from
T. Hondo, C. Ota, Y. Miyake, H. Furutani, M. Toyoda *Analytical Chemistry* 93(17):6589-6593, (2021). https://doi.org/10.1021/acs.analchem.1c00898.

density changes that result in direct changes in the apparent void volume and linear velocity of the column. For this reason, a ultra-violet (UV) diode-array detector and a fluorescence detector have long been applied to monitor both supercritical fluid extraction (SFE) and SFC processes[9,10,3,11].

Mass spectrometry (MS) has also been applied to SFC for some time[12–16]. MS has a higher capability for molecule identification than a UV diode-array detector. The mobile phase CO_2 has fewer chemical background signals than the commonly used organic solvents, which is expected to decrease the limit of detection (LOD). However, development of the SFC-MS interface has been a challenge. The supercritical carbon dioxide ($scCO_2$) holds solutes at a given supercritical condition, which could be crystallized during depressurization into atmospheric pressure. The addition of make-up solvent may prevent crystallization, but it may not be necessary for $scCO_2$ soluble molecules.

Proton-transfer-reaction (PTR)-MS was introduced in 1990s by Lindinger and co-workers[17,18] to determine volatile organic compounds. The advantages of PTR-MS are a low LOD and easy interpretation of mass spectra due to the absence of fragmentation. PTR-MS can detect trace-level volatile organic compounds in gaseous samples in real time; it has become a popular method in the analysis of gaseous samples in many different areas of study[19]. The PTR-MS applications in the literature involve detection of protonated molecules based on the reaction expressed in Equation 1. The proton extraction reaction, which makes a negatively charged ion, has also been reported[20].

The ionization mechanism of PTR is similar to that of atmospheric pressure chemical ionization (APCI), which is one of the common ionization methods for SFC. Different from APCI, the PTR process is carried out under low pressure at approximately 1 to 100 Pa. Ideally, while the $scCO_2$ depressurization occurs above the critical temperature, $scCO_2$ can be vaporized from the subcritical state without a phase-state change and release solute into the vacuum space so it meets the proton source in the flow tube. Furthermore, CO_2 cannot be ionized using H_3O^+, and the carrier CO_2 does not harm the ionization reaction of the solute. In the present work, we have made a supercritical fluid-PTR interface and monitored caffeine ions carried by $scCO_2$ using flow injection (FI). We also have developed an SFE oriented solvent-free direct sample injection method applied for a couple of organic compounds to discuss the feasibility of the PTR ion source as yet another SFC detection method.

2.1 Experimental

2.1.1 Apparatus

A JMS-T100 LP (AccuTOF) time-of-flight (TOF) mass spectrometer (JEOL, Tokyo, Japan) was used. An Acqiris model U5303A ($3.2\,GS \cdot s^{-1}$ 12 bit digitizer, Geneva, Switzerland) was directly connected to the signal and ion-push trigger output from AccuTOF. Data acquisition was carried out by a simultaneous waveform averaging (AVG) and ion counting (PKD) technique[21]. The PKD histogram and AVG waveform were read from the U5303A every 200 ms (3000 ion push triggers).

Figure 2.1 illustrates the block diagram of the PTR flow tube built in-house. It consists of a corona discharge electrode (quartz, stainless steel), a flow tube (stainless steel), and the AccuTOF interface. The general grade helium was connected to a flow tube after passing through a 250 mL volume of the solvent-reservoir bottle, which contained 10 mL of ultrapure water (Millipore, MA, US). The helium flow rate was set to $70\,mL \cdot min^{-1}$, which was controlled using a mass flow controller (MFC) (8500MC-0-1-2, KOFLOC Corp., Kyoto, Japan). The pressure of the flow tube was maintained in a range of 80 to 150 Pa using a NeoDry 15E dry vacuum pump (Kashiyama Industries, Ltd., Nagano, Japan). The model PS350 high voltage power supply (Stanford Research Systems, Inc. Sunnyvale, CA, USA) was used as a corona discharge power supply. The voltage for the discharge electrode was set to $-2.0\,kV$, which resulted in 50 to $100\,\mu A$ of current.

Figure 2.2 illustrates the hydraulics and system schematics. Liquid carbon dioxide in a cylinder was connected to an LC Packings UltiMate Micropump (Thermo Scientific, MA, US), with 3-meter length and 1.0 mm inner-diameter

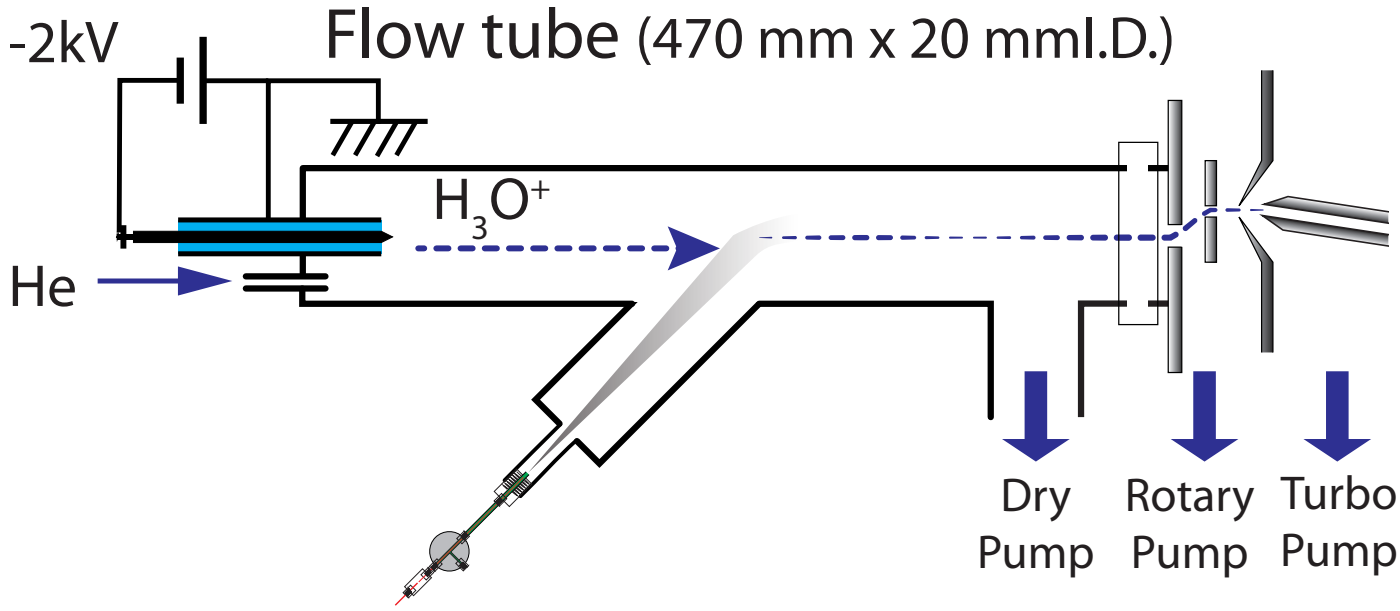

Figure 2.1: Block diagram of the PTR flow tube.

(ID) stainless steel tubing, and passed through an ethanol/dry ice bath that was kept at −25 °C. The pump head was cooled and maintained at 10 °C by a Peltier module (Hebei, TES1-12705, Hebei, China) prepared in-house. The pressurized carbon dioxide from the pump was connected to the Agilent 1100 Series Thermostatted Column Compartment (Agilent, CA, US).

Figure 2.2 (top) shows the FI-PTR schematic diagram. The 20 µm ID inactivated fused silica capillary (GL Science, Tokyo, Japan) was used as a $scCO_2$ pressure restrictor, which holds up to 25 MPa of pressure at the high-pressure end with the other end open to the PTR flow tube, which is at approximately 100 Pa. For FI-PTR monitoring, the pressure restrictor (60 mm) was placed inside the vacuum tube, and the $scCO_2$ output end was aligned to the flow tube wall edge, as shown in the Figure 2.2. A 50 µm inactivated fused silica capillary (GL Science, Tokyo, Japan) was used for plumbing the 6-port injector (Rheodyne 7725, Rheodyne, CA, US) valve and pressure restrictor passing through the quarter-inch HPLC column fitting. A tubing with an approximately 2 µL volume (70 mm length of 0.17 µm ID) was used as sample loop in the injector.

Direct Injection (DI)-PTR Interface: For SFE oriented direct sample introduction into the $scCO_2$ fluid without using organic solvent, was carried out by using ACQUITY Column In-Line Filter (Waters, MA, US) coupled with a two-way switching valve (Rheodyne 7000, Rheodyne, CA, US), as shown in Figure 2.2 (bottom). The same tubing and restrictor configuration from FI-PTR experiments were used.

2.1.2 Chemicals

Caffeine (98.5%), pyrene (98%), reserpine (98%), oleic-acid (65%), and *gamma*-oryzanol (97%) were purchased from FUJIFILM Wako Pure Chemicals Corporation, Osaka, Japan. Methanol (MeOH) and acetonitrile (both LC/MS grade), and reagent-grade acetone (FUJIFILM Wako Pure Chemicals Corporation, Osaka, Japan) were used as solvents to dissolve the chemicals described above.

Water was obtained from a Milli-Q Purification System from Millipore (MA, US). A cylinder of general grade helium (Iwatani Industrial Gases Corp, Osaka, Japan) was used.

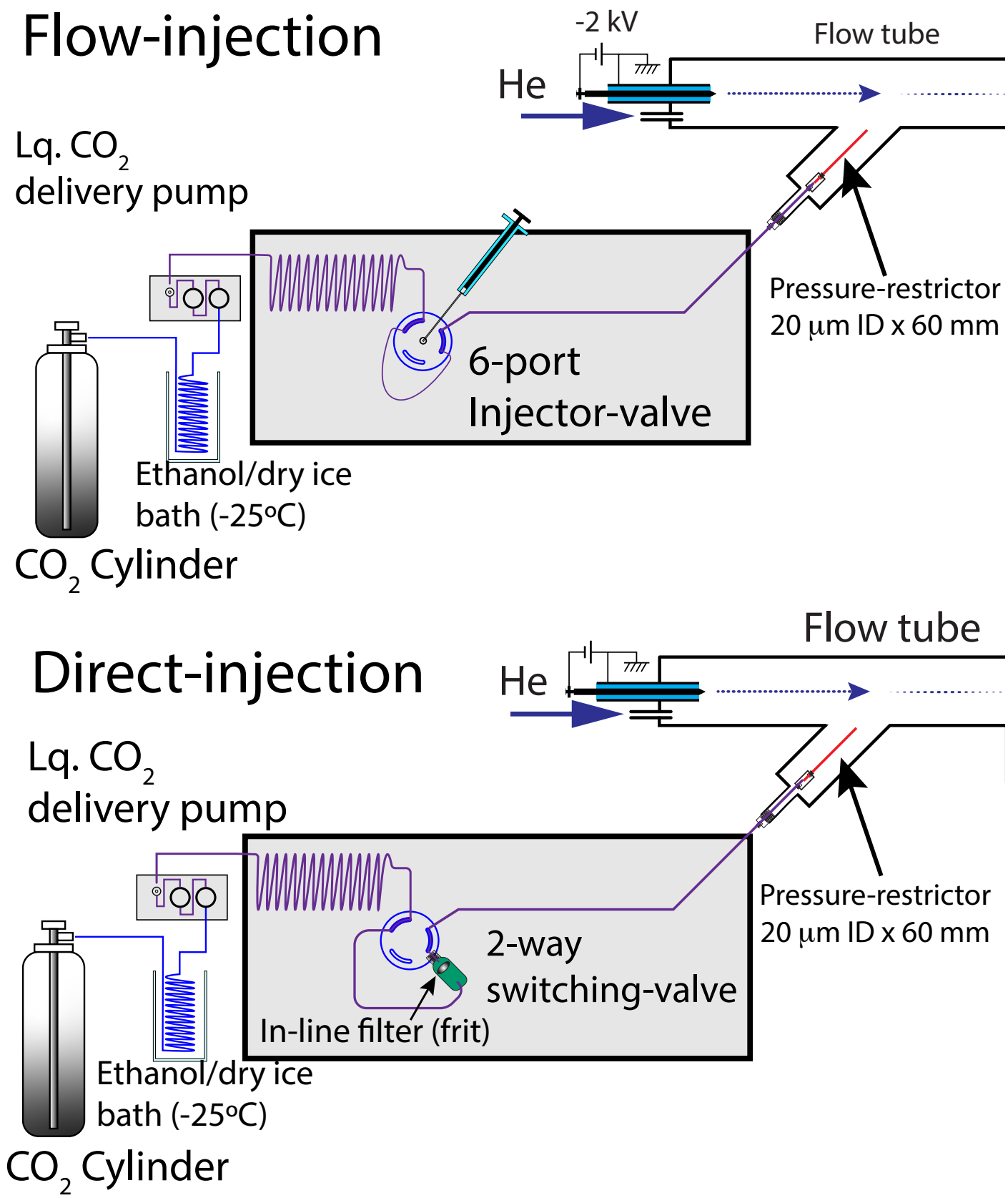

Figure 2.2: System schematics for FI-PTR and DI-PTR analysis.

2.2 Results and Discussion

2.2.1 Mass calibration

Mass calibration was performed using sodium trifluoroacetate, using an electrospray ionization (ESI) source for *m/z* between 159 and 703 and using third-order polynomials. The PTR ion source was then attached by altering the ESI source.

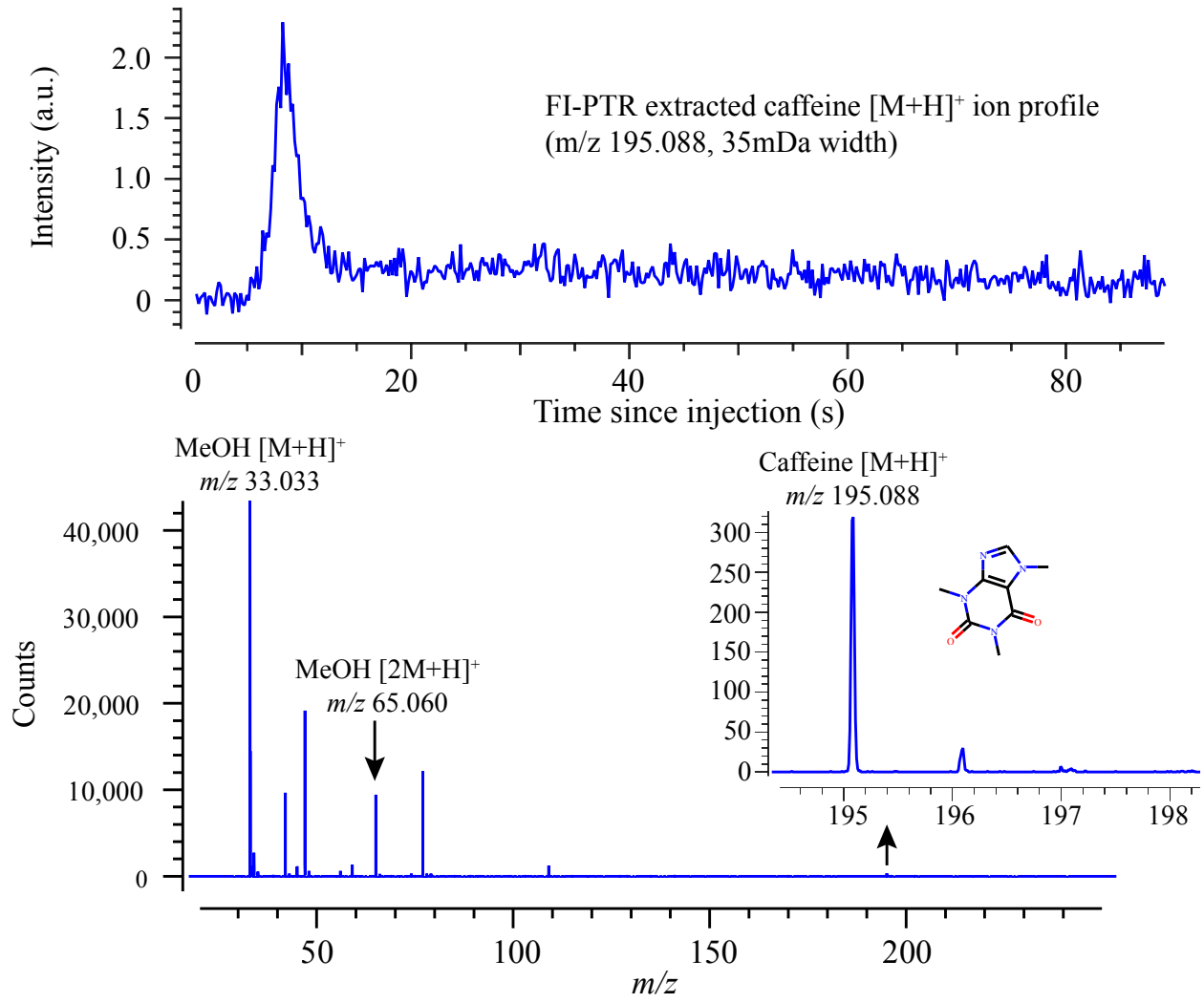

Figure 2.3: Extracted ion FI-PTR profile of 20.5 pmol of caffeine (*m/z* 195.088, 35 mDa width) and caffeine mass spectrum obtained by co-adding a peak half-height region on the profile.

2.2.2 FI-PTR analysis of caffeine

Figure 2.3 shows the caffeine FI-PTR profile and the mass spectrum obtained from a 1 µL injection of 20.5 pmol of caffeine in MeOH. The $scCO_2$ condition was 13 MPa and 50 °C. The capillary tubing dimension from the injector valve to the pressure restrictor was 50 µm by 1.2 m length, which corresponds to a 2.4 µL volume, although the estimated additional volumes of fittings for sample injector, sample loop, and a union for the restrictor totaled approximately 4 to 6 µL and made for a total of approximately 8 µL. The caffeine peak was detected 8.27 s after injection. The estimated $scCO_2$ mass transfer rate calculated from the detection time and tubing volume was approximately 1 $\mu L \cdot s^{-1}$ (60 $\mu L \cdot min^{-1}$. Since the injection volume was 1 µL, the ideal peak width was 1 s, while the obtained peak width was 1.8 s with a peak asymmetry factor of 1.57 The peak parameters for protonated MeOH dimer were 2.5 s for the peak width and 1.29 for the peak asymmetry factor. Peak width was calculated from the width at the half height of the peak. The asymmetry factor was calculated from the width at 5% of the peak height. The peak parameters obtained from caffeine ions and MeOH dimer ions suggest that the instrumental dispersion was approximately 0.5 to 1.5 s for a 1 s peak width.

Figure 2.3 (bottom) shows a co-added mass spectrum for a one second width on the caffeine FI-PTR peak. The spectrum shows the ions of protonated MeOH, MeOH dimer, and caffeine with less than 1.7 mDa mass errors.

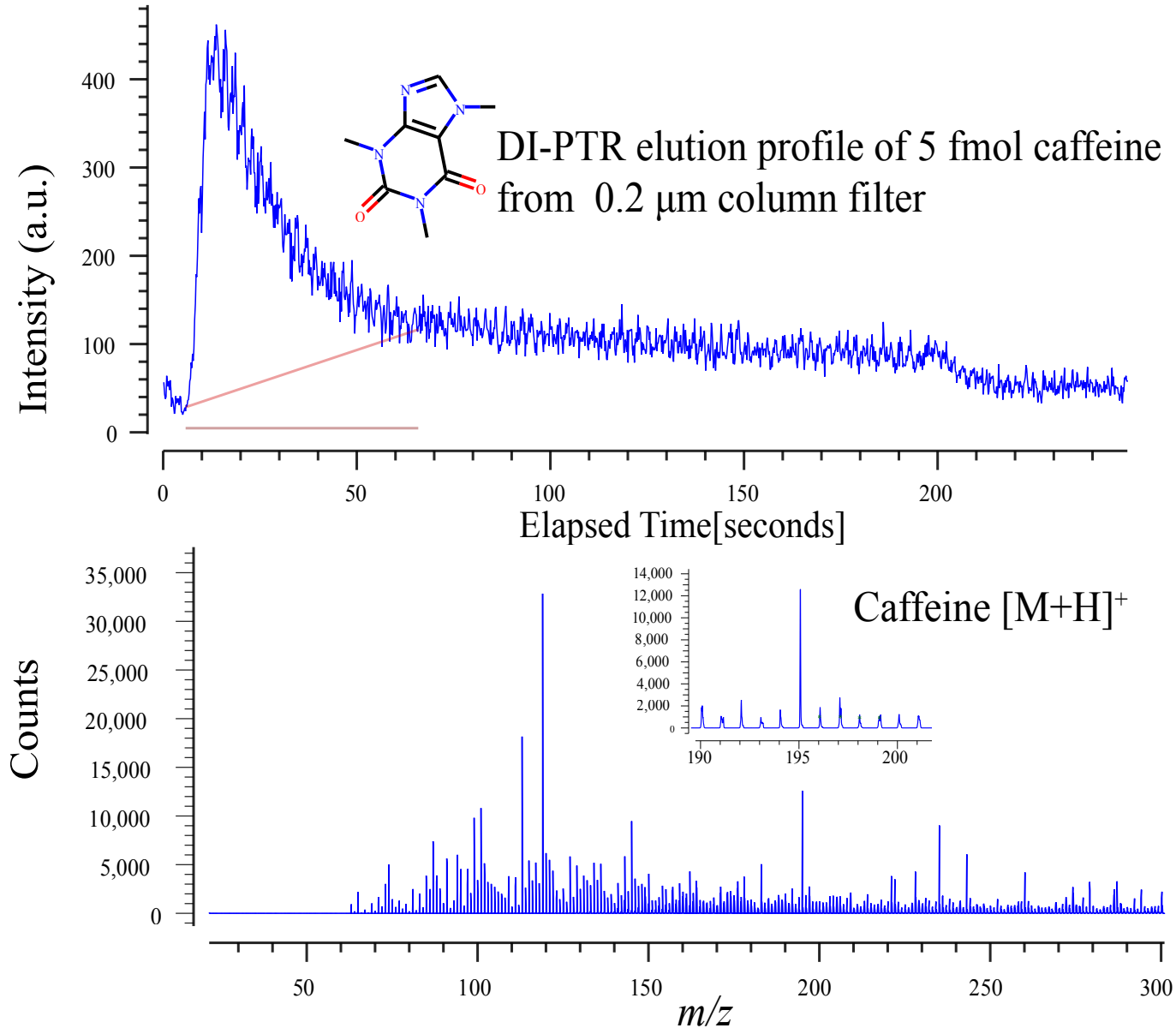

Figure 2.4: Extracted ion DI-PTR SFE profile of 5 fmol of caffeine.

2.2.3 DI-PTR monitoring of caffeine

Figure 2.4 shows the results of DI-PTR analysis of caffeine. Five fmol of caffeine dissolved in acetonitrile was applied to a filter (0.2 µm, 2.1 mm, Waters, MA, US). After a 5-minute wait to evaporate the acetonitrile, the caffeine-containing filter was set into the column in-line filter housing (Waters, MA, US) and attached to the Rheodyne 7000 switching valve. Direct injection (extraction from a filter) was then performed at 22 MPa at 40 °C; the flow rate was set to $0.5\,\mathrm{mL}\cdot\mathrm{min}^{-1}$. The caffeine mass spectrum, shown in Figure 2.4 (bottom), was produced by co-adding the spectra acquired in the elution peak half-height width range 10.1 to 18.9 s.

2.2.4 DI-PTR monitoring of other nonvolatile compounds

Figure 2.5 shows a DI-PTR elution profile of oleic acid $[\mathrm{M}+\mathrm{Cl}]^-$ in negative ion mode. A 32 fmol of oleic acid dissolved in MeOH was applied to the filter, and then the DI-PTR elution profile was monitored.

A detection capability for a couple of other organic compounds besides caffeine and oleic acid were tested by DI-PTR that can avoid using an organic solvent, which suppresses ionization capability in the PTR. The DI-PTR detection sensitivity for each compound (counts/fmol) was: 12941 for caffeine, 5.3 for pyrene in positive ion mode, 573 for oleic acid (sum of $[\mathrm{M}-\mathrm{H}]^-$, $[\mathrm{M}+\mathrm{Cl}]^-$), and 185 for γ-oryzanol (sum of $[\mathrm{M}-\mathrm{H}]^-$ ions for campesteryl ferulate,

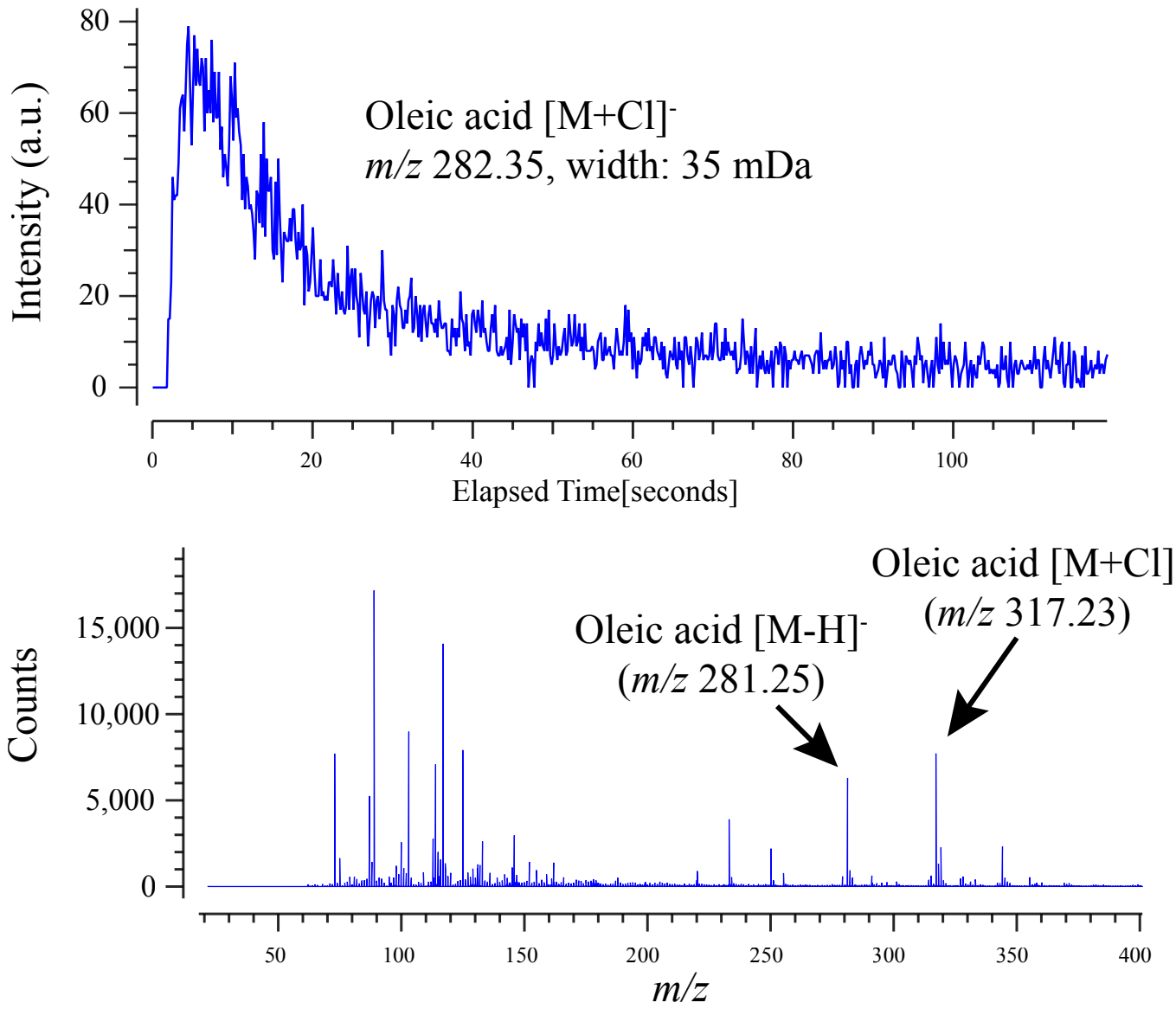

Figure 2.5: DI-PTR elution profile and mass spectrum of oleic acid (32 fmol).

γ-oryzanol A and B) in the negative ion mode. Reserpine ion was able to monitored in both positive (protonated) and negative (deprotonated) mode, which is useful to use as mass reference (data not shown). The spectrum and DI-PTR ion profile were shown in Supporting Information Figures 2.1 and 2.2.

2.3 Conclusion

The $scCO_2$ FI-PTR and DI-PTR were preliminarily evaluated by using caffeine and oleic acid as the model nonvolatile compounds. Very good instrumental dispersion result using the FI-PTR was observed. The DI-PTR method, which extracts caffeine and oleic acid from a column in-line filter, directly monitored PTR ionization with high sensitivity. We have also evaluated the detection capability for a couple of other compounds using DI-PTR. Pyrene was detected in positive ion mode, and $gamma$-oryzanol was detected in negative ion mode.

参考文献

[1] Rajendran, A.; Gilkison, T. S.; Mazzotti, M. *Journal of Separation Science* 2008, **31**, 1279–1289.

[2] Guiochon, G.; Tarafder, A. *Journal of Chromatography A* 2011, **1218**, 1037–1114.

[3] Åsberg, D.; Enmark, M.; Samuelsson, J.; Fornstedt, T. *Journal of Chromatography A* 2014, **1374**, 254–260.

[4] Leśko, M.; Samuelsson, J.; Glenne, E.; Kaczmarski, K.; Fornstedt, T. *Journal of Chromatography A* 2021, **1639**,

461926.

[5] Zosel, K. *Angewandte Chemie International Edition in English* 1978, **17**, 702–709.

[6] Stringham, R. W.; Blackwell, J. A. *Anal. Chem.* 1996, **68**, 2179–2185.

[7] Glenne, E.; Leśko, M.; Samuelsson, J.; Fornstedt, T. *Anal. Chem.* 2020, **92**, 15429–15436.

[8] Glenne, E.; Samuelsson, J.; Leek, H.; Forssén, P.; Klarqvist, M.; Fornstedt, T. *Journal of Chromatography A* 2020, **1621**, 461048.

[9] Sugiyama, K.; Saito, M.; Hondo, T.; Senda, M. *Journal of Chromatography A* 1985, **332**, 107–116.

[10] del Carmen Salvatierra-Stamp, V.; Ceballos-Magaña, S. G.; Gonzalez, J.; Ibarra-Galván, V.; Muñiz-Valencia, R. *Anal Bioanal Chem* 2015, **407**, 4219–4226.

[11] Heiland, J. J.; Geissler, D.; Piendl, S. K.; Warias, R.; Belder, D. *Anal. Chem.* 2019, **91**, 6134–6140.

[12] Arpino, P. J.; Cousin, J.; Higgins, J. *TrAC Trends in Analytical Chemistry* 1987, **6**, 69–73.

[13] Prajapati, P.; Agrawal, Y. K. *Anal. Methods* 2016, **8**, 4895–4902.

[14] Arpino, P. J. In *Mass Spectrometry in the Biological Sciences: A Tutorial*; Gross, M. L., Ed.; NATO ASI Series; Springer Netherlands: Dordrecht, 1992; pp 269–280.

[15] Parr, M. K.; Wüst, B.; Teubel, J.; Joseph, J. F. *Journal of Chromatography B* 2018, **1091**, 67–78.

[16] Ubhayasekera, S. J. K. A.; Acharya, S. R.; Bergquist, J. *Analyst* 2018, **143**, 3661–3669.

[17] Hansel, A.; Jordan, A.; Holzinger, R.; Prazeller, P.; Vogel, W.; Lindinger, W. *International Journal of Mass Spectrometry and Ion Processes* 1995, **149-150**, 609–619.

[18] Lindinger, W.; Jordan, A. *Chem. Soc. Rev.* 1998, **27**, 347.

[19] Yuan, B.; Koss, A. R.; Warneke, C.; Coggon, M.; Sekimoto, K.; de Gouw, J. A. *Chem. Rev.* 2017, **117**, 13187–13229.

[20] Pan, Y.; Zhang, Q.; Zhou, W.; Zou, X.; Wang, H.; Huang, C.; Shen, C.; Chu, Y. *J. Am. Soc. Mass Spectrom.* 2017, **28**, 873–879.

[21] Kawai, Y.; Miyake, Y.; Hondo, T.; Lehmann, J.-L.; Terada, K.; Toyoda, M. *Anal. Chem.* 2020, **92**, 6579–6586.

第 3 章

超臨界流体抽出–中真空化学イオン化質量分析法による有機物正負イオンの測定と定量限界

3.1　緒言

第 2 章において，超臨界流体抽出 (SFE)/超臨界流体クロマトグラフィー (SFC) と中真空化学イオン化 (medum vacuum chemical ionization; MVCI) 質量分析法 (MS) を組み合わせることにより，いくつかの不揮発性有機化合物について，ポジティブイオンあるいは，ネガティブイオンとして高感度に検出できることを述べた[1)].

本章では，MVCI MS の特性や応用可能性をより深く理解する目的で，α-トコフェロール (α-T)，γ-オリザノール，脂肪酸, アセトアミノフェン，多環芳香族など，様々な物質について測定を行い，その結果について述べる．

α-T は，植物により生産される抗酸化物質であり，ヒトは食品から摂取する必要がある物質である．γ-オリザノール[2)] は，米ぬかや米油に多く含まれる天然の抗酸化物質であり医薬品としても利用されている．脂肪酸は，細胞分化などの生命現象に加え，多くの疾病との関わりが指摘されており，細胞内や組織内の濃度の迅速な測定方法が望まれる．アセトアミノフェンは解熱鎮痛剤として広く用いられている．多環芳香族のいくつかは，アスファルトやディーゼルエンジンの排気ガスなどに含まれ，大気汚染物質としての可能性が指摘されている物質である．

現時点で，MVCI 質量分析計を運用する上での課題の１つは，質量較正の試料が見つかっていないことでる．安定で，高感度に測定でき，正負いずれのイオンも検出可能な様々な化合物の探索も本章の目的の１つである．

3.2　実験

3.2.1　試薬

α-T，γ-オリザノール，オレイン酸，ビタミン K_1 (VK_1)，レセルピン，カフェイン，ピレン，リノール酸，アラキジン酸，テトラコセン酸，ステアリン酸，アセトニトリル (LC/MS グレード)，アセトン (試薬グレード) は，富士フィルム和光純薬株式会社（大阪）から購入した．アセトアミノフェン，アラキドン酸，フェナセチンは東京化成工業株式会社 (東京) から購入した．

MVCI MS 測定に用いる試料は α-T 12.3 mg を秤取りアセトン 3 mL に溶解した後，アセトンで 1000 倍希釈し，α-T 10 μmol $\cdot$ L^{-1} 試料溶液とした．

γ-オリザノールは 2.1 mg を秤取りアセトニトリル 1 mL に溶解した後，アセトニトリルで 1000 倍希釈し，γ-オリザノール 3.5 μmol $\cdot$ L^{-1} 試料溶液とした．

オレイン酸は 0.67 mL を秤取りアセトニトリル 2.33 mL に溶解した後，アセトニトリルで 10^6 倍希釈し，オレイン酸 10 μmol $\cdot$ L^{-1} 試料溶液とした．

VK_1 は 13.4 mg を秤取りアセトニトリル 3 mL に溶解した後，アセトニトリルで 10 倍希釈し，VK_1 1 mmol·L^{-1} 試料溶液とした．

レセルピンは 0.4 mg を秤取りアセトニトリル 1 mL に溶解した後，アセトニトリルで 10^6 倍希釈しレセルピン 660 pmol · L^{-1} 試料溶液とした．

アセトアミノフェンは 4.6 mg を秤取りアセトニトリル 3 mL に溶解し，アセトニトリルで希釈を行い試料溶液とした．

フェナセチンは 5.4 mg を秤取りアセトニトリル 3 mL に溶解し，アセトニトリルで希釈を行い試料溶液とした．

カフェインは 4.1 mg を秤取りアセトニトリル 1 mL に溶解し，アセトニトリルで希釈を行い試料溶液とした．

ピレンは 5.0 mg を秤取りアセトニトリル 1 mL に溶解し，アセトニトリルで希釈を行い試料溶液とした．

ステアリン酸は 8.7 mg を秤取りエタノール 3 mL に溶解し，アセトニトリルで希釈を行い試料溶液とした．

リノール酸は 0.67 mL を秤取りヘキサン 2.33 mL に溶解し，アセトニトリルで希釈を行い試料溶液とした．

アラキドン酸は 100 mg を秤取りアセトニトリル 1 mL に溶解し，アセトニトリルで希釈を行い試料溶液とした．

アラキジン酸は 9.5 mg を秤取りヘキサン 3 mL に溶解し，アセトニトリルで希釈を行い試料溶液とした．

テトラコセン酸は 11.1 mg を秤取りアセトン 3 mL に溶解し，アセトニトリルで希釈を行い試料溶液とした．

3.2.2　質量分析装置および試料導入方法

SFE-MVCI 質量分析装置は第 2 章にすでに述べた通り，MVCI イオン源と JMS-T100 LP (AccuTOF) time-of-flight (TOF) mass spectrometer (JEOL, 東京) を接続して用いた．

試料導入方法として，第 2 章で DI-PTR として示した方法，すなわち，アセトニトリルなどに溶解した試料を焼結フィルター（フリット）に浸透させ，有機溶媒の蒸発を待った後，ACQUITY Column In-Line Filter（Waters, US）に取り付け，スイッチングバルブを用いて流路へと導入する方法を用いた．この方法を，以下 SFE-MVCI と示す．

3.2.3　CO_2 送液システム

液体状態でボンベから取り出した CO_2 は，LC Packings Ultimate Micropump (Thermo Scientific, MA, US) のポンプヘッドに，3 枚のペルチェ素子 (Hebei, TES1-12705, Hebei, China) で構成したヘッド冷却機構を取り付け，ポンプヘッドを約 8 °C に冷却した[3)]．冷却機構は，厚さ 5 mm のアルミニウム板をポンプヘッドに密着するようボルトで固定し，そのアルミニウム板に 1 枚のペルチェ素子を取り付け，さらにその背後に 2 枚のペルチェ素子を左右に並べて固定し，その背後から別の厚さ 5 mm のアルミニウム板で挟み樹脂製ボルトおよびナットで固定した．外側アルミニウム板には，市販の CPU ヒートシンク (upHere, Dongguan Zhishang Technology Co., Ltd. Dongguan China) を取り付けた．ペルチェ素子への電流は，市販の ATX 電源 ((KRPW-GA850W/90 ＋，玄人志向) の ATX POWER (12 V) ラインより供給した．ポンプヘッド温度は，ポンプヘッド側アルミニウム板の側面に MAX6675 Cold-Junction-Compensated K-Thermocouple-to-Digital Converter (Max Integrated Inc., CA, US) を埋め込み，その出力信号を DE0-nano-SoC (Terasic, ROC ,Taiwan) にて読み取ることで測定した．

3.2.4　質量較正

質量較正は，AccuTOF にエレクトロスプレーイオン化 (ESI) イオン源を取り付け，1.0 g · L^{-1} トリフルオロ酢酸ナトリウム (TFANa) を導入し，正イオンモード，負イオンモードそれぞれで測定し，159 から 1519 の範囲について飛行時間と $\sqrt{m/z}$ の関係を 3 次多項式でフィッティングすることで行った．質量較正データ測定後 MVCI イオン源に置き換えた．

3.2.5　定量限界

本章では，化合物の焼結フィルターからの SFE 抽出イオンプロファイルについて，そのピーク高さの 1/2 の範囲内のイオンカウント数を求め，100 カウントを与える化合物量を定量下限 (lower limit of quantitation ; LLOQ) とした[4)].

3.2.6　同位体比

それぞれの化合物イオンに対する同位体ピークの理論相対強度，ならびに *m/z* は，データシステムソフトウエア QtPlatz (http://github.com/qtplatz) 5.2 を用い，質量分解能 (mass resolving power) 5000，最小相対強度 (minimum RA limit) 10^{-4} をパラメータとして計算した値を用いた.

3.3　結果・考察

3.3.1　ネガティブイオンモードでの α-T の SFE-MVCI MS

α-T の測定は 3.2 節に述べた 10 µmol · L^{-1} の α-T 試料溶液 0.2 µL (2 pmol) をフリットに載せ SFE-MVCI 測定を行った．Figure 3.1に，ネガティブイオンモードでの SFE-MVCI MS で得られた 2 pmol の α-T スペクトルを示す．α-T プロトン脱離分子 (*m/z* 429.374) が最大強度ピークとして観測された．Table 3.1にこの測定で得られた α-T の同位体比の実測値と計算値を示す．α-T のモノアイソトピックピークに対して，同位体パターン上の M+1, M+2, M+3 に対応するピークのカウント数の統計誤差，20, 10, 5 は，それぞれ 5.2 %, 10.0 %, および 22 % に相当し，得られた同位体比は，計算値に比較してやや高い値を示す結果が得られた．得られたスペクトルは，広範囲にわたってバックグラウンドイオンが検出されており，その影響による誤差ではないかと考えられる．これらを考慮すると，ネガティブイオンモードで測定した α-T 同位体プロフィールは計算値と比較的良好に一致したといえる．この点は，次章に述べるポジティブイオンモードでの α-T スペクトルの挙動とは大きく異なっている.

3.3.2　ネガティブイオンモードでのオリザノールおよびレセルピンの SFE-MVCI MS

Figure 3.2 にネガティブイオンモードで得られた 700 fmol の γ-オリザノールの質量スペクトルを示す．γ-オリザノールの測定は，3.2.2節に述べた方法で γ-オリザノール 700 fmol をフリットに載せた後，さらにレセルピン 0.13 fmol を載せ測定した．γ-オリザノールとレセルピンはいずれもプロトン脱離分子（$[M-H]^-$）として観測さ

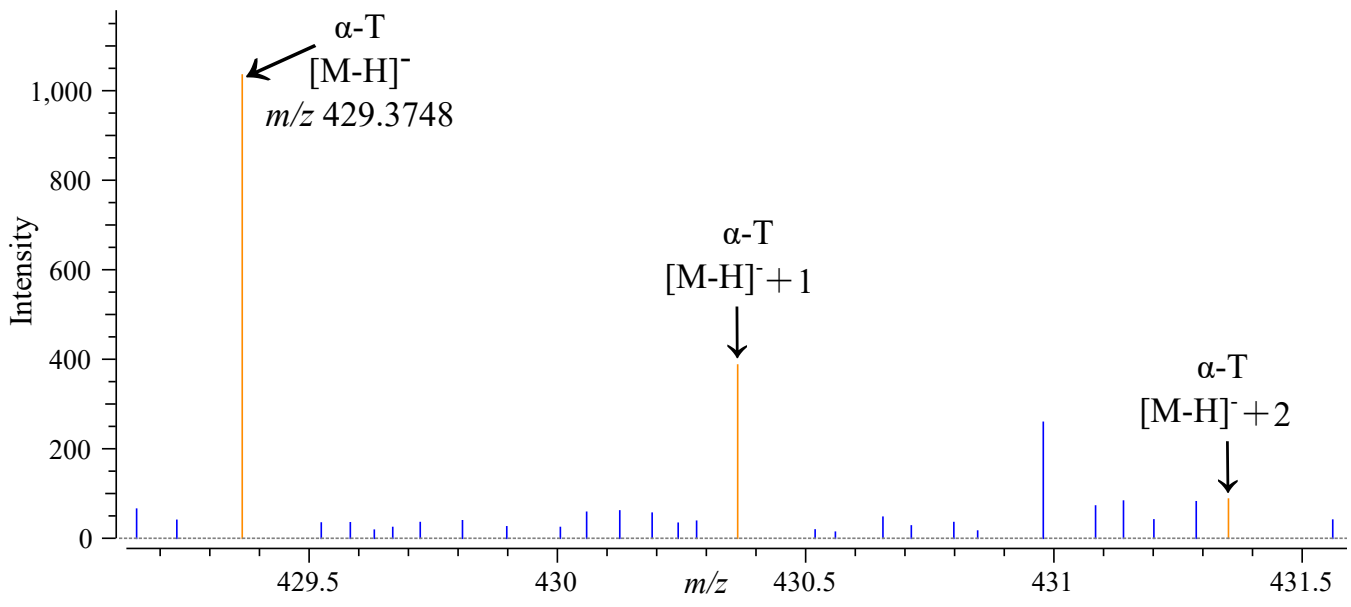

Figure 3.1: SFE-MVCI mass spectrum of 2 pmol of α-T in negative ion mode.

Table 3.1: Relative abundance (RA) of α-T isotopes. Exact RA was calculated based on a mass resolving power of 5000. The peak with RA 0.1% for the most abundant peak has been removed.

Compound	ion form	*m/z*	Counts	RA (%)	RA (exact)
α-T	$[M-H]^-$	429.374	1027 ± 32	100	100
	$[M-H]^-$ +1	430.377	379 ± 20	37 ± 2	32.0
	$[M-H]^-$ +2	431.380	100 ± 10	20 ± 2	5.4
	$[M-H]^-$ +3	432.383	22 ± 5	2.0 ± 0.4	0.6

れた.

Figure 3.3 に得られた γ-オリザノール[5] の主要成分である，カンペステリルフェルラート，γ-オリザノール A (シクロアルテニルフェルレート)，γ-オリザノール B (24-メチレンシクロアルタニルフェルレート)，およびレセルピンのプロトン脱離分子（ $[M-H]^-$ ）の抽出イオンプロファイルを示す.

γ-オリザノールの SFE 抽出プロファイルのピーク幅（半値幅）は 15.0 s，半値幅内のイオンカウントはカンペステリルフェルラート，γ-オリザノール A，および B がそれぞれ 15459，31274，36458 であった．レセルピンは測定時間 300 s 経過後もイオンが観測され続け，その後数回の SFE-MVCI MS 測定に渡ってピークが観測され続け，イオンが確認されなくなるには数時間を要した.

Table 3.2 にカンペステリルフェルラート，γ-オリザノール A，γ-オリザノール B，それぞれの同位体ピークのスペクトルから得られた強度比と計算で得られた同位体存在比を示す． Table 3.2 に示す通り，測定で得られた同位体パターンは計算値と良好な一致を示した.

Table 3.2: Relative Abundance (RA) of γ-oryzanol isotopes

Compound	ion form	*m/z*	Counts	RA (%)	RA(exact)
Campesteryl ferulate	$[M-H]^-$	575.411	2148 ± 46	100	100
	$[M-H]^-$ +1	576.413	971 ± 31	45.2	41.9
	$[M-H]^-$ +2	577.417	278 ± 17	13.0	9.1
	$[M-H]^-$ +3	578.420	110 ± 10	5.1	0.3
γ-Oryzanol A	$[M-H]^-$	607.266	4965 ± 70	100	100
	$[M-H]^-$ +1	608.269	2674 ± 52	53.9	37.2
	$[M-H]^-$ +2	609.272	1040 ± 32	20.9	8.4
	$[M-H]^-$ +3	610.274	280 ± 17	5.6	0.7
γ-Oryzanol B	$[M-H]^-$	615.442	6661 ± 82	100	100
	$[M-H]^-$ +1	616.445	3474 ± 59	52.2	45.2
	$[M-H]^-$ +2	617.448	1037 ± 32	15.6	10.5
	$[M-H]^-$ +3	618.451	268 ± 16	4.0	1.4

3.3.3　複数化合物の同時検出におけるピーク強度への影響

ネガティブイオンモードにおいて，オレイン酸 2 fmol，α-T 50 pmol，レセルピン 133 pmol，VK_1 400 pmol，および γ-オリザノール 16 pmol それぞれ個別に測定して得られたピーク強度と，これらをフリット上で混合し，混合物として一斉に測定した場合について得られるピーク強度を測定した．それぞれ得られた結果から LLOQ を求め Table 3.3 に示した．この際，混合物として一斉に測定した場合の質量スペクトルを Figure 3.4 に示す.

Table 3.3 に示すとおり，化合物を個別に測定した場合と比較して，混合物として一斉に測定した場合，オレイン酸 1.9 倍，α-T 1950 倍，レセルピン 443.9 倍，VK_1 750 倍，γ-オリザノール 66.3 倍に LLOQ が上昇した．すな

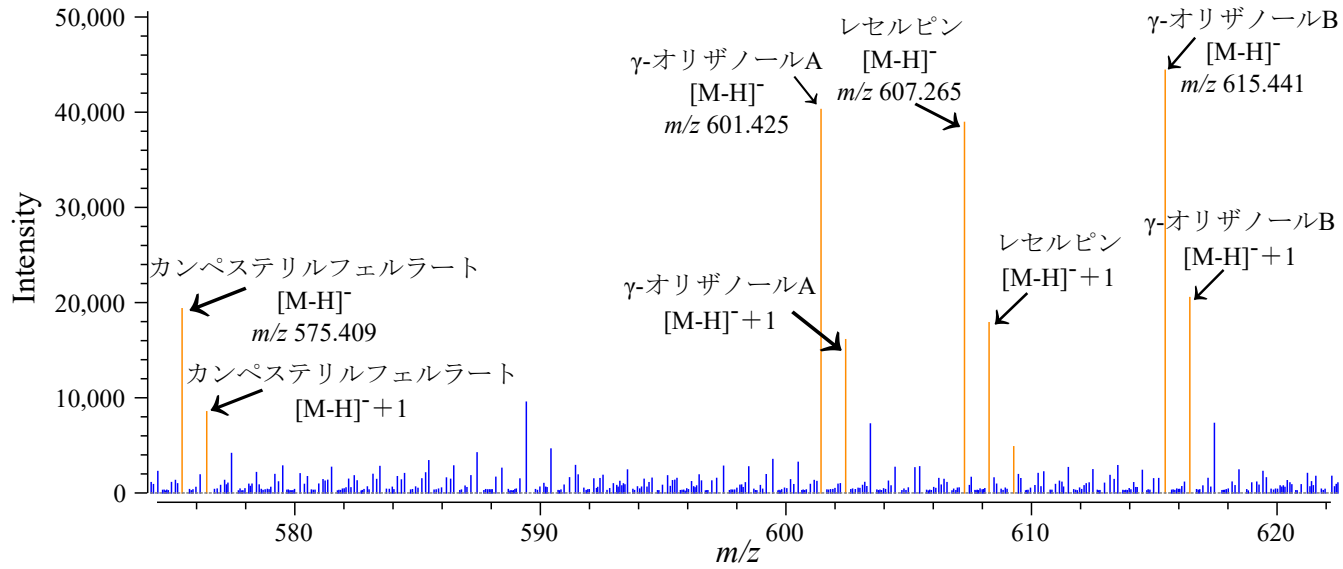

Figure 3.2: Mass spectrum of 700 fmol γ-oryzanol obtained by SFE-MVCI MS in negative ion mode.

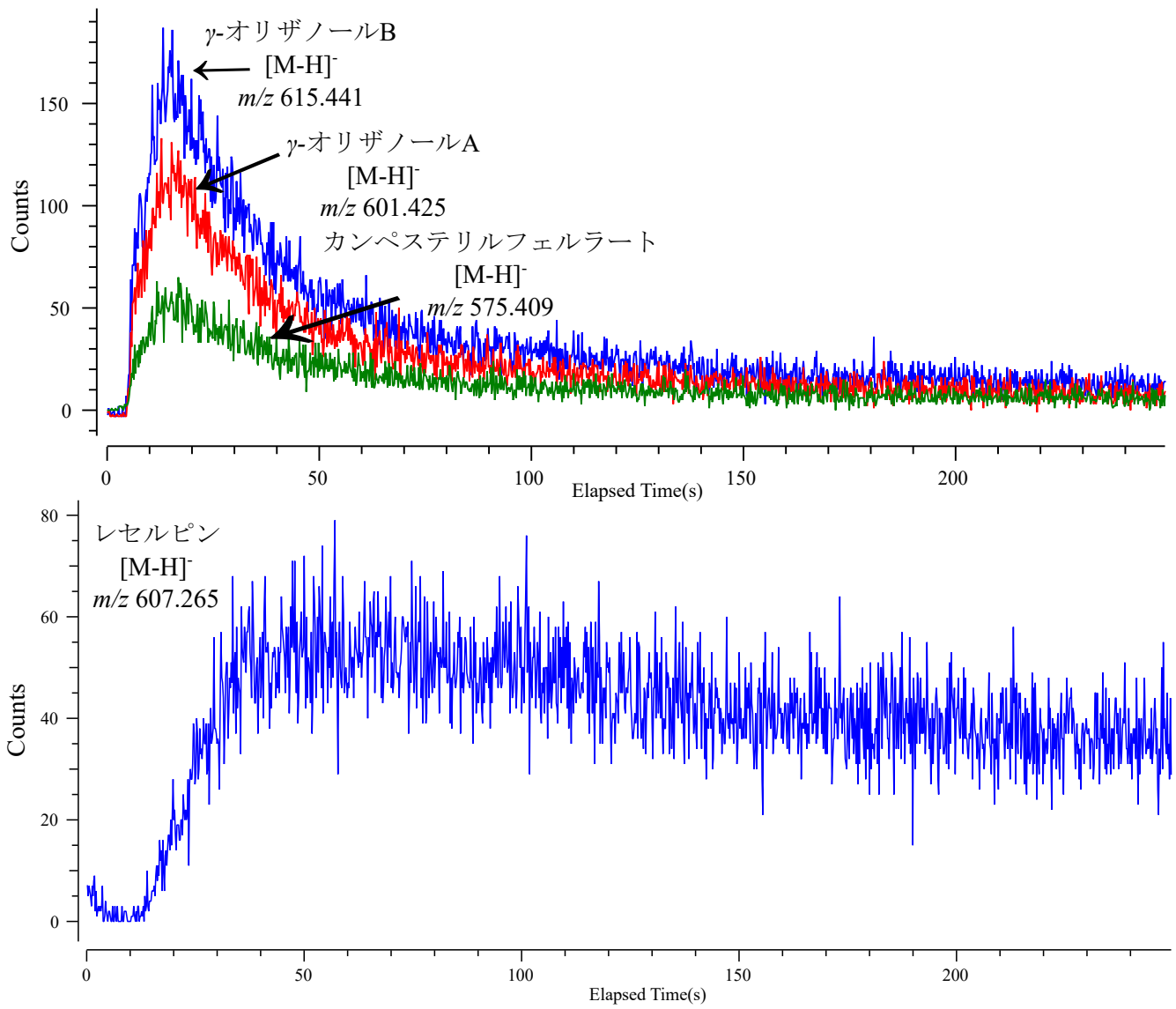

Figure 3.3: Extracted ion profiles of γ-oryzanol $[M-H]^-$ (top) and reserpine $[M-H]^-$ (bottom).

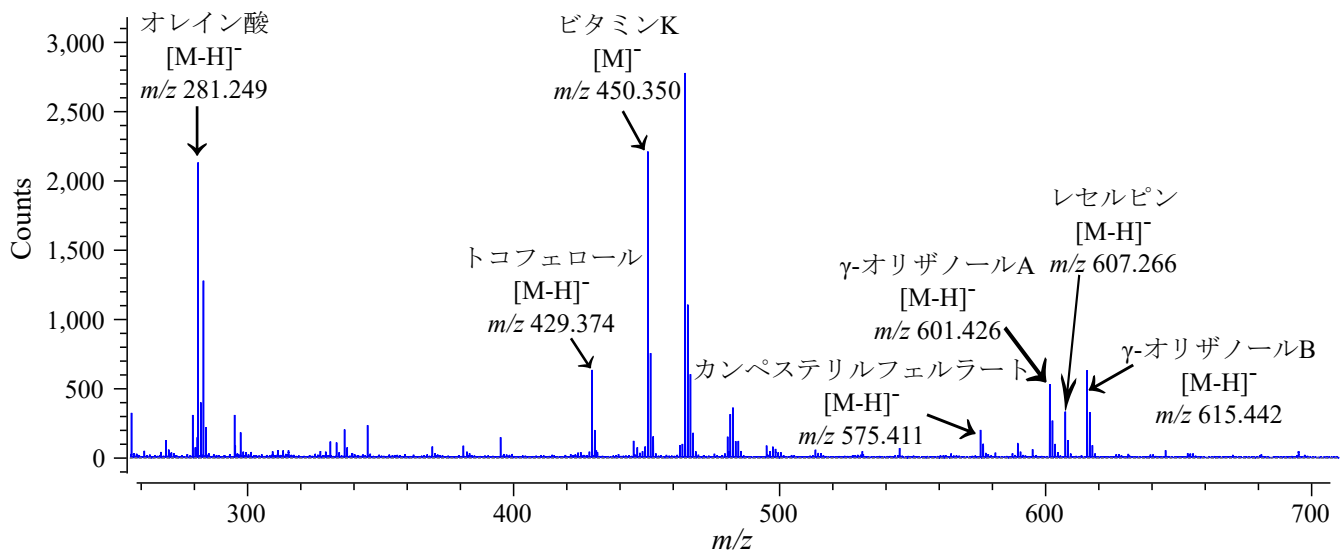

Figure 3.4: Mass spectrum of a mixture of oleic acid (2 fmol), α-T (50 pmol), VK_1 (400 pmol), γ-oryzanol (16 pmol), and reserpine (133 pmol).

わち，これらの化合物が混合物として同時にイオン化される条件では，いずれの化合物も LLOQ が大きく押し上げられることが分かった．今回の混合試料測定ではオレイン酸がより速くイオン化され，試薬イオンである OH^- をレセルピン，VK_1，γ-オリザノールより早く消費し，OH^- が枯渇したためではないかと考えられる．

Table 3.3: Lower Limit of Quantitation (LLOQ) for various authentic samples.
A sum of intensities for peaks obtained from m/z 602.434, 615.442, and 675.411 was used as the γ-oryzanol intensity.

Compound	ion	*m/z*	LLOQ (fmol)	
			Individual analysis	Mixture analysis
Oleic acid	$[M-H]^-$	282.256	0.048	0.091
α-T	$[M-H]^-$	430.381	4	7800
VK_1	$[M]^-$	450.350	41	18200
γ-Oryzanol	$[M-H]^-$	(602.434)	1.6	1200
Reserpine	$[M-H]^-$	608.273	590	39100

複数の化合物が同時にイオン化されることによるイオン化の抑制は ESI など他のイオン化法でも広く知られており，その一般的な回避方法はクロマトグラフィーによる分離機構を測定系に加えることである．このことから超臨界流体クロマトグラフィー (SFC) を導入し，それぞれの物質を時間的に分離してイオン源に到達するようにすることで，混合試料を測定する場合のイオン化の抑制の影響を少なくできると考えられる．SFC は SFE とオンラインで接続することができ，物質の前処理に相当する抽出操作とクロマトグラフィー分離を一連の操作として行える．試料を装置に導入するまでの前処理操作を最小にすることができ，抽出から測定にいたる過程でのコンタミネーションのリスクを低く抑えることができる．さらに超臨界流体特有の高速な抽出により，分析スループットの向上が期待できる．SFC は極めてカラム効率が高く，高い線流速を用いながら，高い理論段数を実現でき，一般的に得られるピーク幅は 0.5 s 以下に達する．MVCI イオン源に対してそのような極めて狭いバンド幅で試料がピークとして導入された場合の時間的広がり (longitudinal dispersion) については解明されておらず，本論文の第 5 章で詳しく議論する．

3.3.4　その他の有機化合物の定量下限

Table 3.4 に SFE-MVCI MS ポジティブイオンモードとネガティブイオンモードで測定した化合物について，100 カウントあたりの化合物量を定量下限として示した．多くの化合物で，ポジティブイオン，あるいはネガティブイオンで fmol から amol オーダーの定量下限が得られた．アセトアミノフェン，フェナセチン，レセルピンはポジティブイオンで高感度に検出され，ネガティブイオンモードでも感度は劣るものの検出は可能であった．脂溶性ビタミンである α-T，VK_1 はネガティブイオンモードで良好な感度で検出された．またポジティブイオンモードでもやや感度は劣るものの良好な感度で検出されている．カフェインおよび多環芳香族であるピレンはポジティブイオンモードでのみ検出可能であった．脂肪酸はネガティブイオンモードでのみ検出可能であった．また，ステアリン酸 (C18:0)，オレイン酸 (C18:1)，リノール酸 (C18:2)，アラキジン酸 (C20:0)，およびアラキドン酸 (C20:1) の LLOQ から，程度の違いはあるものの同一炭素数の場合，二重結合を含む脂肪酸がより高感度となる傾向が認められた．カフェインを除く化合物では， log P 2.0 から 10.2 の範囲でポジティブイオンモード，ネガティブイオンモードで化合物が検出できた．ESI では，α-T, VK_1, γ-oryzanol など極端に log P の大きな化合物は感度が低い傾向にあるが，MVCI では log P の大きさに関わりなく良好な感度が得られており，超臨界 CO_2 に溶解させることができる化合物は検出できるのではないかと考えられる．

Table 3.4: Lower Limit of Quantitation for various authentic samples. The log P values were calculated using a function on the rdkit.[6)]

Compound	mass	log(P)	positive ion mode		negative ion mode	
Acetaminophen	151.063	2.0	4.9 fmol	$[M+H]^+$	274 fmol	$[M-H]^-$
Phenacetin	179.095	2.0	1.4 fmol	$[M+H]^+$	203 fmol	$[M-H]^-$
Caffeine	194.080	-1.0	0.077 fmol	$[M+H]^+$	–	
Pyrene	202.078	4.6	9.5 fmol	$[M+H]^+$	–	
Oleic acid	282.256	6.1	–		0.048 fmol	$[M-H]^-$
Stearic acid	284.272	6.3	–		10 fmol	$[M-H]^-$
Linolic acid	280.240	5.9	–		0.20 fmol	$[M-H]^-$
Arachidic acid	312.303	7.1	–		27 fmol	$[M-H]^-$
Arachidonic acid	304.240	6.2	–		19 fmol	$[M-H]^-$
Tetracosanoic acid	368.365	8.7	–		17 fmol	$[M-H]^-$
α-T	430.381	8.8	63 fmol	$[M+H]^+$	4 fmol	$[M-H]^-$
VK_1	450.350	9.2	406 fmol	$[M+H]^+$	41 fmol	$[M]^-$
γ-Oryzanol	602.434	10.2	–		1.6 fmol	$[M-H]^-$
Reserpine	608.273	4.2	8.3 fmol	$[M+H]^+$	8000 fmol	$[M-H]^-$

3.4　結言

ポジティブイオンモードの測定では，アセトアミノフェン，フェナセチン，カフェイン，ピレン，α-T，VK_1，およびレセルピンがいずれもプロトン付加分子として検出でき，得られた LLOQ は，それぞれ 4.9, 1.4, 0.077, 9.5, 63, 406, および 8.3 fmol であった．

ネガティブイオンモードの測定では，オレイン酸，α-T，γ-オリザノール，レセルピンはプロトン脱離分子として検出された．しかしながら，VK_1 は，ラジカルアニオン ($M^{-\bullet}$) としてのみ検出され，プロトン脱離分子は観測されなかった．オレイン酸，α-T, γ-オリザノール，レセルピン，および VK_1 に対する LLOQ は，それぞれ 0.048, 4, 1.6, 8000, 41 fmol であった．

オレイン酸，α-T，VK_1，γ-Oryzanol，およびレセルピンを混合した試料の SFE-MVCI MS 測定では，それぞれの化合物のみを試料として測定した場合に比べ，得られた定量下限は，それぞれ 1.9, 1950, 449, 750, および 66 倍上昇し，化合物によって程度の違いはあるものの，共存する化合物によって相互に強くイオン化阻害していることが示唆された．したがって，細胞など，より複雑な試料の測定には，SFC などによる分離が重要と考えられる．

参考文献

[1] Hondo, T.; Ota, C.; Miyake, Y.; Furutani, H.; Toyoda, M. *Anal. Chem.* 2021, **93**, 6589–6593.

[2] Kayathi, A.; Chakrabarti, P. P.; Bonfim-Rocha, L.; Cardozo-Filho, L.; Bollampalli, A.; Jegatheesan, V. *Process Safety and Environmental Protection* 2021, **148**, 179–188.

[3] 太田千尋 超臨界流体抽出/クロマトグラフィ-プロトン移動反応質量分析計（SFE/SFC-PTR-MS) の開発. 卒業論文, 関西大学, 2021.

[4] Kawai, Y.; Miyake, Y.; Hondo, T.; Lehmann, J.-L.; Terada, K.; Toyoda, M. *Anal. Chem.* 2020, **92**, 6579–6586.

[5] Nakano, H.; Takai, T.; Kondo, M. *Cereal Chem* 2018, **95**, 800–810.

[6] Wildman, S. A.; Crippen, G. M. *J. Chem. Inf. Comput. Sci.* 1999, **39**, 868–873.

第 4 章

α-トコフェロールの中真空化学イオン化とエレクトロスプレーイオン化の質量スペクトルの比較

4.1　緒言

第3章までに脂肪酸，脂溶性ビタミンなどの生理活性物質について fmol オーダーの定量限界が，超臨界流体抽出 (SFE)-中真空化学イオン化 (MVCI) 質量分析法 (MS) で得られることを示した．これらの化合物を基質として反応する酵素のミカエリス定数がおよそ $\mu mol \cdot L^{-1}$ から $mmol \cdot L^{-1}$ オーダーと報告されている[1–7]．このことから，細胞内ではこの付近での基質濃度変化によって代謝反応の調節が行われていると考えられる．シングルセル内の濃度が $250\,\mu mol \cdot L^{-1}$ の場合，細胞の体積を 4 pL[8] と仮定すると，1 細胞内の脂質存在量は，およそ 1 fmol と推定できる．3章に示した通り，SFE-MVCI MS を用いたオレイン酸の定量下限として 48 amol を得ており，本法で amol から fmol 量の遊離脂肪酸 (FFA) を定量できる可能性があることがわかった．この章では，その極性の低さから液体クロマトグラフィー (LC) での分離が困難で，エレクトロスプレーイオン化 (ESI) での感度が得られにくい脂質の代表例として，脂溶性ビタミンの測定を検討する．

α-トコフェロール (α-T) はヒトにとっては必須ビタミンであり，食品から摂取する必要がある脂溶性化合物の１つである．植物は光合成を行う際に生成する有害な一重項酸素 ($^1O_2$) による細胞膜などの破壊に対する防御システムとして，抗酸化作用をもつ α-T を自身で生成している[9,10]．α-T は，植物においても，また動物においても，重要な生理活性物質であり，様々な定量方法が開発されてきたが，α-T は log P が 8.8 と極性が極めて低く，血漿や組織からの抽出が容易ではないうえ，液体クロマトグラフィー (LC) での分離も困難であり，ESI イオン化でも十分な感度が得られ難い[11]．SFE-MVCI MS は，微細な細胞試料であっても，細胞を破砕することなく SFE により脂溶性成分を抽出し，MVCI MS で測定可能であることから，チラコイド膜上での α-T の抗酸化反応を SFE 抽出ベッセル上で再現する *in vitro* 測定や，あるいは光合成領域の組織 *in situ* での量の変化などを捉えることができる可能性を持っている．3 章までに測定した化合物は，ポジティブイオンモードにおいてすべてプロトン付加分子で検出されていたことから，α-T もプロトン付加分子の生成を期待した．しかしながら，α-T の SFE-MVCI MS 測定の結果，m/z 429.4, 430.4, および 431.4 の 3 種のイオンが同時に得られた．これらは，それぞれ α-T の $[M-H]^+$，$[M]^+$，および $[M+H]^+$ に一致するが，測定を繰り返した結果，これら 3 ピークの強度比が測定日によって異なり，著しく再現性に乏しい結果が得られた．α-T の定量に関する文献は，主に LC とタンデム質量分析法 (MS/MS) を組み合わせる方法が複数存在する．それらによれば，プリカーサーとして選択するイオンとして，$[M-H]^+$ (m/z 429)[12], $[M]^+$ (m/z 430)[13], あるいは $[M+H]^+$ (m/z 431)[14] など様々である．実験に使用した α-T は，規格含量 98.0% (HPLC) であるものの，MVCI イオン化では化合物によっては amol 程度の量で極めて強いイオン信号が得られることから，購入した α-T に含まれる痕跡程度の不純物を検出している可能性も否定できない．MVCI MS で得られた，これら 3 つのピークが α-T に由来するものか，それ以外であるか不明瞭であった．

この章では，文献に報告例のある α-T の LC-ESI-MS 測定を行い，SFE-MVCI MS で得られる質量スペクトル

と比較・検討する．なお，第 2 章に述べた Direct Injection (DI)-PTR 測定法は，本章では SFE-MVCI と表記する．

4.2　実験

4.2.1　試薬

α-T，ギ酸，アセトニトリル (LC/MS グレード)，アセトン (試薬グレード) は，富士フィルム和光純薬株式会社（大阪）から購入した．

LC-ESI-TOF に用いる試料は α-T 12.3 mg を秤取りアセトニトリル 3 mL に溶解した後，アセトニトリルで 100 倍希釈を行い，0.1 % ギ酸を含むアセトニトリル/水 90/10 混合液で 2 倍希釈した．SFE-MVCI MS 測定に用いる試料は α-T 12.3 mg を秤取りアセトン 3 mL に溶解した後，アセトンで 1000 倍希釈した．

4.2.2　MVCI 質量分析装置

SFE-MVCI 質量分析装置は第 2 章にすでに述べた通り，MVCI イオン源と JMS-T100 LP (AccuTOF) time-of-flight (TOF) mass spectrometer (JEOL, 東京) を接続して用いた．

4.2.3　LC-ESI-TOF MS

液体クロマトグラフは，ACQUITY UPLC H-Class PLUS (Waters，MA，US) を用い，AccuTOF を標準構成 (ESI イオン源) で用いた．カラムは Phenomenex Luna Omega PS C18 (1.6 µm C18 2.1 mmID，長さ 50 mm) を使用した．移動相は 0.1 % ギ酸を含むアセトニトリル/水 10/90 混合液 (A) と 0.1 % ギ酸を含むアセトニトリル (B) を ACQUITY 低圧混合装置にて，A/B 5/95 アイソクラティック，流量 0.2 mL $\cdot$ min^{-1} で送液した．カラムオーブンの設定はオフ，測定時の室温は 25 °C，カラム操作圧力は 1300 psi (8.96 MPa) であった．

AccuTOF は ESI ポジティブイオンモード，ピーク間電圧 400 V，ニードル電圧 2000 V，リングレンズ電圧 7 V，オリフィス 1 電圧 40 V，オリフィス 2 電圧 5 V に設定した．

4.2.4　質量較正

質量較正は，AccuTOF にエレクトロスプレーイオン化 (ESI) イオン源を取り付け，1.0 g $\cdot$ L^{-1} トリフルオロ酢酸ナトリウム (TFANa) を導入し，正イオンモード，負イオンモードそれぞれで測定し，159 から 703 の範囲について飛行時間と $\sqrt{m/z}$ の関係を 3 次多項式でフィッティングすることで行った．質量較正データ測定後 MVCI イオン源に置き換えた．

4.3　結果・考察

4.3.1　α-T の SFE-MVCI MS による測定

典型的な α-T の SFE 溶出プロファイルを Figure 4.1 に示す．Figure 4.2 に示した上下 2 つのスペクトルは，調整日の異なる α-T 2 pmol の SFE-MVCI MS 測定で得られた結果である．α-T に対する $[M + H]^+$ (m/z 431.4), $[M]^+$(m/z 430.4), および $[M-H]^+$ (m/z 429.4) の溶出プロフィールは同一測定データ内で相似であった．しかしながら，Figure 4.2 に示す通り，α-T 由来と考えられる 3 つのイオンの強度は，α-T 試料の調整日や測定日によって大きなばらつきが見られた．様々な試行錯誤の結果，購入した α-T (−80 °C，暗所で保存) 標品を採取，希釈し，ただちに測定を行うことで，再現性よく m/z 431.4 が最大強度となるようなスペクトルが得られることがわかった．以降，測定に用いる α-T 試料は，測定当日に希釈，調整することとした．なお，この 3 イオンの強度比が変化する理由は，５章において詳細に検討し，原因を明確にする．

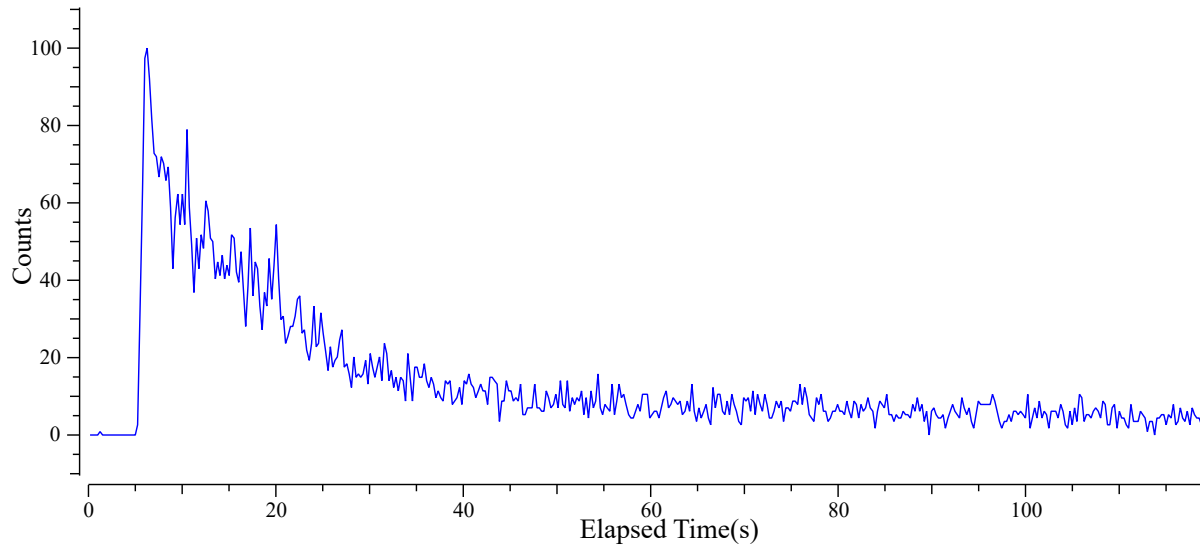

Figure 4.1: The extracted ion profile of α-T ($[M + H]^+$, *m/z* 431.388) by SFE-MVCI MS, corresponding to Figure 4.2 (top).

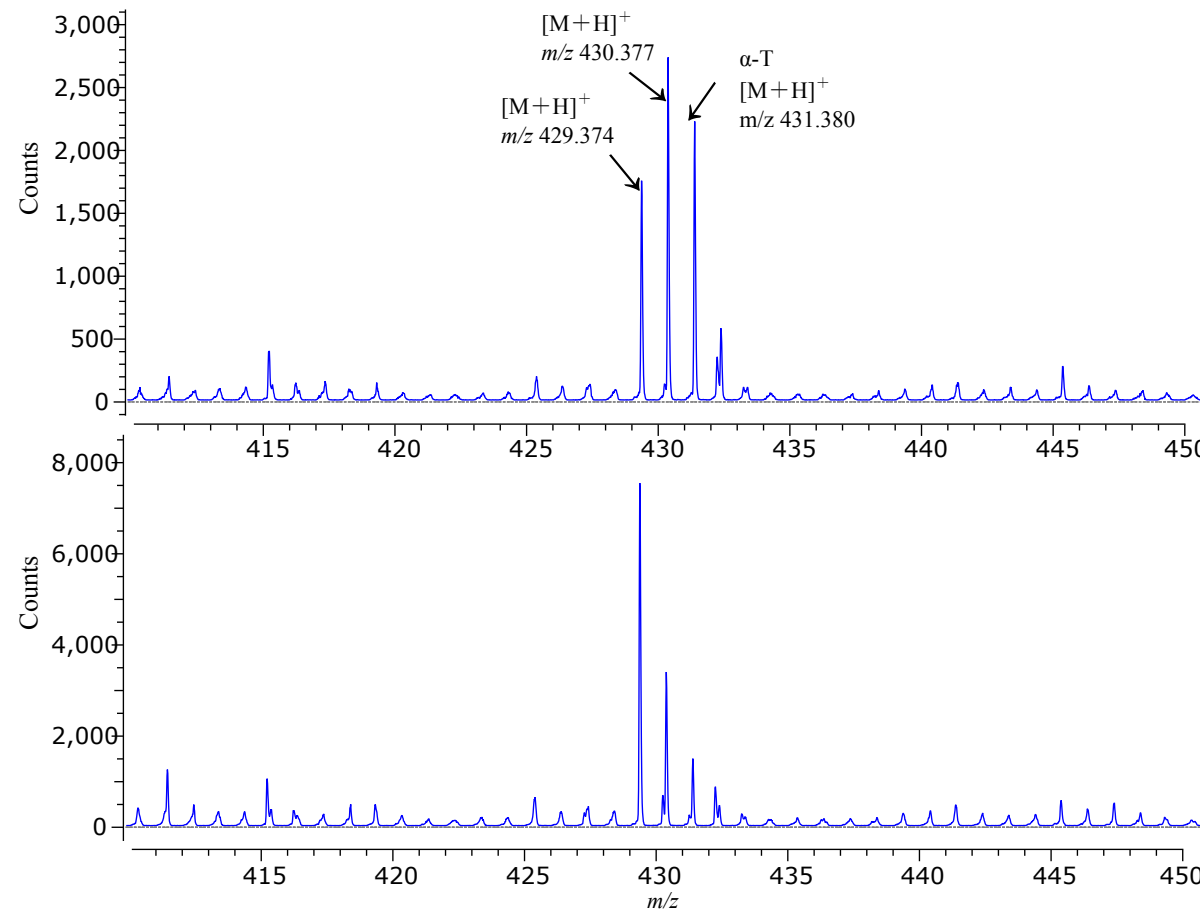

Figure 4.2: Comparison of α-T SFE-MVCI MS spectra acquired on 2021-06-14 (top) and 2021-06-15 (bottom). Each spectrum was obtained by co-added a series of the spectrum in between 2 to 20 s on the SFE monitoring.

4.3.2　α-T の LC-ESI MS による測定

Figure 4.3 に，50 pmol α-T の LC-ESI MS で得られた *m/z* 430.381 の抽出イオンクロマトグラムを示す．得られた α-T 溶出ピーク頂点のスペクトルを Figure 4.4 (上）に示す．Figure 4.4（下）は，後述する SFE-MVCI MS により得られた α-T 質量スペクトルである．Figure 4.4（上）に示す通り，α-T クロマトグラムのピーク頂点の質量スペクトルからは，*m/z* 430.4 が最大強度であることがわかる．また，α-T の $[M-H]^+$　に対応する *m/z* 429.4 にもピークが確認できる．*m/z* 431.4 にみられるピークは，*m/z* 430.4 のピーク強度の 26%（理論計算値は 32%)

であることから，*m/z* 430.4 をモノアイソトピックピークとする分子の +1 同位体と考えるのが妥当である．すなわち，α-T のプロトン付加分子は生成していないか，生成していたとしても量的に極めて少ないと考えられる．注目すべきは，*m/z* 447.4 に観測されるピークで，これは α-T 酸化過程で生成することが報告されている[15] 5-formyl-γ-tocopherol (5-f-γ-T) のプロトン付加分子であると考えられる．LC-ESI MS で得られた質量スペクトル上のピーク *m/z* 429.4, 430.4, および 447.4 それぞれの抽出イオンクロマトグラムを Figure 4.5 に示す．これら 3 種のイオンは，保持時間が一致していることから，いずれも ESI イオン化の過程で生成したイオンと考えられる．特に，*m/z* 447.4 に観測される 5-f-γ-T は，α-T が酸化を受ける過程で生成する化合物であることが報告[15,16] されており，同じ構造を持つ分子が ESI イオン化の過程でも生成している様子がうかがえる．

4.3.3　α-T の ESI および MVCI MS スペクトルの比較

4.2.1節に示した手順で調整した α-T 10 µmol·L^{-1} アセトン溶液 0.2 µL を，SFE-MVCI MS で測定し，得られた溶出ピークから得られた質量スペクトルを，Figure 4.4（下）に示す．先に述べた通り，同図（上）は LC-ESI MS により得られた質量スペクトルである．LC-ESI MS では，α-T 由来のイオンは，*m/z* 430.4, 429.4 に観測され，同時に 5-f-γ-T のプロトン付加分子も観測された．これに対して，SFE-MVCI MS では，α-T のプロトン付加 *m/z* 431.4 が最大強度と観測され，また，α-T ラジカルカチオン *m/z* 430.4 も観測された．SFE-MVCI MS 法は，クロマトグラフィー分離を伴わないため，試料中の夾雑物と思われるピークもみられるものの，少なくとも 5-f-γ-T は確認できなかった．

Tang ら[15]，および Kumar ら[16] によると，α-T の一重項酸素 ($^1O_2$) による酸化の過程で最初に生成される分子は，α-T ラジカルであることが確認されている．このことから類推すると，MVCI および ESI イオン化の過程で類似の反応が起こり，α-T のラジカルカチオンが生成したことが考えられる．3章に述べた通り，MVCI MS のネガティブイオンモード測定では，α-T 由来のラジカルイオンは確認されなかった．SFE-MVCI MS で観測される α-T の $[M + H]^+$ および $M^{+\bullet}$ が測定試料中に異なる分子として存在していたものか，イオン化の過程で生成したものかについては，クロマトグラフィー分離を行っていないため，判断できない．

4.4　結言

α-T について LC-ESI MS と SFE-MVCI MS で得られた質量スペクトルを比較した．SFE-MVCI MS で得られた質量スペクトルからは，*m/z* 429.4, 430.4, 431.4 にピークが確認され，この 3 種の強度比は試料調製からの経過時間に依存して大きく変化することが判明した．α-T 試料調製直後に測定した MVCI イオン化による質量スペクトルでは，α-T プロトン付加分子 *m/z* 431.4 が最大強度で得られ，α-T ラジカルカチオンと考えられる 430.4 も確認された．しかしながら，α-T 試料調製直後に測定した質量スペクトルからは *m/z* 429.4 ($[M-H]^+$) は確認できなかった．

LC-ESI MS では α-T のラジカルと考えられる *m/z* 430.4 の抽出イオンクロマトグラムの保持時間 667.9 s にピークが確認できた．同時に，α-T の $[M-H]^+$, ラジカルカチオン ($M^{+\bullet}$), および 5-f-γ-T のプロトン付加分子に対応する，それぞれ *m/z* 429.4, 430.4, および 447.4 が確認された．これらの抽出イオンクロマトグラムから，いずれも同一の保持時間に溶出が見られたことから，ESI イオン化過程で生成したものと考えられる．とりわけ，5-f-γ-T は，α-T 酸化過程で生成することが報告されており[15]，同様の反応が ESI 過程でも生じていることは興味深い．また，MVCI イオン化では，この 5-f-γ-T に該当するイオンは確認されなかった．

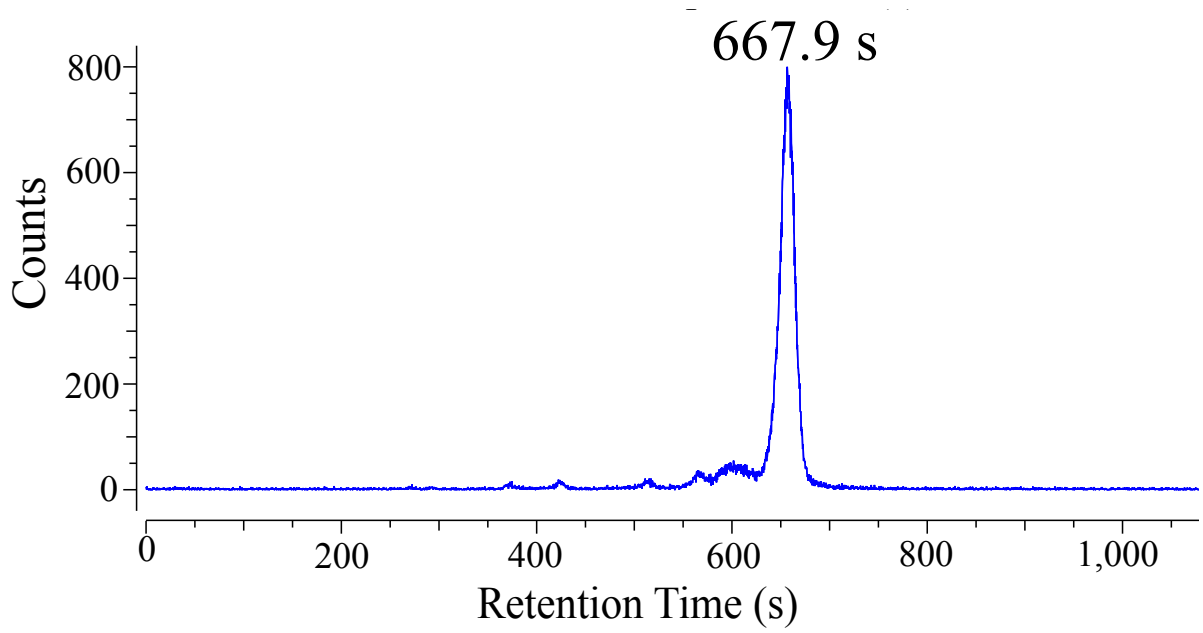

Figure 4.3: The extracted ion chromatogram of α-T radical ($M^{+\bullet}$, *m/z* 430.381) by LC-ESI MS. Fifty picomole of α-T (1 µL) were injected into the column. A retention time for α-T was 667.9 s, the asymmetry factor was 0.88, and the theoretical plate was 10 210. Chromatographic conditions are described in the text.

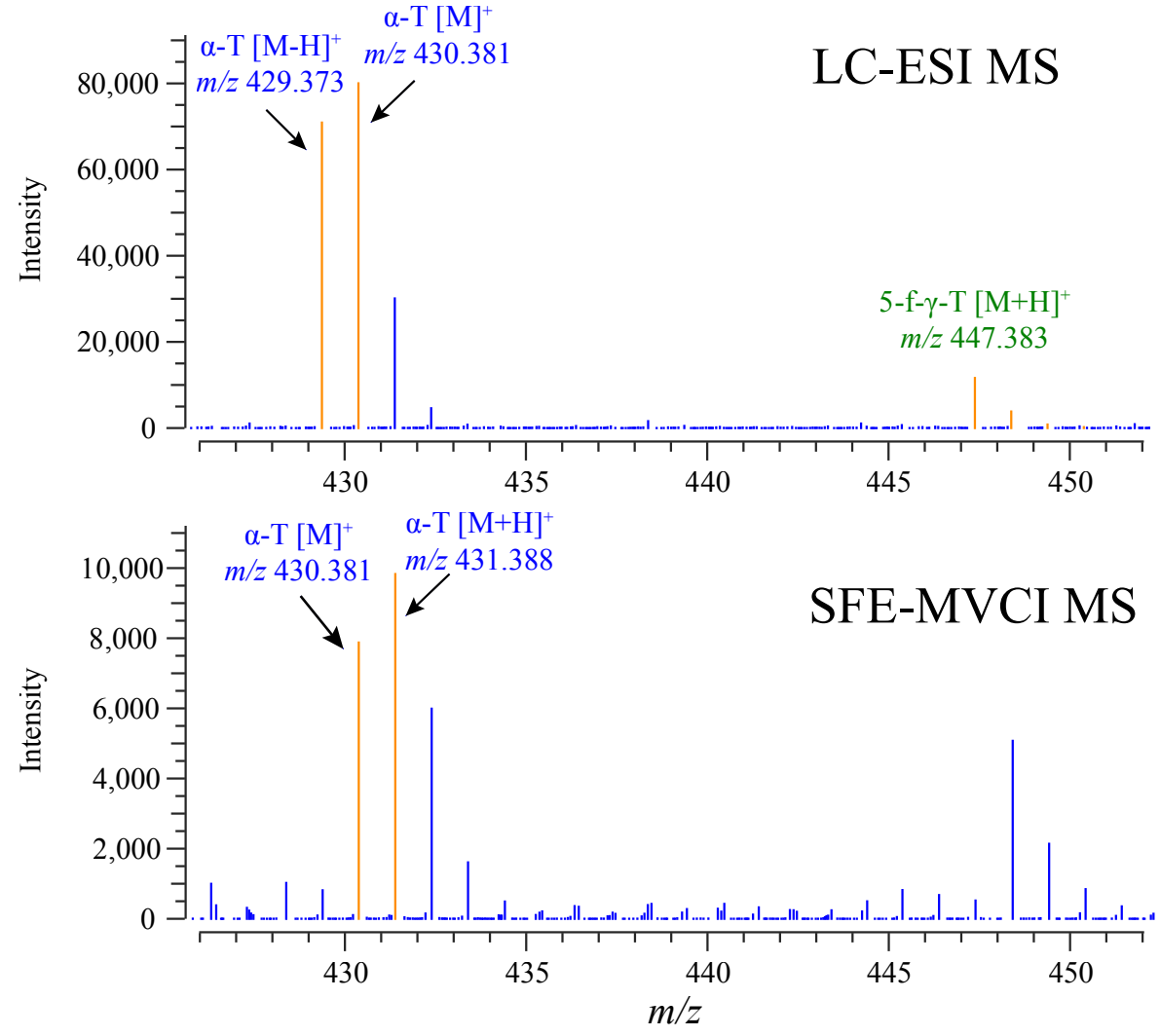

Figure 4.4: Comparison of α-T mass spectra acquired on LC-ESI MS (top) and SFE-MVCI MS (bottom). Top: LC-ESI MS spectrum of α-T obtained from retention time of 669.7 s on Figure 4.3. Bottom: SFE-PTR MS spectrum of α-T obtained from the apex on the SFE profile of *m/z* 431.388.

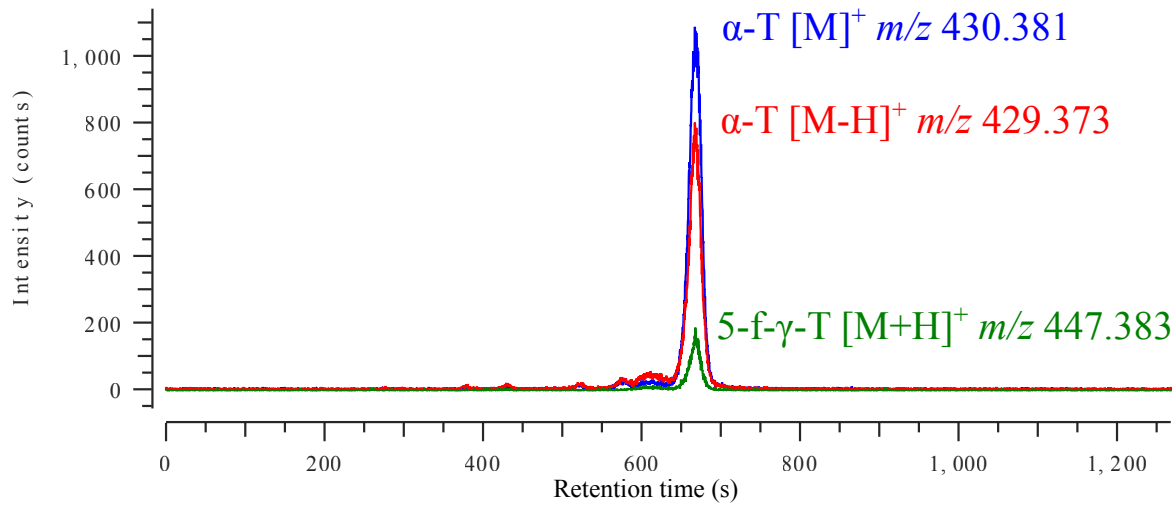

Figure 4.5: Overlay extracted ion chromatograms of α-T derived ions of $[M-H]^+$, $M^{+\bullet}$; and protonated 5-formyl-γ-tocopherol obtained from LC-ESI MS chromatogram, described in Figure 4.3.

参考文献

[1] Moate, P. J.; Boston, R. C.; Jenkins, T. C.; Lean, I. J. *J Dairy Sci* 2008, **91**, 731–742.

[2] Katiyar, S. S.; Cleland, W. W.; Porter, J. W. *J Biol Chem* 1975, **250**, 2709–2717.

[3] Hou, J.; Reid, N. E.; Tromberg, B. J.; Potma, E. O. *Biophysical Journal* 2020, **119**, 258–264.

[4] Clausen, M. R.; Mortensen, P. B. *Gastroenterology* 1994, **106**, 423–432.

[5] Ruppe, S.; Mains, K.; Fox, J. M. *Proc. Natl. Acad. Sci. U.S.A.* 2020, **117**, 23557–23564.

[6] Rand, A. A.; Barnych, B.; Morisseau, C.; Cajka, T.; Lee, K. S. S.; Panigrahy, D.; Hammock, B. D. *Proc. Natl. Acad. Sci. U.S.A.* 2017, **114**, 4370–4375.

[7] Liu, Y.; Roth, J. P. *Journal of Biological Chemistry* 2016, **291**, 948–958.

[8] Nakatani, K.; Izumi, Y.; Hata, K.; Bamba, T. *Mass Spectrometry* 2020, **9**, A0080–A0080.

[9] Mottier, P.; Gremaud, E.; Guy, P. A.; Turesky, R. J. *Analytical Biochemistry* 2002, **301**, 128–135.

[10] Cela, J.; Tweed, J. K. S.; Sivakumaran, A.; Lee, M. R. F.; Mur, L. A. J.; Munné-Bosch, S. *Plant Physiology and Biochemistry* 2018, **127**, 200–210.

[11] Tomai, P.; Bosco, C. D.; D'Orazio, G.; Scuto, F. R.; Felli, N.; Gentili, A. *Journal of Chromatography Open* 2022, **2**, 100027.

[12] Hryniewicka, M.; Karpinska, A.; Kijewska, M.; Turkowicz, M. J.; Karpinska, J. *Journal of Mass Spectrometry* 2016, **51**, 1023–1029.

[13] Lauridsen, C.; Leonard, S. W.; Griffin, D. A.; Liebler, D. C.; McClure, T. D.; Traber, M. G. *Analytical Biochemistry* 2001, **289**, 89–95.

[14] Hinchliffe, E.; Rudge, J.; Reed, P. *Ann Clin Biochem* 2016, **53**, 434–445.

[15] Tang, C.; Tao, G.; Wang, Y.; Liu, Y.; Li, J. *J. Agric. Food Chem.* 2020, **68**, 669–677.

[16] Kumar, A.; Prasad, A.; Pospíšil, P. *Sci Rep* 2020, **10**, 19646.

第 5 章

Rapid analysis of α-tocopherol and its oxidation products using supercritical carbon dioxide and proton transfer reaction ionization mass spectrometry.

We have developed a rapid and sensitive analytical method for α-tocopherol and its oxidative products by using supercritical fluid extraction (SFE) online supercritical fluid chromatography (SFC) with proton-transfer-reaction (PTR) ionization mass spectrometry (MS). α-Tocopherol is a well-known antioxidant that plays a vital role in the antioxidant defense system in a plant cell. However, the study of its mechanisms in a cell is limited due to the lack of a rapid analytical method. It requires complex sample preparation and long chromatography separation time. Additionally, most molecules involved are a combination of isomers, which must be separated before applying the tandem mass spectrometry. α-Tocopherol produces α-tocopheroxyl radical as the first step of antioxidant action; the ion with the same mass may also be generated in-source. Separation by SFC effectively distinguished them from their oxidative products in the sample and produced on the fly in-source. This method enabled the measurement of α-tocopherol and oxidative products such as α-tocopheroxyl radical and α-tocopheryl quinone with a throughput of about 3 min per sample, including sample preparation.

5.1 Introduction

Since its development by Lindinger *et al.* [1] in the late 1990s, proton transfer reaction (PTR) mass spectrometry (MS) has been used as a susceptible method for measuring volatile organic compounds (VOCs) in gaseous samples. It has been used for a wide variety of applications involved in VOCs, such as volcanic gases, forest fires, the metabolite analysis of breath, identification of microorganisms, and so forth [2–6]. In addition to it, we have expanded the application area for non-volatile molecules by using a supercritical fluid as a mobile phase that effectively transports the analyte molecules into the PTR MS [7].

Supercritical fluid extraction (SFE) is a rapid and safe method for extracting lipophilic compounds from a complex sample matrix. Still, it can also extract polar molecules using an entrainer when applicable. It was developed by Zosel

Reprinted with permission from
C. Ota, T. Hondo, Y. Miyake, H. Furutani, M. Toyoda *Mass Spectrometry* (2022). https://doi.org/10.5702/massspectrometry.A0108.

in the 1970s[8], and it has been applied for industrial-scale extraction of food and fine chemicals since carbon dioxide, the most common fluid for SFE, is safe to use in foods. The supercritical fluid dissolves compounds selectively by changing the temperature, pressure, and modifiers that can transport a range of molecules to another vessel, which is convenient for industrial-scale extraction and analytical scale sample preparation.

Since supercritical fluid has a lower viscosity than liquid and an almost identical density to liquid, SFC has higher separation efficiency than liquid chromatography (LC). Thus, it has also been used for the optical separation of racemic compounds[9] and the steroids[10] where they are hard to optimize the separation in LC. By combining SFE and SFC, unique applications such as bioactive lipids in aqueous solution were also reported[11]. In recent years, significant advances in fluid control technology have led to new developments such as ultrafast separation by SFC[12,13].

Plant cells have several self-defense mechanisms for antioxidation enzymatically and non-enzymatically. In particular, α-tocopherol (α-T) is the well known to prevents lipid peroxidation[14–16]. The α-T oxidization reaction scheme reported by Kumar *et al.*[17] and Tang *et al.*[18] was summarized in Figure 5.1. The log P values indicated in the figure were calculated using a function on the Crippen module in the RDKit[19]. Kumar *et al.* investigated the formation of α-tocopheroxyl radical and α-T-hydroperoxide by thylakoid membrane and rose bengal as singlet oxygen ($^1O_2$) source. They used a combination of analytical instruments such as LC with a photodiode array (PDA) detector, fluorescence spectroscopy, and electron paramagnetic resonance (EPR) spectrometry to detect α-tocopherol hydroperoxide, α-T-radicals and $^1O_2$. A key role of α-T is quenching $^1O_2$ rapid enough before the fatty acids oxidize. Tang *et al.* reported the detailed chemical structure of α-T oxidization products using LC-PDA detection coupled with quadrupole time-of-flight mass spectrometry.

Although the details of the self-defense system of plant cells against $^1O_2$ by α-T are recently being determined by combining several analytical methods, the analytical process requires complex procedures and over 30 min of a chromatographic run. It is desired to be a more rapid and sensitive method for investigating the defense system in individual cells. In addition, oxidation is progressing in the ambient; therefore, the sample processing needs to be done as quickly as possible to avoid artifacts.

As we have reported, SFE-PTR MS also detects non-volatile small molecules with high sensitivity, at least up to *m/z* 1000 so far tested. Adding chromatography separation to the SFE-PTR MS improves the analytical efficiency, such as the separation of isomers and better detection sensitivity. We further evaluated our PTR flow tube prototype, which observed about 2 s of longitudinal peak dispersion, practically applicable to the SFC, which makes a narrow peak width in general. In this study, we have investigated a preparation-free rapid analysis of α-tocopherol (α-T) and its oxidation products by SFE/SFC-PTR MS.

5.2 Experimental

5.2.1 Chemicals

α-T, Hexamethoxyphosphazine (P321), Hexakis (2,2-difluoroethoxy) phosphazene (P621), ethanol, acetonitrile (LC/MS grade) were purchased from FUJIFILM Wako Pure Chemicals Corporation, Osaka, Japan. Water was obtained from a Milli-Q Purification System (Merck, Germany). A cylinder of general grade helium and carbon dioxide (siphon type) (Iwatani Industrial Gases Corp, Osaka, Japan) was used.

The purchased α-T was stored in the dark at −80 °C until use. Purchased α-T samples were prepared as a 10 µmol·L^{-1} acetonitrile solution in 1 mL total volume without further purification and used after incubation at room temperature (25 °C) in Eppendorf sample tubes for a given period as needed.

InertSustain C18 3 µm, 1.0 mm inner-diameter (i.d.)× 30 mm length (GL Science, Tokyo, Japan) (InertSustain), and L-column3 C18 3 µm, 2.1 mmi.d.× 100 mm length (CERi, Chemicals Evaluation and Research Institute, Saitama, Japan) (L-column3) were used for SFC separation.

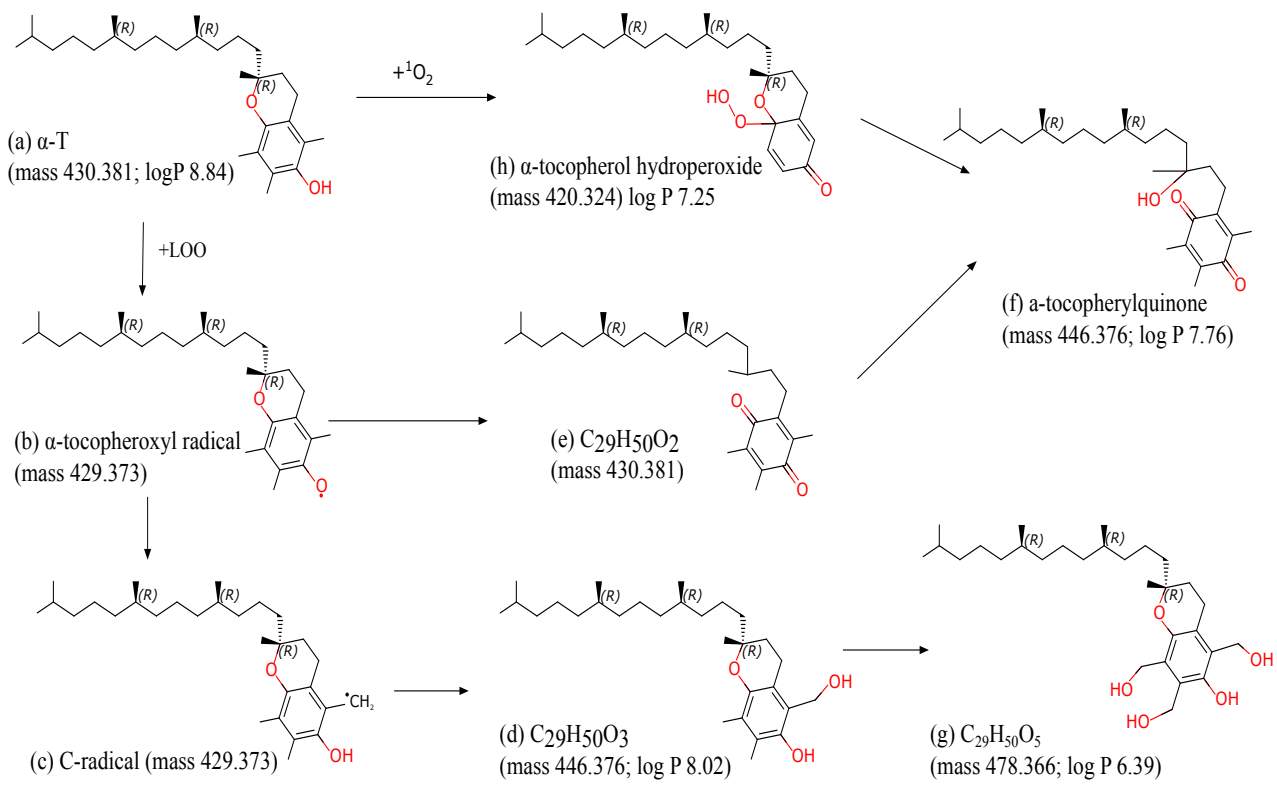

Figure 5.1: Oxidative reaction schematics of α-tocopherol described in the literature. The log P values were calculated using a function on the Crippen module in the RDKit[19)]

.

5.2.2 Mass spectrometer

A JMS-T100 LP (AccuTOF) time-of-flight (TOF) mass spectrometer (JEOL, Tokyo, Japan) was used with a minor modification, which altered the data acquisition system to an Acqiris Model U5303A ($3.2\,\mathrm{GS}\cdot\mathrm{s}^{-1}$ 12-bit digitizer, Geneva, Switzerland). Data acquisition was carried out using open-source software "QtPlatz" (https://github.com/qtplatz/qtplatz) with a modified field programmable gate array (FPGA) configuration for acquiring "peak detection" (PKD) and waveform averaging (AVG) simultaneously[20)]. The PKD histogram and AVG waveform were taken from the U5303A every 200 ms.

Figure 5.2 illustrates the PTR ion source block diagram, which consists of a flow tube with a corona discharge electrode. Helium was connected to a flow tube after passing through a 250 mL volume of the solvent-reservoir bottle, which contained $\approx$10 mL of ultrapure water (Millipore, MA, US). The helium flow rate was set to $70\,\mathrm{mL}\cdot\mathrm{min}^{-1}$, which was controlled by a mass flow controller (8500MC-0-1-2, KOFLOC Corp., Kyoto, Japan). The pressure of the flow tube was maintained in a range of 90 to 105 Pa by an AccuTOF vacuum system. The model PS350 high voltage power supply (Stanford Research Systems, Inc. Sunnyvale, CA, US) was used as a corona discharge power supply. The voltage for the discharge electrode was set to -2.0 kV, which resulted in 80 to 100 µA of current.

5.2.3 SFE/SFC splitless injection

Figure 5.3 shows the hydraulics of splitless injection. Liquid carbon dioxide from a cylinder was pre-cooled to $-5\,^\circ$C in an ethanol/dry ice bath and delivered for $0.5\,\mathrm{mL}\cdot\mathrm{min}^{-1}$ at 25 MPa with an LCPackings UltiMate Micropump (Thermo Scientific, US), then equilibrated to 40 °C in an oven (Agilent 1100 Series Thermostatted Column Compartment (Agilent, CA, US)) and connected to an SFC column of InertSustain. The outlet from the column was connected to a PTR flow tube passed through a 20 µm i.d. $\times$ 25 mm length fused silica capillary (GL

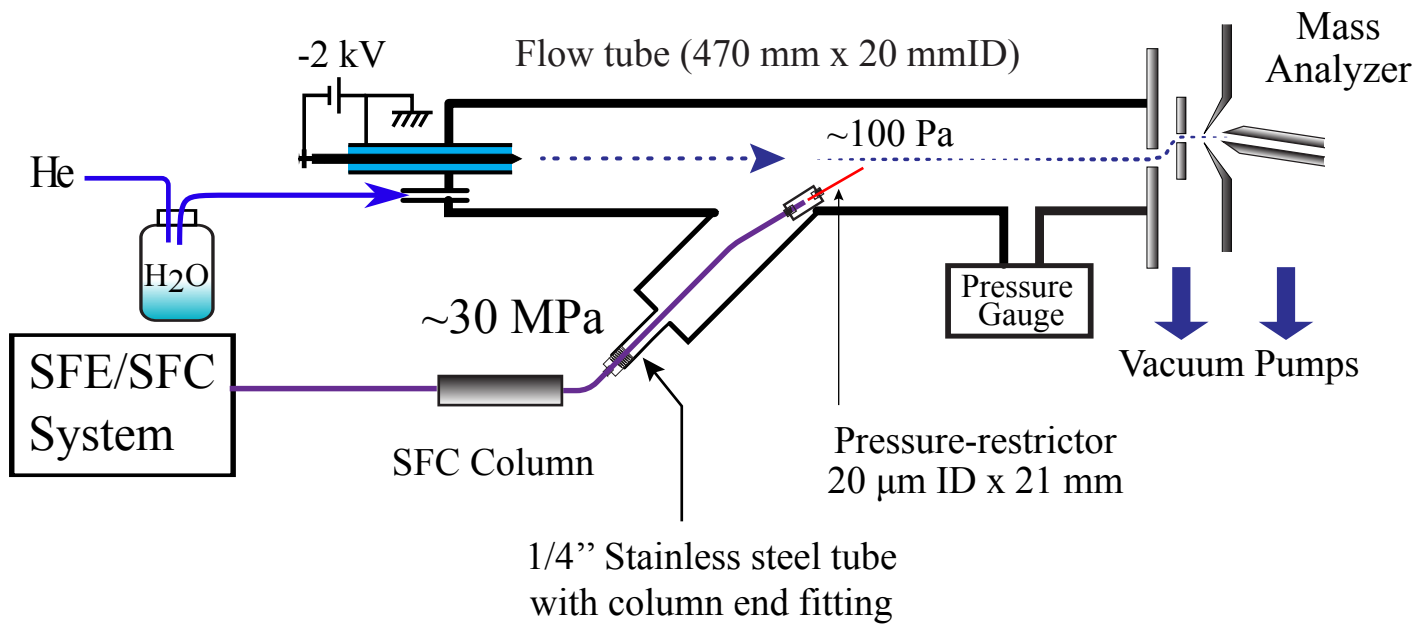

Figure 5.2: Schematics of PTR flow tube.

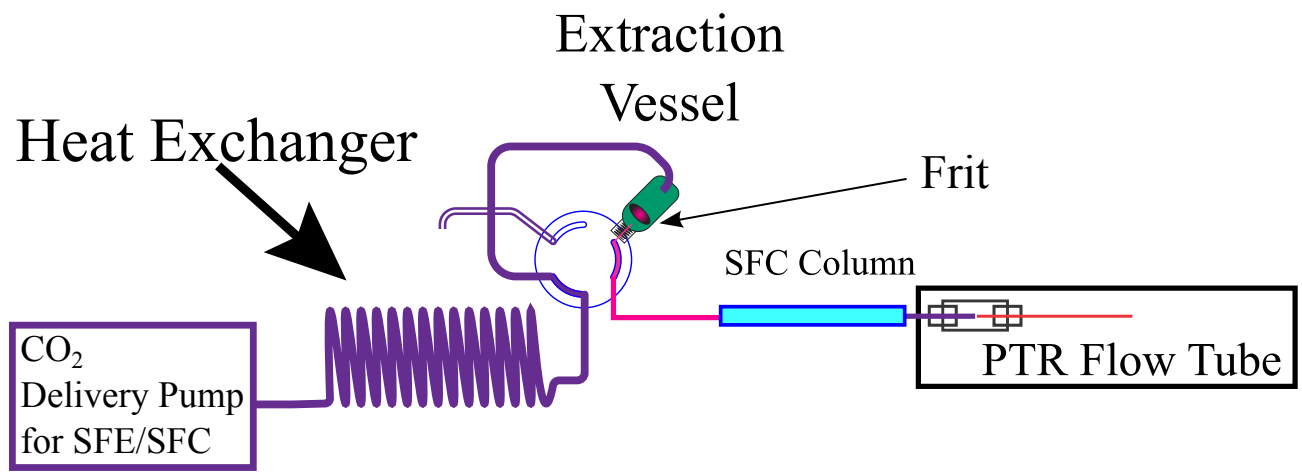

Figure 5.3: Hydraulics of SFE/SFC with the splitless injection.

Science, Tokyo, Japan) as a pressure restrictor.

The sample dissolved in acetonitrile was applied on the stainless steel frit, waited for the evaporate acetonitrile, and then attached to an in-line filter (ACQUITY Column In-Line Filter (Waters, US)) and introduced into the SFC flow by switching the valve (Rheodyne 7000, Rheodyne, USA) position.

5.2.4　SFE/SFC split injection

Figure 5.4 shows the hydraulics of SFE/SFC split injection, where SFE and SFC have independent CO_2 delivery systems. In the SFE hydraulics, liquid carbon dioxide from a cylinder was pre-cooled to −5 °C in an ethanol/dry ice bath and delivered for 200 µL/min at 25 MPa with an LCPackings UltiMate Micropump. Carbon dioxide from the pump was equilibrated to 40 °C in an oven and then passed through Rheodyne 7000 switching valves V1 and V2, and then went to the waste through a 20 µm i.d. × 250 mm length pressure restrictor.

In the SFC hydraulics, liquid carbon dioxide was pre-cooled to −5 °C in an ethanol/dry ice bath and delivered for 1.0 mL · min^{-1} at 30 MPa by a PU-980 pump (JASCO, Tokyo, Japan), equilibrated to 40 °C in an oven, and connected to the separation column via valve V2. The mobile phase from the column was connected to a pressure restrictor in the PTR flow tube. This method used either an InertSustain or an L-column3 for SFC separation. SFC hydraulics shared V2 with the SFE hydraulics, in which the 1 µL portion of the fluid is split and introduced into the column. The

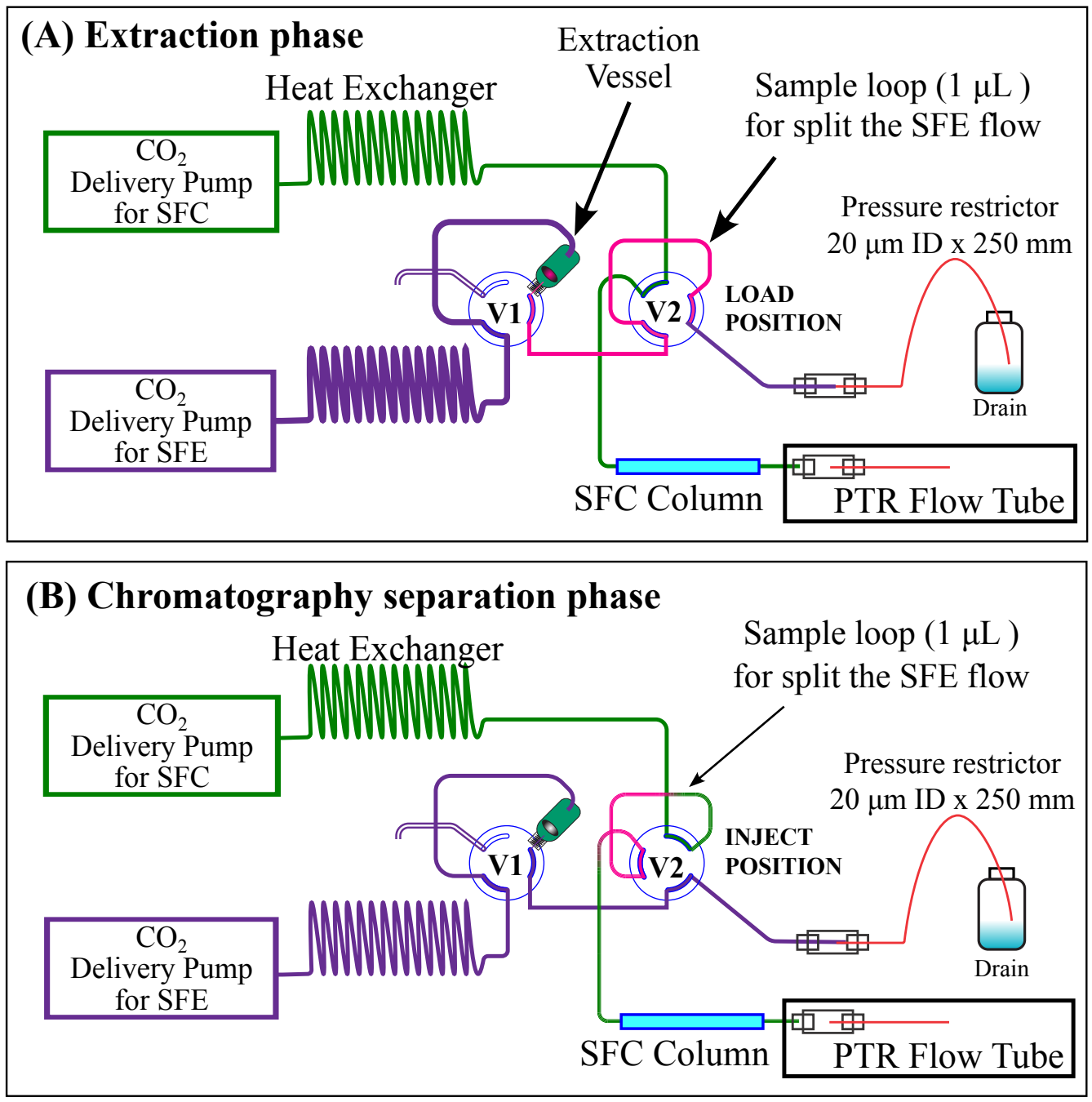

Figure 5.4: Hydraulics of SFE/SFC with the split injection.

CO_2 flow rate, temperature, pressure, and timing of the split since SFE starts may affect the composition and amounts of the sample to be injected.

All pump heads for CO_2 delivery were cooled to approximately 8 °C by a Peltier module (TES1-12705, Hebei, China).

5.2.5 Mass calibration

Mass calibration was performed using sodium trifluoroacetate, an electrospray ionization (ESI) source for *m/z* between 159 and 703 and third-order polynomials. The PTR ion source was then attached by altering the ESI source.

5.3 Results and Discussion

5.3.1 SFE/SFC analysis of α-T incubate

The α-T incubates for 0, 1, and 7 days of incubation at ambient temperature (≈25 °C) was applied to SFE/SFC splitless injection analysis applied each of five pmol equivalents of α-T. The obtained extracted ion chromatograms for

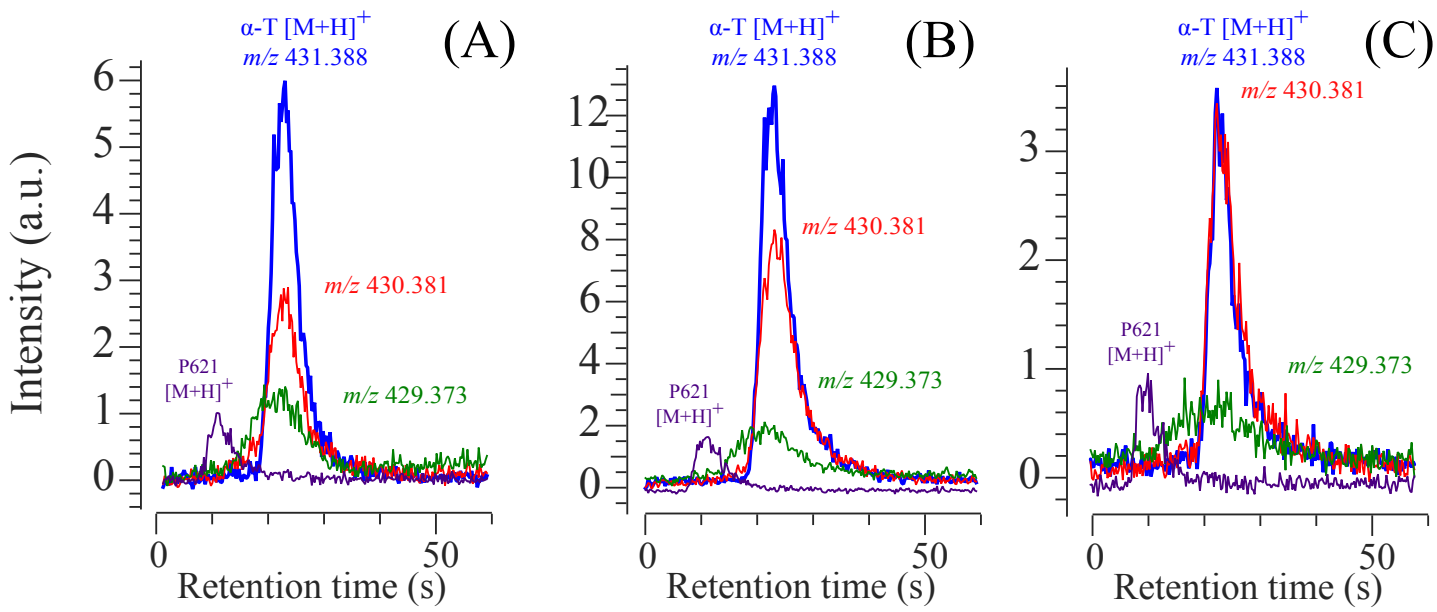

Figure 5.5: Extracted ion chromatograms of α-tocopherol and suspected oxidative products analyzed by splitless injection. A: freshly prepared sample, B: sample incubated for a day at ambient, and C: sample incubated for seven days at ambient temperature. Each of the 5 pmol equivalents of the α-T sample was applied on the frit. SFC condition: InertSustain C18, mobile phase: CO_2 0.5 mL/min, 25 MPa.

m/z 431.388, 430.381, and 429.373, which correspond to $[M+H]^+$, $[M]^+$, and $[M-H]^+$ of α-T respectively were shown in Figure 5.5. An *m/z* 431.388 chromatogram in each of (A), (B), and (C) shows a single chromatographic peak with the highest intensity. The relative intensity of *m/z* 430.381 is drastically changed as a course of the incubation period. Although an *m/z* 429.373 chromatogram shows a broad peak on all three chromatograms, the retention time seems to be moving forward, giving a shorter retention time. As shown in Table 6.1, the relative peak area for *m/z* 430.381 over 431.388 increased to folds of 1.45 and 2.20 for 1 and 7 days incubation, respectively. The relative peak area of *m/z* 430.381 significantly changed, though no apparent chromatographic changes such as separation and retention factor changes were obtained. Since Figure 5.1 suggested that many of the reported oxidative products may have the *m/z* 430.381 and 431.388 if they are protonated, obtained chromatographic peak consists of a couple of co-elute. To discover those molecules, better chromatography separation seems to be required.

An extraction vessel has a volume of approximately one microliter, which is small enough to make a narrow peak bandwidth compatible with SFC. However, chromatographic peaks were obtained between three to five seconds of peak width (Table 6.1 during the SFE process and additional molecule-specific extraction delay. Each molecule goes into the column as a slightly separated series of bands, each of which has a few seconds of peak width. An easy and effective method is split injection to make a narrow sample bandwidth introduced to SFC to get better peak resolution.

5.3.2 Determination of split timing

As described in the previous section, SFE extraction profiles show a peak with a few seconds of width. The best timing for splitting an SFE flow is to find a peak apex point; however, an apex timing depends on both molecule and SFE conditions. Therefore a compromised timing for the given sample matrix needs to be determined experimentally. Figure 5.6 shows a series of sample injections splitting SFE flow into SFC hydraulics without a separation column. An extracted ion profile monitored at *m/z* 431.388 gave the best split timing of 20 s, which offers the most intense peak. However, a profile monitored at *m/z* 430.381 and 429.373 gave the most intense peak at 10 s split timing. Since

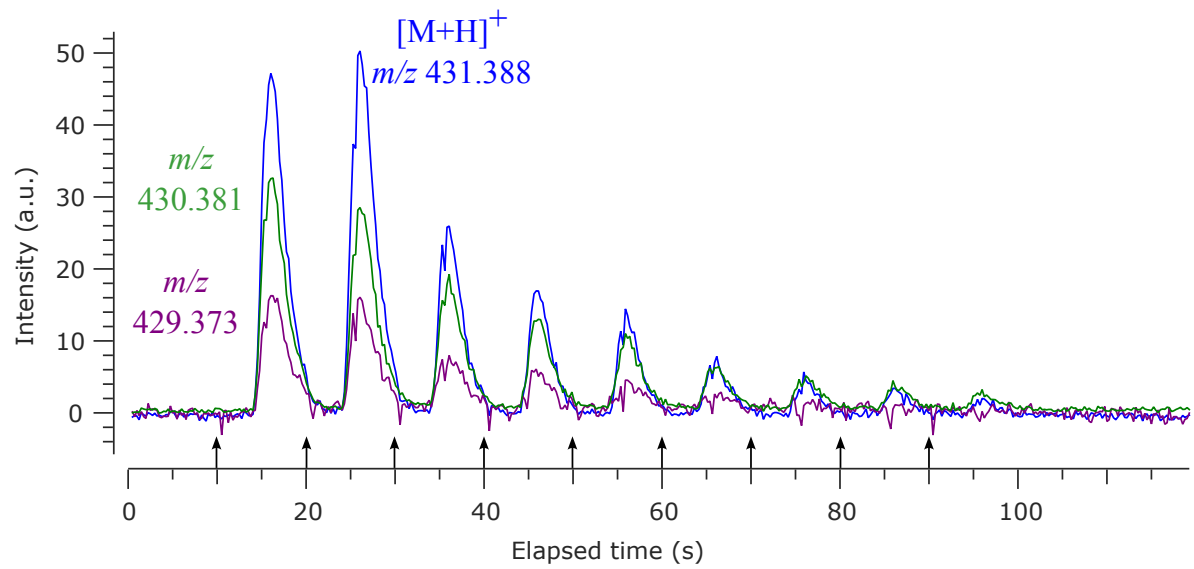

Figure 5.6: Determination of the split timing after SFE start. Time course of peak intensity by 1 µL split injection since SFE starts without a column.

peak intensity for *m/z* 431.388 at 10 and 20 s has no significant difference, we determined the 10 s split timing for further experiments.

5.3.3 Comparison of chromatograms of splitless and split injection.

Figure 5.7 shows a chromatogram of 10 pmol equivalents of α-T sample using split injection, which corresponds to Figure 5.5 (B). An extracted ion chromatogram for *m/z* 431.388 shows a single peak at a retention time of 15.1 s with a width of 2.7 s, which is half the peak width obtained compared to splitless injection. A chromatogram for *m/z* 430.381 gave a peak with the same retention time with *m/z* 431.388; however, it also shows an unresolved shoulder peak at 11.15 s. Sample amounts applied to the frit for split injection were ten pmol, double the amounts of splitless injection (5 pmol) chromatogram; however, obtained peak intensity on split injection was about 30-fold larger than the peak heights on splitless injection chromatogram. It made us discover that the other ions are supposed to be oxidative products of α-T described in the literature, such as *m/z* of 445.368, 463.378, and 447.383. (See Figure 5.1).

5.3.4 Separation of α-T oxidative products

Although split injection shows drastic improvement in column efficiency compared to splitless injection, extracted ion chromatograms for *m/z* 429.373 and 430.381 shows an unresolved peak. The molecules that appeared on the same *m/z* need to be resolved on chromatography to apply the tandem mass spectrometry technique to select a precursor ion effectively. We have further evaluated using L-column3 C18 that has 2.1 mm i.d. with 100 mm length. Figure 5.8 shows α-T chromatograms using L-column3 with split injection applied ten pmol equivalents of α-T sample on the SFE frit. Extracted ion chromatograms for *m/z* 430.381 and 431.388 for freshly prepared α-T sample are shown at the bottom. No chromatographic peak at *m/z* 429.373, 447.383, or 445.368 was detected from this sample. In contrast, we have seen several chromatographic peaks at extracted ion chromatograms for masses supposed to appear α-T oxidative products. The peak parameter for all detected peaks was listed in Table 6.2, and the mass spectra taken at the peak apex were illustrated in Figure 5.9.

An ion appeared at *m/z* 430.381, which corresponds to α-T-radical seems always shown together with protonated α-T ion at precisely the same retention time without exception. Therefore it might be generated during the PTR process. However, chromatographic peaks at retention times of 40.9, 57.1, and 62.0 s on *m/z* 430.381 are considered an incubation product.

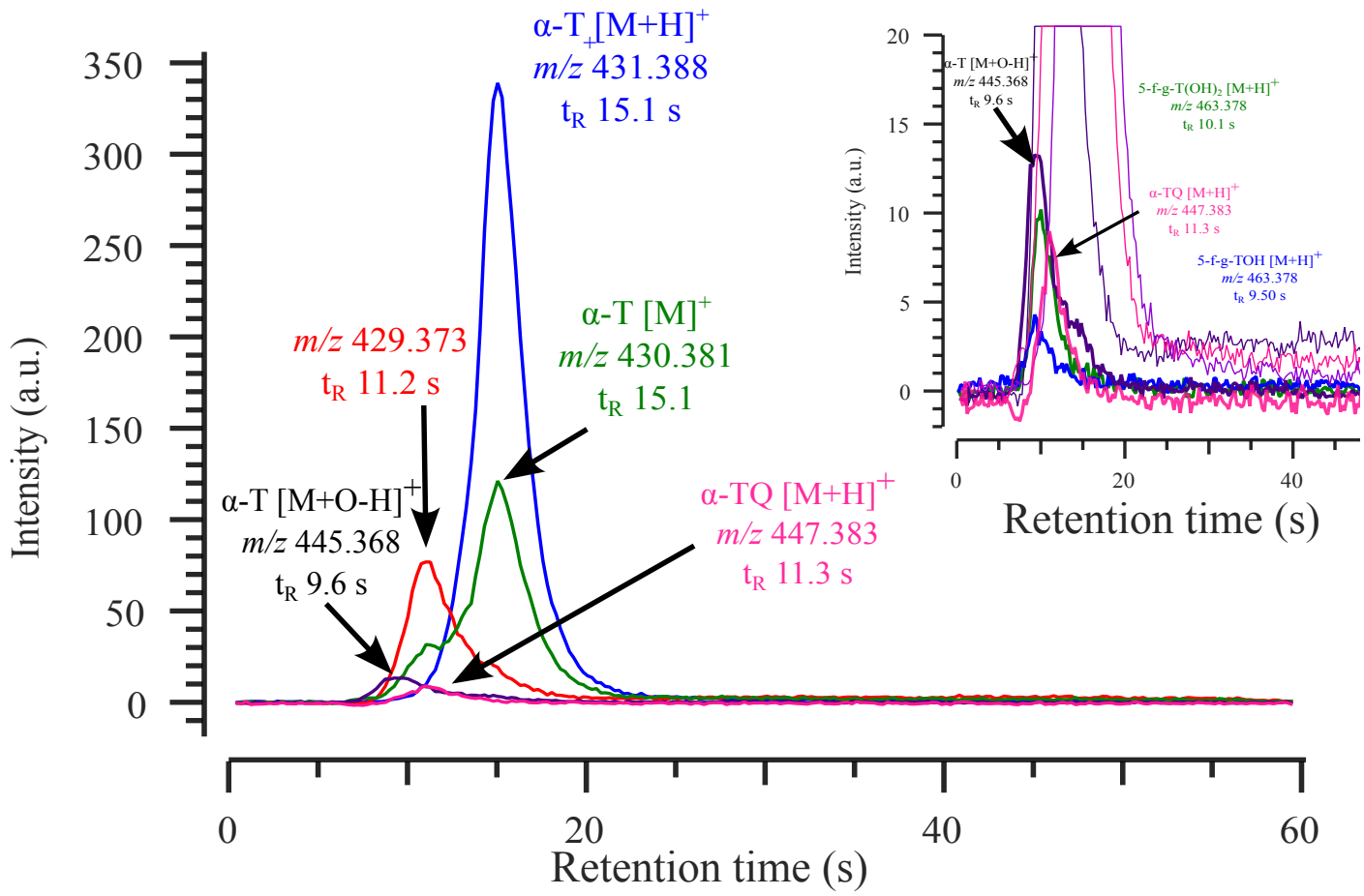

Figure 5.7: Extracted ion chromatograms of α-tocopherol and suspected oxidative products analyzed by split injection. 10 pmol equivalents of α-T applied on the frit. The inset is scaled on the vertical axis for visibility. SFE condition: 40 °C, 25 MPa, 200 µL · min^{-1}; SFC condition: InertSustain C18, mobile phase: CO_2 1.0 mL/min 25 MPa.

From the reaction schematics illustrated in Figure 5.1, the molecules of (B) and (C) gives *m/z* 430.381 if protonated. The molecules (D) and (F) provide *m/z* 447.383, where we have seen two peaks at retention times of 46.5 and 56.9. There is no evidence where those peaks correspond to (D) and (F); however, α-TQ (F) may have a shorter retention time compared to (D) from a suggestion of logP value. For this reason, 46.5 s peak at *m/z* 447.383 add a label as α-TQ.

There are two significant peaks on *m/z* 429.373 at 57.0 and 62.0, besides 82.5 s, though we do not have any information to assign them either (B), (C), or something else. Two peaks shown on *m/z* 430.381 at 57.1 and 62.0 s may be an isotope of *m/z* 429.373. A peak on *m/z* 449.399 at 82.8 s is possibly the α-tocopherylhydroquinone; one of the two peaks on *m/z* 479.373 might be (G), and one of the *m/z* 463.378 peaks might be 5-formyl-γ-tocopherol + OH according to Tang *et al.* [18].

All peaks that appear on the chromatogram of the same *m/z* are separated by the resolution (Rs) of 1.7 or better, which is possible to select precursor ions for tandem mass spectrometry. We keep working on reducing an instrumental dispersion at the PTR flow tube, which is currently about 2 s. We aim to minimize the dispersion by at least less than 1 s, where all peaks listed here will be fully resolved as of $Rs > 2.0$.

5.4 Conclusion

We have evaluated the SFE/SFC-PTR MS to separate α-T and its oxidative products that have a significant role as an antioxidant defense system in a plant cell during photosynthesis. The mechanism and reaction scheme of α-T antioxidant function have been recently investigated using multiple analytical instruments, including chromatographic

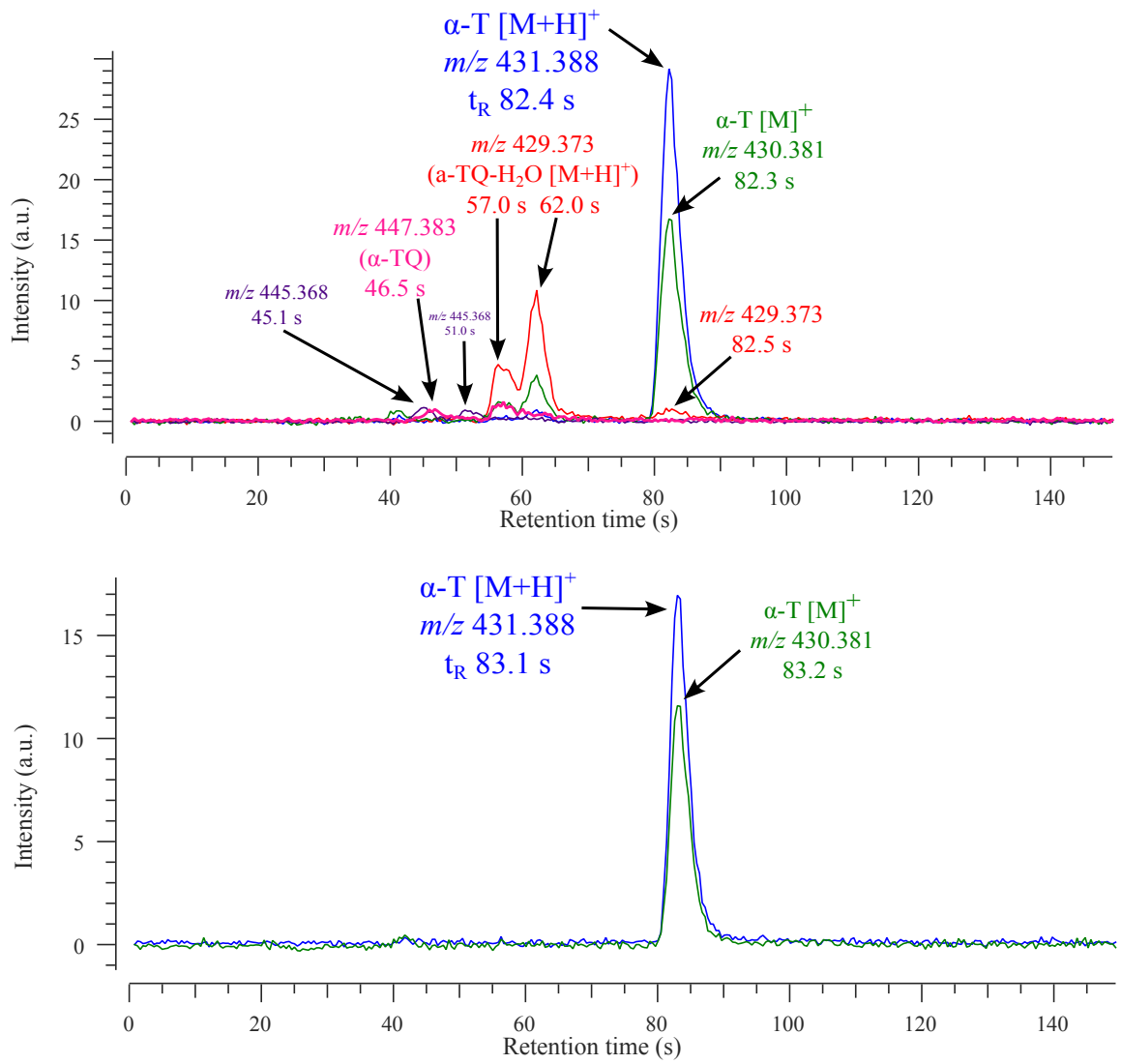

Figure 5.8: SFE/SFC split injection chromatograms of α-tocopherol (10 pmol) and suspected oxidative product separated on L-column3 C18 columns. Bottom plots are freshly prepared samples; top plots are samples incubated for twenty-one days at ambient temperature. SFE condition: 40 °C, 25 MPa, 200 µL · min^{-1}; SFC condition: L-column3 C18, mobile phase: CO_2 1.0 mL/min, 30 MPa.

separation and complex sample processing. Using an SFE combined with SFC and PTR MS, it has achieved nearly complete separation of isomers reported in the literature by less than 2 min of chromatography by simply applying the sample on the stainless steel frit. Identifying molecules with structure determination still requires using tandem mass spectrometry; the isomers must be separated before ionization to select precursor ions. The present study demonstrated that the SFE/SFC split injection could efficiently separate α-T oxidative products without dedicated sample preparation like solid phase extraction. It has achieved fast chromatography separation with high detection sensitivity. This method has excellent potential for analyzing complex sample matrices, including cells and tissues; it may help to detect molecules from a single cell or small amounts of tissues.

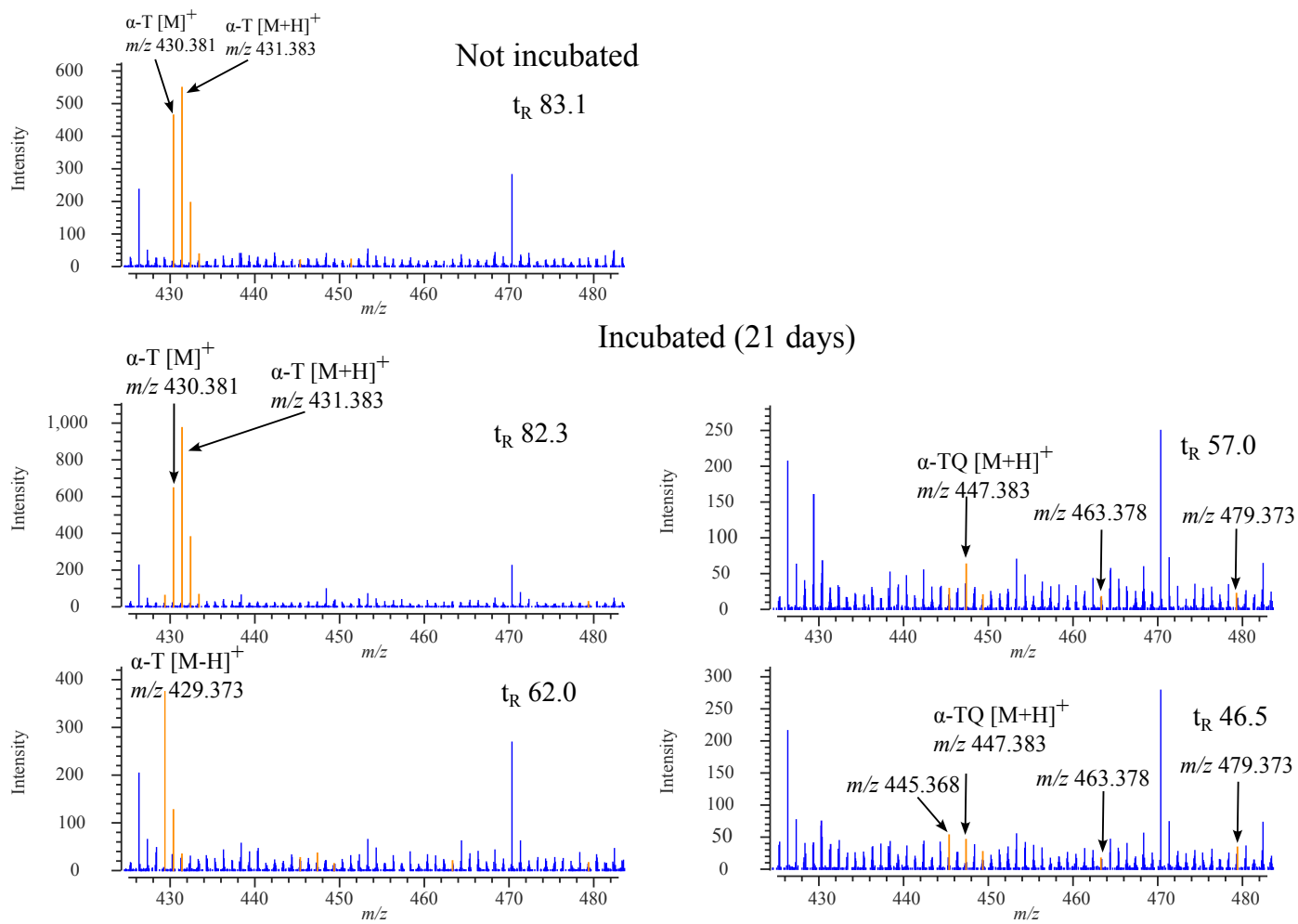

Figure 5.9: Mass spectra at peak apex on chromatograms shown in Figure 6.8.

Table 5.1: Peaks obtained from chromatograms shown in Figure 5.5

	m/z	t_R(s)	Area	Height	Width(s)	Area ratio (A/A_{431})	fold
A	622.029	11.20 ± 0.06	9.0 ± 2.6	1.45	4.07		
	431.388	23.1 ± 0.5	34.4 ± 2.0	5.38	5.04	n/a	n/a
	430.381	23.0 ± 0.4	18.8 ± 4.5	2.34	5.74	0.543	100.0 %
	429.373	22.6 ± 1.5	12.03 ± 0.01	1.25	6.58	0.351	100.0 %
B	622.029	12.1 ± 0.6	10.72 ± 0.68	1.73	4.79		
	431.388	23.0 ± 0.2	58.3 ± 26.3	9.24	5.25	n/a	n/a
	430.381	23.5 ± 0.3	48.4 ± 26.5	6.22	6.63	0.810	149.2 %
	429.373	22.1 ± 0.5	18.7 ± 8.6	1.60	6.71	0.319	91.0 %
C	622.029	11.4 ± 0.3	3.84 ± 0.97	0.98	2.27		
	431.388	25.6 ± 1.8	15.67 ± 3.11	3.11	4.13	n/a	n/a
	430.381	25.8 ± 1.7	18.81 ± 3.02	3.02	4.94	1.196	220.2 %
	429.373	22.4 ± 3.6	7.92 ± 2.97	0.65	2.61	0.497	141.8 %

Table 5.2: Peak parameter for peaks appeared on chromatograms shown in Figure 5.8

m/z	t_R(s)	Area	Height	Width(s)	NTP	*Rs*	Asymmetry	k
429.373	57.0	8.95	3.37	3.46	1505	–	1.1	1.22
	62.0	22.52	8.82	2.44	3577	1.7	1.0	1.42
	82.5	2.08	0.66	2.29	7168	8.6	1.1	2.22
430.381	40.9	4.25	0.97	2.72	1255	–	2.4	0.59
	57.1	3.80	1.21	3.27	1691	5.4	1.0	1.23
	62.0	10.44	3.44	2.47	3484	1.7	1.1	1.42
	82.3	63.09	16.72	3.40	3244	6.9	1.5	2.21
431.388	62.2	2.85	0.96	2.69	2955	–	0.8	1.43
	82.4	103.27	29.19	3.17	3742	6.9	1.5	2.21
445.368	45.1	4.12	1.19	3.12	1159	–	1.1	0.76
	51.0	3.03	0.84	3.20	1407	1.9	1.9	0.99
447.383	46.5	5.14	1.05	3.09	1260	–	1.4	0.81
	56.9	4.99	1.43	3.44	1516	3.2	1.7	1.22
463.378	44.6	1.35	0.34	2.80	1408	–	1.4	0.74
	48.6	1.27	0.43	3.2	1279	2.2	1.5	0.90
479.373	44.5	1.78	0.44	2.69	1511	–	1.2	0.73
	49.5	1.46	0.36	2.69	1883	1.9	1.2	0.93
449.399	82.8	2.86	0.57	3.12	3895	–	1.2	2.23

参考文献

[1] Lindinger, W.; Jordan, A. *Chem. Soc. Rev.* 1998, **27**, 347.

[2] Ninomiya, S.; Iwamoto, S.; Usmanov, D. T.; Hiraoka, K.; Yamabe, S. *International Journal of Mass Spectrometry* 2021, **459**, 116440.

[3] Bottiroli, R.; Pedrotti, M.; Aprea, E.; Biasioli, F.; Fogliano, V.; Gasperi, F. *J Mass Spectrom* 2020, e4505.

[4] Bodner, M.; Morozova, K.; Kruathongsri, P.; Thakeow, P.; Scampicchio, M. *Eur Food Res Technol* 2019, **245**, 1499–1506.

[5] Pan, Y.; Zhang, Q.; Zhou, W.; Zou, X.; Wang, H.; Huang, C.; Shen, C.; Chu, Y. *J. Am. Soc. Mass Spectrom.* 2017, **28**, 873–879.

[6] Zhan, X.; Duan, J.; Duan, Y. *Mass Spectrom. Rev.* 2013, **32**, 143–165.

[7] Hondo, T.; Ota, C.; Miyake, Y.; Furutani, H.; Toyoda, M. *Anal. Chem.* 2021, **93**, 6589–6593.

[8] Zosel, K. *Angewandte Chemie International Edition in English* 1978, **17**, 702–709.

[9] Stringham, R. W.; Blackwell, J. A. *Anal. Chem.* 1996, **68**, 2179–2185.

[10] Parr, M. K.; Wüst, B.; Teubel, J.; Joseph, J. F. *Journal of Chromatography B* 2018, **1091**, 67–78.

[11] Koski, I. J.; Jansson, B. A.; Markides, K. E.; Lee, M. L. *Journal of Pharmaceutical and Biomedical Analysis* 1991, **9**, 281–290.

[12] Yamamoto, K.; Machida, K.; Kotani, A.; Hakamata, H. *Chemical and Pharmaceutical Bulletin* 2021, **69**, 970–975.

[13] Sakai, M.; Hayakawa, Y.; Funada, Y.; Ando, T.; Fukusaki, E.; Bamba, T. *Journal of Chromatography A* 2019, **1592**, 161–172.

[14] Yamauchi, R.; Yagi, Y.; Kato, K. *Bioscience, Biotechnology, and Biochemistry* 1996, **60**, 616–620.

[15] Cela, J.; Tweed, J. K. S.; Sivakumaran, A.; Lee, M. R. F.; Mur, L. A. J.; Munné-Bosch, S. *Plant Physiology and Biochemistry* 2018, **127**, 200–210.

[16] Mottier, P.; Gremaud, E.; Guy, P. A.; Turesky, R. J. *Analytical Biochemistry* 2002, **301**, 128–135.

[17] Kumar, A.; Prasad, A.; Pospíšil, P. *Sci Rep* 2020, **10**, 19646.

[18] Tang, C.; Tao, G.; Wang, Y.; Liu, Y.; Li, J. *J. Agric. Food Chem.* 2020, **68**, 669–677.

[19] Wildman, S. A.; Crippen, G. M. *J. Chem. Inf. Comput. Sci.* 1999, **39**, 868–873.

[20] Kawai, Y.; Miyake, Y.; Hondo, T.; Lehmann, J.-L.; Terada, K.; Toyoda, M. *Anal. Chem.* 2020, **92**, 6579–6586.

第 6 章

Microscale supercritical fluid extraction combined with supercritical fluid chromatography and proton-transfer-reaction ionization time-of-flight mass spectrometry for a magnitude lower limit of quantitation of lipophilic compounds.

The application of proton transfer ionization reaction mass spectrometry (PTR MS) combined with microscale supercritical fluid extraction (SFE) and supercritical fluid chromatography (SFC) aiming to quantitate single-cell fatty acid analysis levels was investigated. Using a microscale extraction vessel, the obtained lower limits of quantitation (LLOQs) of arachidonic acid and arachidic acid were 1.2 and 2.7 fmol, respectively, by using less than 1 µL of sample on stainless steel frit. A series of phthalate, vitamin K_1, and α-tocopherol were also tested, and the LLOQ was less than one femtomole for phthalate and 35 and 13 fmol for vitamin K_1 and α-tocopherol, respectively. A microliter portion of SFE extracts was introduced into the SFC column by split injection, improving the reproducibility of the chromatography and separation efficiency. The method in the present study has great potential to quantitate lipophilic molecules on the nanogram scale of a sample without complex preparation procedures.

6.1 Introduction

Morphogenesis and cell differentiation are essential phenomena in an organism. A combination of metabolic pathways regulates these processes. A metabolic pathway is a sequence of biochemical reactions. An increase or decrease in a key metabolite across a threshold concentration causes a pathway to go further, stop, or reverse. The chain of these reactions regulates the cell life cycle and signaling between cells, forming cell-to-cell interaction networks. Out-of-regulated cells may be removed from the organism, such as “programmed cell death.” The integrity of such a cell-to-cell signaling network performing morphogenesis and homeostasis establishes the organism. Therefore, it is

Reprinted with permission from
T. Hondo, C. Ota, Y. Miyake, H. Furutani, M. Toyoda *Journal of Chromatography A* **1682**, 463495 (2022). https://doi.org/10.1016/j.chroma.2022.463495.

crucial to understand the metabolism in a single cell and find the difference between cells and their population in a tissue.

Notably, it is well known that free fatty acids (FFAs) play significant roles in mammalian bodies[1,2]. The arachidonic acid cascade is a well-known pathway that controls the level of a group of prostanoids, which are involved in many diseases, such as cancers, fever, pain, and bipolar disorders[3]. Additionally, it is well known that various lipid-soluble compounds are contained in biological tissues, which are strongly involved in biological phenomena[4–7]. However, their measurement at a single cell is not always easy due to small amounts, the presence of isomers, and complex extraction/preparation procedures. Chen *et al.*[7] reported that the amounts of various FFAs in a colon tumor cells using LC/MS/MS, which was in the range of 0.02 to 2 nmol $\cdot$ mg^{-1} of tissue. By assuming a weight of a single cell is four nanograms, amounts of FFA in a single cell can be estimated in the range of 0.08 to 8 fmol. The traditional FFA analysis methods require several steps, such as homogenizing a tissue sample, extracting organic solvents, evaporating the organic solvents, and dissolving it into LC mobile-phase friendly solvents for LC/MS/MS analysis. Solid phase extraction may also be applied before injecting into LC[8,9]. The derivatization of extracted FFA samples is also used for both GC/MS and LC/MS analysis[10,11] since either GC/MS and use of positive ion mode in electrospray ionization (ESI) have advanced sensitivity than ESI negative ion mode. It is necessary to use tandem mass spectrometry to identify molecules in possible isomers, which also requires good chromatography separation to isolate isomers and select a precursor ion appropriately. An excellent opportunity for our method is keeping low detection limits in negative ion mode. In contrast, the sensitivity of ESI in negative ion mode is not as good as in positive ion mode.

One other example, tocopherol, is a well-known antioxidant that plays a crucial role in the antioxidant defense system in plants; however, the study of the formation of its oxidative products is limited[12,13]. Furthermore, their measurement is difficult due to the progress of autooxidation during sample preparation.

Proton transfer reaction ionization-mass spectrometry (PTR MS) has been used to analyze real-time trace-level volatile organic compounds; however, it also detects nonvolatile small molecules by a combination with supercritical fluid extraction (SFE), as we have previously reported[14]. Although traditional PTR-MS instruments selectively use H_3O^+ as reagent ion[15] by use of drift tube, that makes the protonate the analyte molecule. Pan *et al.*[16] introduces the proton-ejection reaction mass spectrometry (PER-MS), which can switch the PTR-MS and PER-MS modes. The ion source we have invented does not have a drift tube; thus, the equimolar of H_3O^+ and OH^- generated by corona discharge reacts with the sample molecules. Therefore, the proton transfer reaction happens in both directions for protonation/deprotonation of the analyte simultaneously. Due to no drift tube, the ion source assembly stays simple mechanical structure and thus robust. In this method, a sample applied on frit is directly introduced into the PTR mass spectrometer by supercritical carbon dioxide ($scCO_2$) without any sample preparation, which is a tremendous advantage for analyzing trace levels of lipids and fatty acids in the tissue and a cell. SFE has a significant advantage over other preparation methods and is capable of selective extraction of lipophilic molecules from a complex sample matrix by choosing $scCO_2$ pressure, temperature, and entrainer appropriately. Dušica Ivanov *et al.*[17] showed that SFE is a well-suited and recommended sample preparation method for fatty acid analysis. As we have already reported[14], SFE-PTR MS is well suited to detecting lipophilic molecules with high sensitivity. However, a combination with chromatography has not yet been studied.

The online hyphenation technique for supercritical fluid extraction (SFE) and supercritical fluid chromatography (SFC) has been studied for approximately four decades[18,19], and it is well established today. Hofstetter *et al.* reported that online solid-phase SFE/SFC-MS applies to a small number of clinical samples[20]. Sakai *et al.* reported an SFE/SFC system integrated with a split-flow and precolumn trap method for a broad polarity range of compounds in the presence of modifiers[21]. Several review articles are largely documented for recent progress on online SFE coupling to SFC[22**?** –24]. An advantage of the online SFE coupling method enhancing analytical sensitivity and accuracy due to less chance of getting contaminant for trace analysis, rapid sample extraction/preparation, and eliminating sample

handling in advance. A couple of SFE configurations have been introduced, which can be classified into static and dynamic extraction. The static extraction is performed in a closed vessel without fluid flow, while dynamic extraction is performed in the fluid keep flowing. The SFE-PTR we have previously reported uses dynamic extraction, in which the $scCO_2$ keeps flowing, and analytes containing fluids go into the PTR flow tube. A problem with this method is that many unwanted co-extracts get into an ion source simultaneously, which may suppress ionization. A possible solution is to add a chromatography separation step following to SFE process.

An expected benefit of hyphenating SFC following SFE is that it produces a series of compounds with a narrow bandwidth (chromatographic peaks), preventing ionization suppression by a complex sample matrix. A narrow chromatographic peak also improves the low detection limit. A significant concern is an SFC to PTR MS interface and whether longitudinal dispersion remains small since $scCO_2$ (~30 MPa) blows into a relatively large space of vacuum (100 Pa) via a narrow (20 µm) channel, which may have a different flow velocity with an SFC. An essential advantage of SFC over liquid chromatography (LC) is its enhanced column efficiency at a higher optimum linear velocity[25], which means that more peaks can be separated in a short period and achieve higher sample throughput. However, a reasonably narrow peak width is required on the chromatogram. The short response time is listed as an advantage of PTR ionization in many literatures; however, existing applications monitor concentration changes in the gas phase, such as volcano gas, forest fires, breath, and so forth. It is still unknown whether the response time is fast enough for the narrow peak width of the SFC chromatogram, expecting less than a half second.

We have studied online SFE/SFC-PTR MS for chromatography peak width and the quantitative analysis capability for authentic samples of α-tocopherol (α-T), vitamin K_1 (VK_1), and phthalate in positive ion mode; arachidic acid, and arachidonic acid in negative ion mode. A series of phthalate was used as the reference material for obtaining systematic information on chromatographic peak width and retention factor for fewer retention times of peaks.

6.2 Experimental

6.2.1 Mass Spectrometer

A JMS-T100 LP (AccuTOF) time-of-flight (TOF) mass spectrometer (JEOL, Tokyo, Japan) was used with a minor modification, which altered the data acquisition system to an Acqiris Model U5303A ($3.2\,GS \cdot s^{-1}$ 12-bit digitizer, Geneva, Switzerland). Data acquisition was carried out using open-source software "QtPlatz" (https://github.com/qtplatz/qtplatz) with a modified field programmable gate array (FPGA) configuration for acquiring "peak detection" (PKD) and waveform averaging (AVG) simultaneously[26]. The PKD histogram and AVG waveform were taken from the U5303A every 200 ms.

Figure 6.1 illustrates the block diagram of the PTR flow tube built in-house, which is the same as previously reported[14]. It consists of a corona discharge electrode (quartz, stainless steel), a PTR flow tube (stainless steel), and the AccuTOF interface.

Approximately 21 mm length of 20 µm inner-diameter (ID) inactivated fused silica capillary (GL Science, Tokyo, Japan) was used as a $scCO_2$ pressure restrictor, which holds up to 30 MPa at a liquid CO_2 flow rate set to $1.0\,mL \cdot min^{-1}$ at the high-pressure end and the other end open to the PTR flow tube, which is at approximately 100 Pa. The pressure restrictor was connected through the 1/16-inch outer diameter, 0.1 mm ID stainless steel tubing, and the capillary end was placed to the center of the transverse plane of the PTR flow tube, with an approximately 30° angle for the longitudinal axis.

General grade helium (Iwatani Industrial Gases Corp, Osaka, Japan) was connected to a PTR flow tube after passing through a 250 mL volume of the solvent-reservoir bottle, which contained 10 mL of ultrapure water (Millipore, MA, US). The helium flow rate was set to $70\,mL \cdot min^{-1}$, which was controlled using a mass flow controller (MFC) (8500MC-0-1-2, KOFLOC Corp. Kyoto, Japan). The pressure of the PTR flow tube was maintained in a range of 90

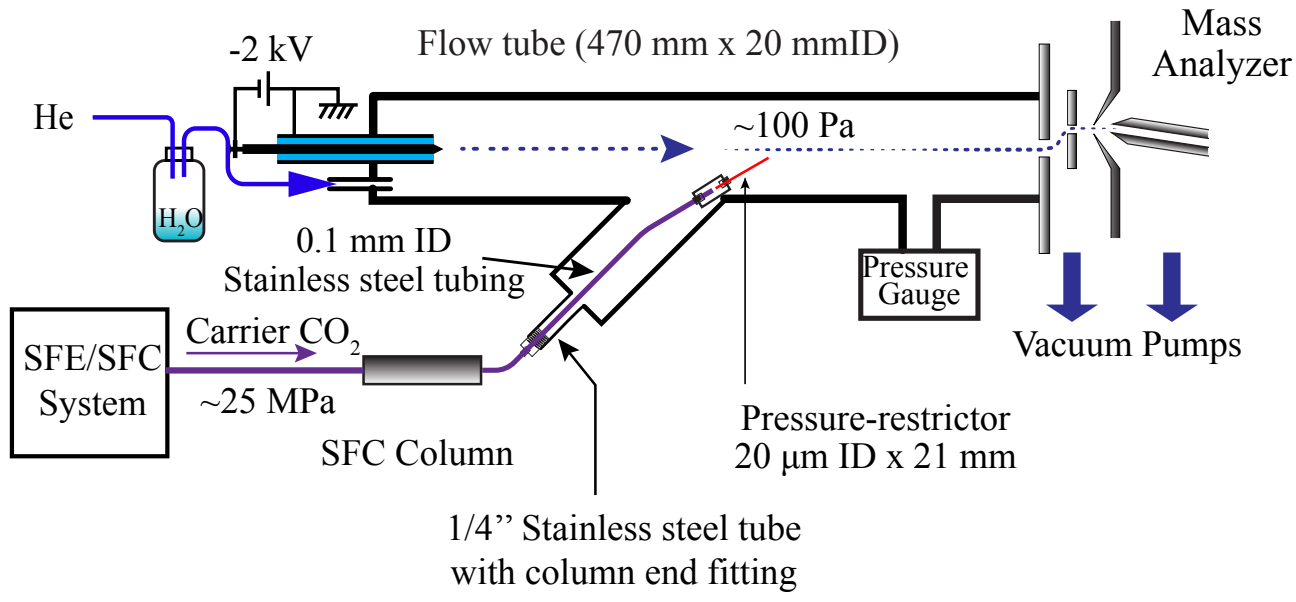

Figure 6.1: Block diagram of the PTR flow tube and the $scCO_2$ restrictor for SFC monitoring.

to 105 Pa by an AccuTOF vacuum system. The model PS350 high voltage power supply (Stanford Research Systems, Inc. Sunnyvale, CA, US) was used as a corona discharge power supply. The voltage for the discharge electrode was set to −2.0 kV, which resulted in 80 to 100 µA of current.

6.2.2　SFE/SFC System

Figure 6.2 illustrates the hydraulics and system schematics for SFE coupled with SFC in the split injection method. The system consists of two independent $scCO_2$ hydraulics for SFE and SFC, and they share a 6-port 2-way switching valve illustrated as V2, which acts as an injector.

SFE: Liquid CO_2 from a cylinder (Iwatani Industrial Gases Corp, Osaka, Japan) was precooled to −5 °C using an ethanol/dry ice bath and then pressurized up to 25 MPa at 200 µL · min^{-1} by an LC Packings UltiMate Micropump (Thermo Scientific, MA, US). The pressurized carbon dioxide from the pump was connected to the Agilent 1100 Series Thermostatted Column Compartment (Agilent, CA, US) and through the Rheodyne 7000 switching valves V1 and V2 and then waste after 20 µm ID × 250 mm length of pressure restrictor.

SFC: Liquid CO_2 from a cylinder was precooled to −5 °C using an ethanol/dry ice bath and then pressurized up to 30 MPa at 1.0 mL · min^{-1} by a PU-980 pump (JASCO, Tokyo, Japan). Then, the pressurized carbon dioxide was passed through an Agilent 1100 Series Thermostatted Column Compartment (Agilent, CA, US) and V2 and then flowed into a separation column and PTR flow tube. InertSustain C18 3 µm, 1.0 mm ID × 30 mm length (GL Science, Tokyo, Japan), and L-column3 C18 3 µm, 2.1 mm ID × 100 mm length (CERi, Chemicals Evaluation and Research Institute, Japan, Saitama, Japan) were used as SFC columns.

Pump heads for CO_2 delivery for both SFE and SFC were cooled to approximately 8 °C by the Peltier module (Hebei, TES1-12705, Hebei, China) prepared in-house.

An ACQUITY column in-line filter (Waters, MA, US) connected to V1 was used as the SFE vessel. A total of 0.2 to 1.0 µL of sample dissolved in acetonitrile was applied on the frit and set to a column in-line filter after waiting a few minutes to evaporate the acetonitrile. Switching both V1 and V2 to the LOAD position, as illustrated in Fig. 6.2 (A), will start SFE, and the supercritical fluid containing extracts will move toward the drain passing through 1 µL of the sample loop on V2. After a given time, the V2 position is switched to INJECT, as illustrated in Fig. 6.2 (B), to start SFC. The optimum time for V2 switching after starting SFE was determined by switching the V2 valve periodically without the SFC column.

Figure 6.3 shows the extracted ion profile by switching the V2 position to INJECT and LOAD every five seconds,

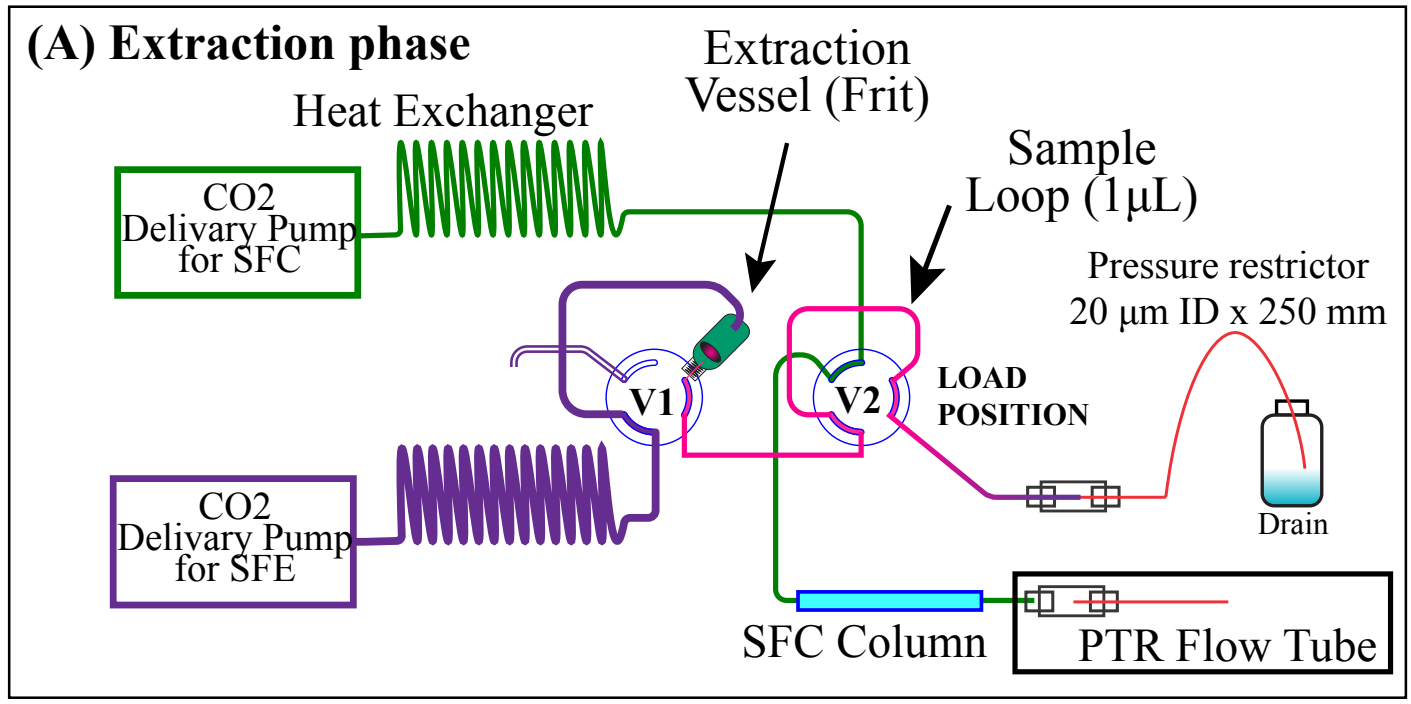

Figure 6.2: Hydraulics of SFE coupled with SFC with the split injection method.
A sample is applied on the frit and set in the extraction vessel while the extraction vessel is under atmospheric pressure. Set valve V1 and V2 positions as shown in (A), in which the starting SFE and extracts are passed by the sample loop. After a given time (10 s), the V2 valve position switches to the INJECT position, as shown in (B), which makes 1 μL of SFE extract into the SFC hydraulics flow.

injecting a 1 μL portion of SFE extracts into the SFC flow every 10 seconds. Although the 20 s injection timing (second peak) appears to have the most intense peak for α-T, all other molecules show the most intense peak at the 10 s injection timing (the first peak). Therefore, for future experiments, we determined that the sample injection timing was set to 10 seconds after SFE started.

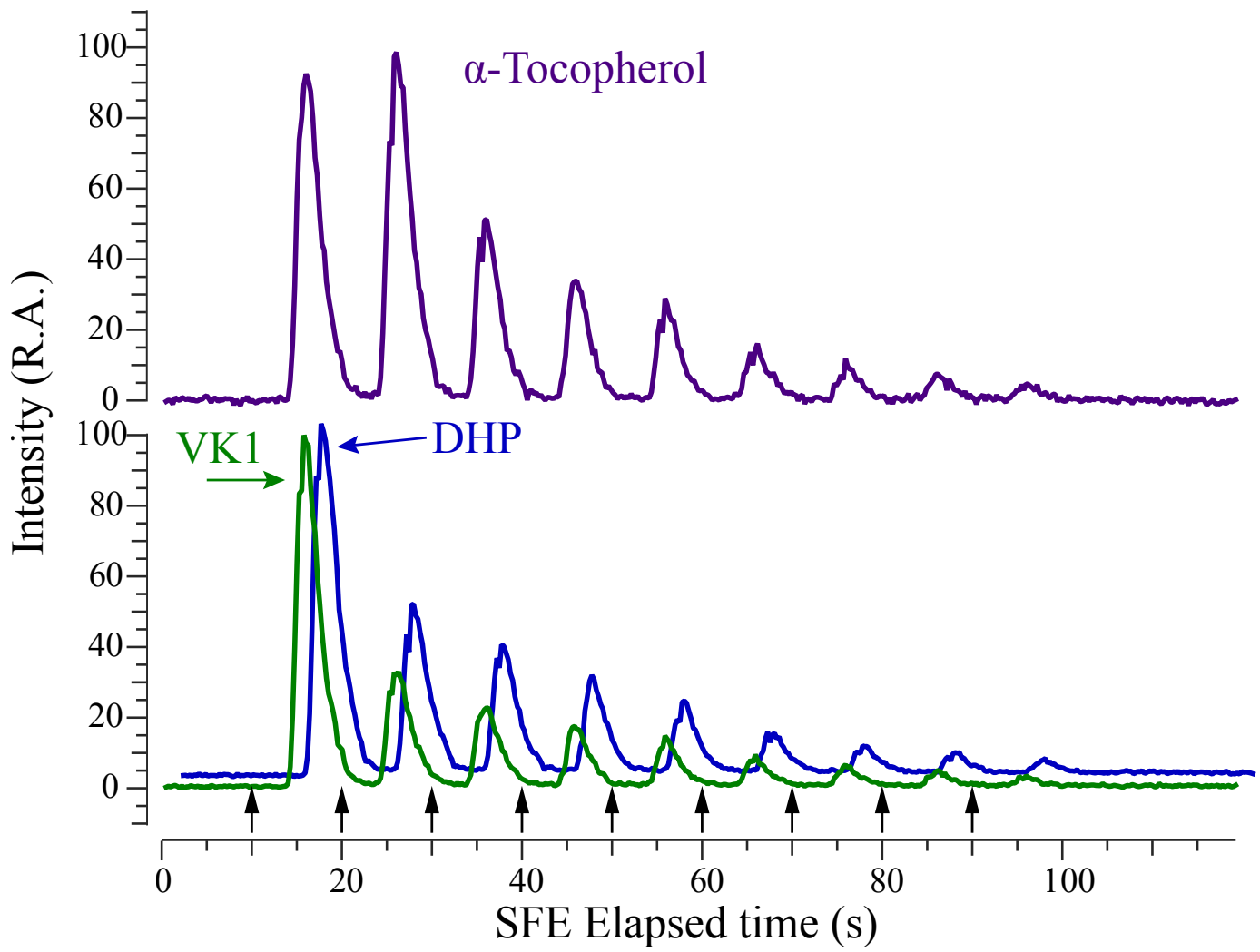

Figure 6.3: Optimization of SFE/SFC split injection timing.

6.2.3 Chemicals

Eight phthalate mixture standard solutions (each 100 µg · mL^{-1}in hexane), which contain diethyl phthalate (DEP), dipropyl phthalate (DPP), di-n-butyl phthalate (DBP), di-n-pentyl phthalate (DnPP), di-n-hexyl phthalate (DHP), benzyl butyl phthalate (BBP), bis (2-ethylhexyl) phthalate (DEHP), dicyclohexyl phthalate (DCHP), α-T, and arachidic acid (C20:0) were purchased from FUJIFILM Wako Pure Chemicals Corporation, Osaka, Japan. α-T was stored at −80 °C until use. One hundred microliters of LC/MS grade acetonitrile were added to arachidonic acid (100 mg) and stored at −80 °C until use. Arachidonic acid (ARA) was purchased from Tokyo Chemical Industry Co., Ltd, Tokyo, Japan. Human pool serum was purchased from Cosmo Bio Co., Ltd, Tokyo, Japan. LC/MS grade acetonitrile and acetone for pesticide residue and polychlorinated biphenyl tests (FUJIFILM Wako Pure Chemicals Corporation, Osaka, Japan) were used as solvents to dissolve the chemicals described above. Water was obtained from a Milli-Q Purification System from Millipore (MA, US).

6.2.4 Mass calibration

Mass calibration was performed using sodium trifluoroacetate, an electrospray ionization (ESI) source for *m/z* between 159 and 703 and third-order polynomials. The PTR ion source was then attached by altering the ESI source.

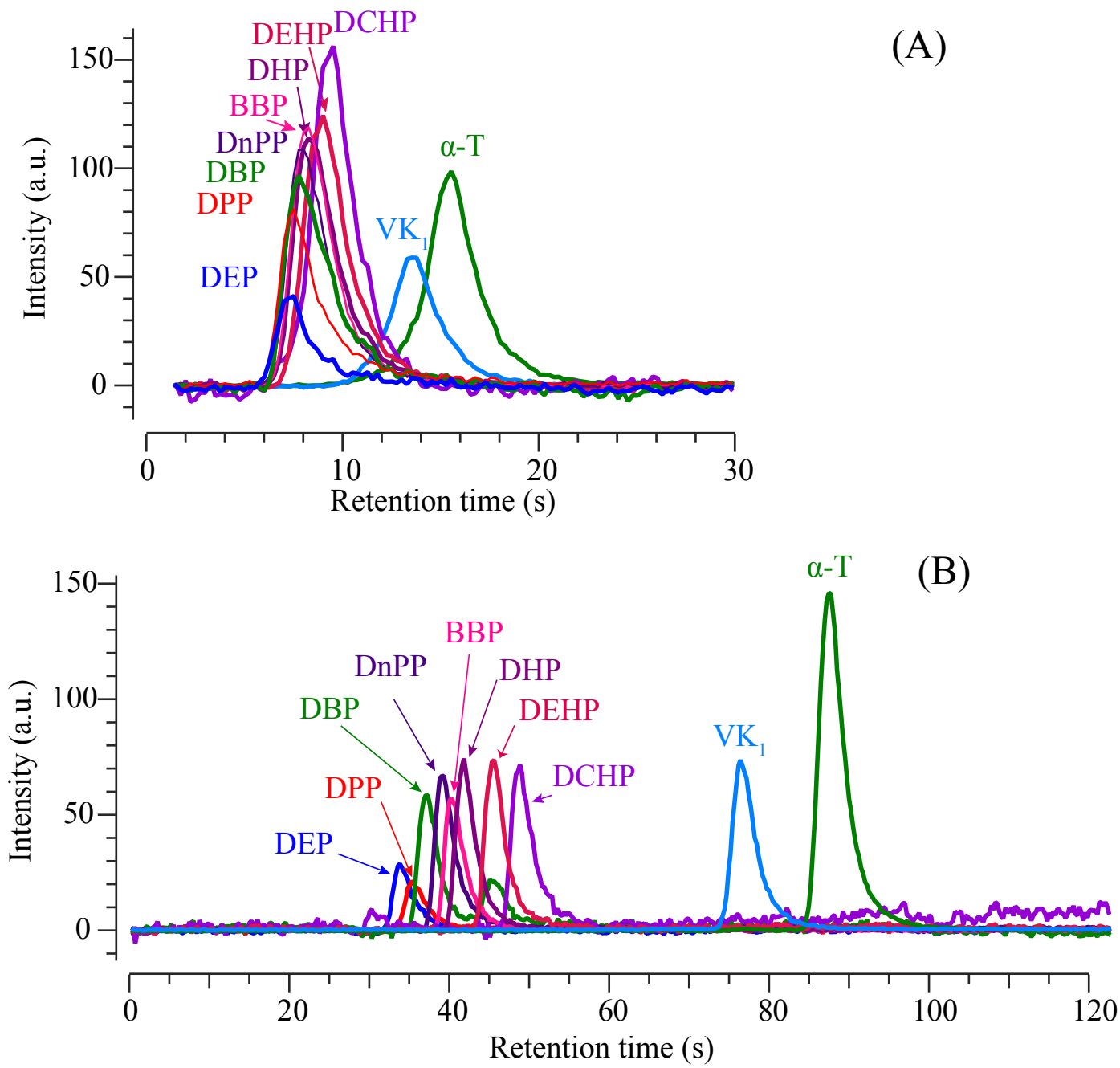

Figure 6.4: Extracted ion chromatograms of phthalates, VK_1, and α-T separated on the SFC columns. (A) The InertSustain C18 (3 µm, 1.0 mm×30 mm) column. A total of 0.2 pg each of 8 phthalates and 2 pmols each of VK_1 and α-T were applied to the frit. (B) The L-column3 C18 (3 µm, 2.1 mm×100 mm) column. A total of 1 pg each of 8 phthalates and 10 pmols each of VK_1 and α-T were applied to the frit. All chromatograms were extracted in the ion form of $[M + H]^+$.

6.3 Results and Discussion

6.3.1 Chromatography peak parameters

The retention time and peak width for all peaks shown in Fig. 6.4 are listed in Tables 6.1 and 6.2, and the relationship between the retention factor (k) and theoretical plate (N) is plotted in Fig. 6.5. The smallest retention time of extracted ion chromatograms for ion peaks at retention times of approximately 0 to 8 s (InertSustain C18) and 0 to 35 s (L-column3 C18) was used as the void time (t_0). No correlation between k and N was shown for eight phthalates ($k < 0.3$) separated on InertSustain C18, but VK_1 and α-T peaks, which are $k > 1.0$, had a positive correlation of 0.87. The samples were injected with one microliter volume at 1 mL · min^{-1} of flow rate, expecting to obtain about half a

Table 6.1: Chromatographic peak parameters for extracted ion chromatograms on InertSustain C18 (3 µm, 1.0 mm×30 mm, t_0 = 7.08 s)

name	t_R (s)	width (s)	k	N
DEP $[M + H]^+$	7.4 ± 0.1	1.8	0.04	93
DPP $[M + H]^+$	7.5 ± 0.2	1.9	0.05	93
DBP $[M + H]^+$	8.0 ± 0.2	2.6	0.13	57
DnPP $[M + H]^+$	8.0 ± 0.1	2.2	0.13	75
DCHP $[M + H]^+$	8.1 ± 0.2	3.7	0.14	29
BBP $[M + H]^+$	8.2 ± 0.1	2.2	0.16	81
DHP $[M + H]^+$	8.4 ± 0.1	2.4	0.18	73
DEHP $[M + H]^+$	8.9 ± 0.1	2.5	0.26	75
VK_1 $[M + H]^+$	13.5 ± 0.2	2.7	0.91	145
α-T $[M + H]^+$	15.4 ± 0.2	2.7	1.18	179

Table 6.2: Chromatographic peak parameters for extracted ion chromatograms on L-column3 C18 (3 µm, 2.1 mm×100 mm, t_0 = 30.5 s)

name	t_R (s)	width (s)	k	N
DEP $[M + H]^+$	34.1 ± 0.2	2.6	0.12	1026
DPP $[M + H]^+$	35.5 ± 0.3	2.8	0.16	1021
DBP $[M + H]^+$	37.2 ± 0.2	2.9	0.22	948
DnPP $[M + H]^+$	39.1 ± 0.3	2.6	0.28	1271
BBP $[M + H]^+$	40.5 ± 0.1	2.8	0.33	1195
DHP $[M + H]^+$	41.8 ± 0.3	2.6	0.37	1584
DEHP $[M + H]^+$	45.4 ± 0.3	2.8	0.49	1424
DCHP $[M + H]^+$	48.7 ± 0.3	2.9	0.60	1631
VK_1 $[M + H]^+$	76.7 ± 0.4	3.2	1.52	3232
α-T $[M + H]^+$	87.7 ± 0.5	3.6	1.87	3301

second of peak width. However, the obtained minimum peak width was approximately two seconds. The peaks should get broadened with a course of retention time under isobaric SFC conditions. Although short retention of peaks does not clearly correlate with width over k in general, the obtained result suggests that our ion source has two seconds of peak dispersion, which limits an N value for the short retention time of peaks on the short column. In contrast, N for all peaks is well correlated with k on L-column3 C18 even for the peaks of $k < 0.3$. The instrumental longitudinal dispersion of 2 s for injecting a sample bandwidth of 0.06 s computed from the pump flow rate is suggested by Fig. 6.3, which bypasses the SFC column. Therefore, any chromatographic peak narrower than 2 s broadens, which reduces the resolution (through lower N). The peak width of VK_1 and α-T on the InertSustain C18 column was 2.7 s, as listed in Table 6.1, which is competitive to 2 s and shows clear correlations between k and N relationships. On the other hand, for L-column3 C18, which has 4.3-fold larger t_0 value over InertSustain C18, the peak width for all peaks was 2.6 s or higher, as listed in Table 6.2; thus, better resolution (through higher N) was obtained. Due to a limitation of our PTR flow tube assembly, we cannot address the cause of such peak dispersion, although the width of the peak was highly dependent on the position and angle of the restrictor end in the PTR flow tube. By relocating the restrictor exit position in the PTR flow tube, we observed the peak width change between 3.5 s and 2.0 s, where 2.0 s was the best result thus far.

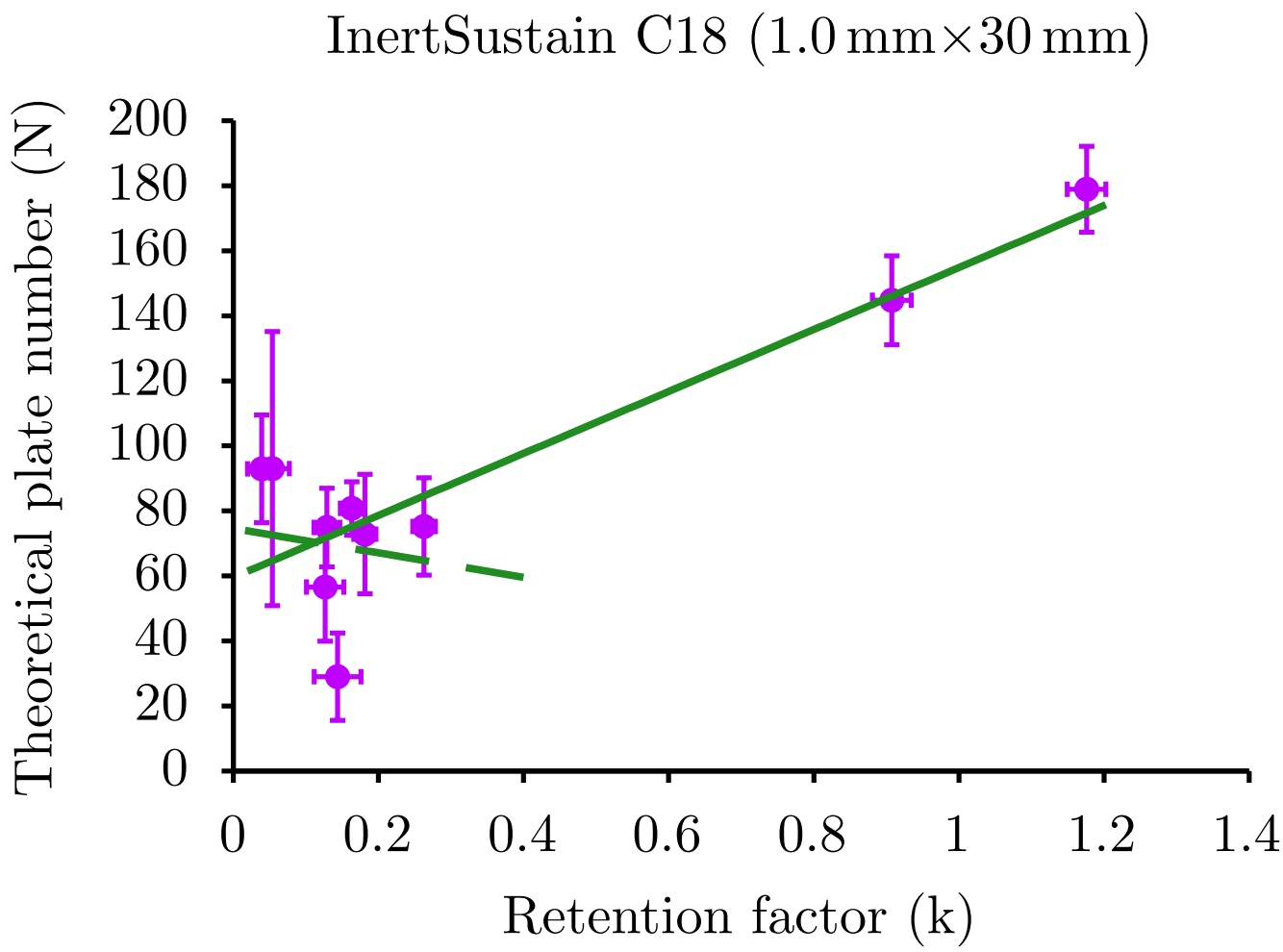

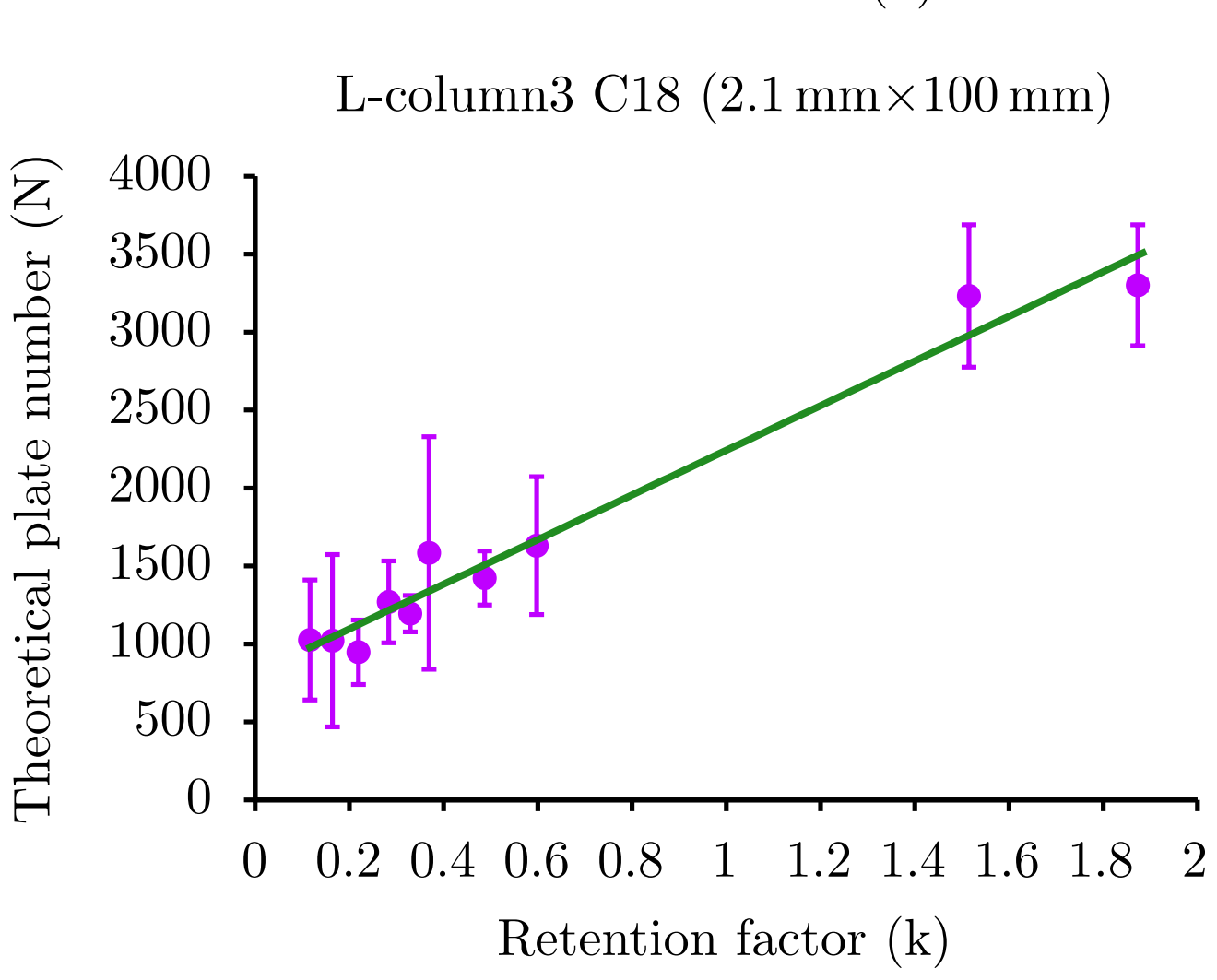

Figure 6.5: Relationship between retention factor (k) and theoretical plate (N) on InertSustain C18 (3 µm, 1.0 mm×30 mm) and L-column3 C18 (3 µm, 2.1 mm×100 mm)
The void times (t_0) for InertSustain C18 and L-column3 C18 were 7.08 and 30.5 s, respectively. The correlation coefficients were 0.869 and 0.984 for IntertSustain C18 and L-column3 C18, respectively; however, the correlation coefficient for peaks with retention times less than 10 s (k < 0.4) on IntertSustain C18 was -0.115 (dashed line).

Table 6.3: Lower limit of quantitation.

name		LLOQ (fmol)
DEP	$[M+H]^+$	0.53
DPP	$[M+H]^+$	0.66
DBP	$[M+H]^+$	0.77
DnPP	$[M+H]^+$	0.68
BBP	$[M+H]^+$	0.57
DCHP	$[M+H]^+$	0.61
DHP	$[M+H]^+$	0.62
DEHP	$[M+H]^+$	0.60
α-T	$[M+H]^+$	13.30
VK_1	$[M+H]^+$	34.50
C20:0	$[M-H]^-$	2.65
ARA	$[M-H]^-$	1.18

The relative standard deviation (RSD) of the retention time for each molecule was 1.7 % throughout the entire chromatographic run of this study, and the RSD for the peak area for each triplicate was between 1 and 30 %. The authors consider that the stability of the pressure restrictor for SFE hydraulics is responsible for the peak area variance.

6.3.2 Lower limit of quantitation

Figs. 6.6 and 6.7 illustrate the calibration curves for α-T, VK_1, C20:0 and ARA. The calibration curves for all compounds acquired in this study are illustrated in Supporting Information Figure S1. A linear relationship between peak area and amounts was observed up to 5 pmol for α-T and VK_1, and two picomoles for C20:0 and 150 fmol for ARA were both obtained from PKD and AVG waveforms. The previously reported method[26] converted a chromatographic peak area from the AVG waveform to corresponding area counts.

A lower limit of quantitation (LLOQ) was then estimated from the slope of the linear regression line as an amount that gives 100 counts. A list of the obtained LLOQs is shown in Table 6.3. The LLOQ on the SFE-PTR, a direct injection from SFE to PTR MS as previously reported for α-T and VK_1 (positive ion mode), C20:0, and ARA (negative ion mode) was 63, 406, 27, and 19 fmol, respectively. Using online SFE/SFC in the present study, LLOQ for α-T, VK_1, C20:0, and ARA listed in Table 6.3 decreased 4.7, 12, 10, and 16-fold compared to the previous method.[14]

Gachet *et al.*[9] reported that the LLOQ for ARA was 6250 fmol on a column by using LC/MS/MS. Chen *et al.*[7] reported an LC/MS/MS method for FFA quantitation in clinical samples. The reported LLOQs for C20:0 and C20:4 were 0.059 and 0.037 $\mu g \cdot mL^{-1}$, respectively, which corresponds to approximately 1900 to 1200 fmol per sample injected (10 µL) into the HPLC. They also quantitated FFAs in colon tumor tissue (using 21-27 mg) in the 0.01 to 0.5 $nmol \cdot mg^{-1}$ range. Assuming a cell is one microgram, it corresponds to 10 to 500 fmol per cell, which is in the quantitative range of the method described in this study (SFE/SFC-PTR MS). We used a frit as a sample holder and an in-line column filter as an SFE vessel, which is well fit for holding a single cell and tissues.

6.3.3 Quantitative dynamic range

Calibration curves for α-T, VK_1, C20:0, and ARA on IntertSustain C18 column are shown in Fig. 6.6 and 6.7. All calibration curves are also drawn in Supporting Information Figure S1. The upper limit of the linear response range for the IntertSustain C18 column was up to 500 pg (≈1.6 pmol) for phthalates, 5 pmol for α-T and VK_1, 2 pmol for

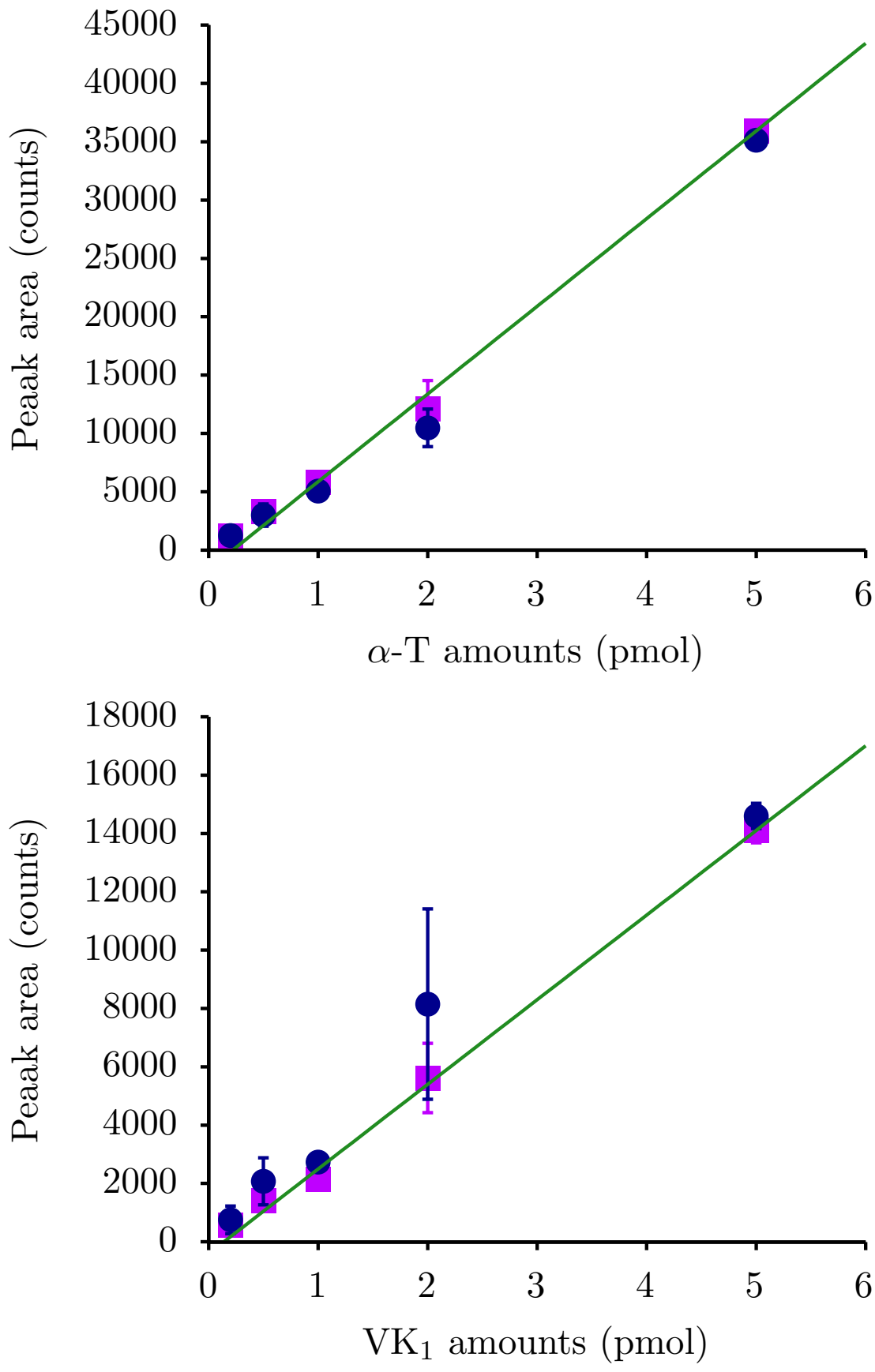

Figure 6.6: Calibration curves for α-T (top) and VK_1 (bottom). SFC separation was carried out on the InertSustain C18 column. The closed circle indicates a peak area (counts) from the PKD waveform, and the closed square indicates a peak area from the AVG waveform, normalized as counts.

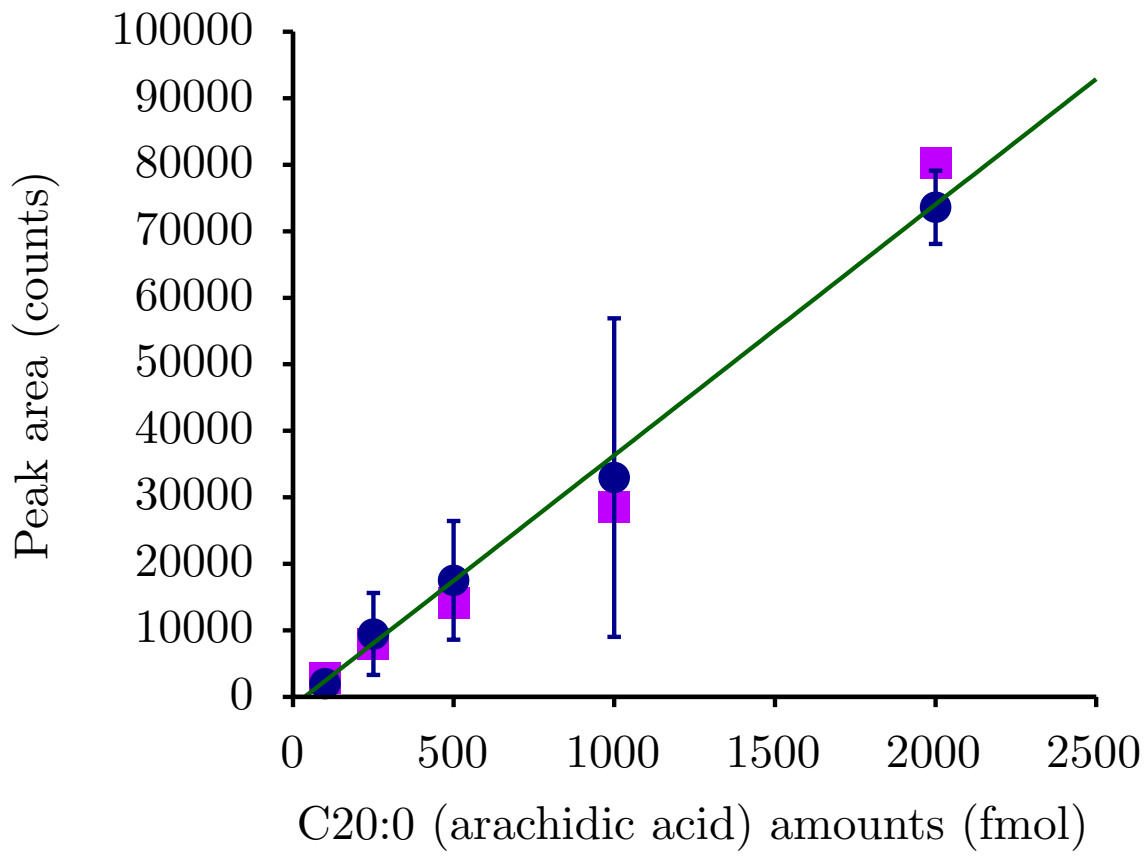

Figure 6.7: Calibration curves for C20:0 (top) and ARA (bottom). SFC separation was carried out on the InertSustain C18 column. The closed circle indicates a peak area (counts) from the PKD waveform, and the closed square indicates a peak area from the AVG waveform, normalized as counts.

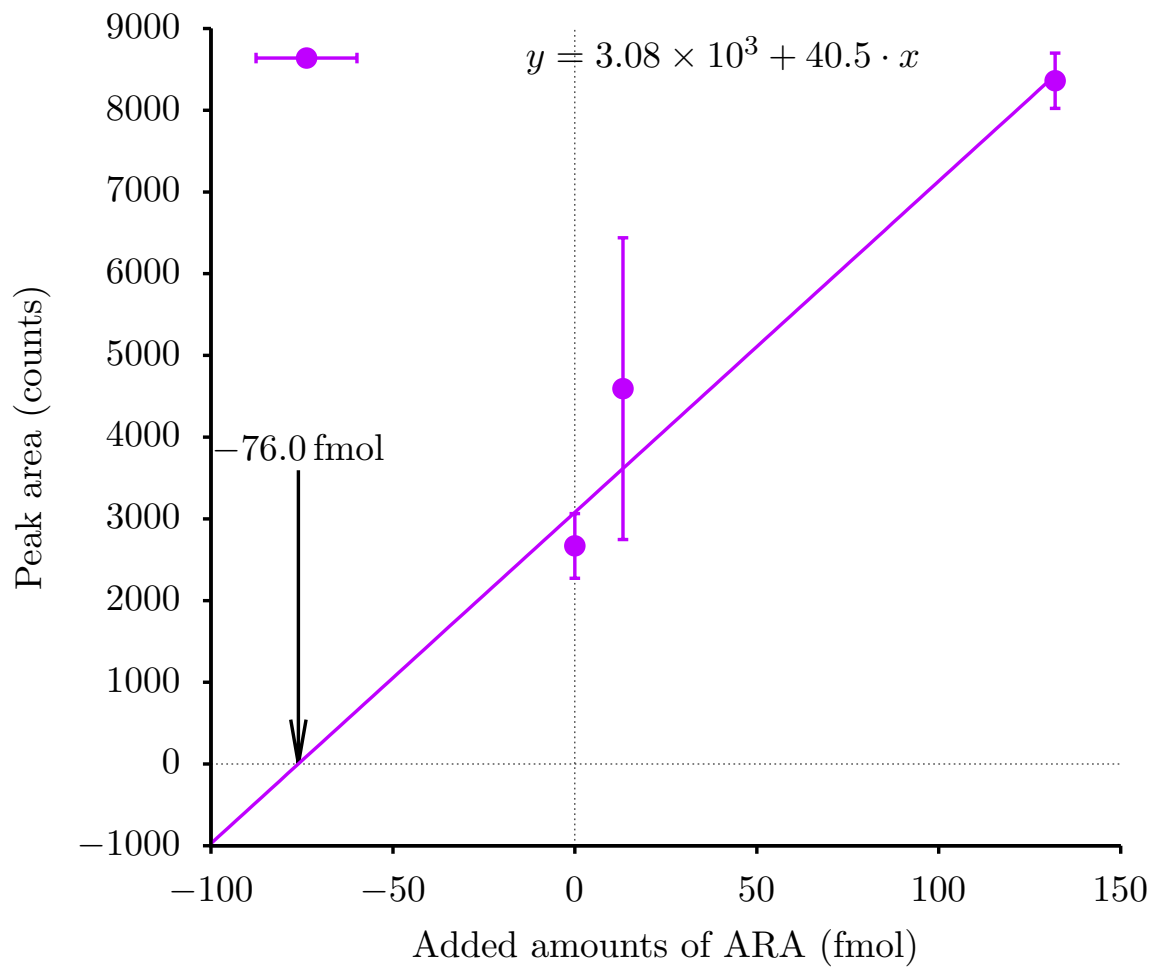

Figure 6.8: Peak areas for extracted ARA $[M-H]^-$ chromatograms for ARA added human pool serum.

ARA amounts of zero, 13.2, and 132 fmol were added to the human pool serum. SFC separation was carried out on L-column3 C18 column. The square root of χ^2 for the linear regression line was 1049. The calculated ARA amount in the 0.1 µL human pool serum was estimated as 76 fmol, which is 0.76 µmol · L^{-1} in human pool serum.

C20:0, and 0.17 pmol for ARA.

6.3.4 FFA analysis of human pool serum

ARA amount in the human pool serum was evaluated using standard sample additions. One microliter of ten times diluted human pool serum by acetonitrile was applied on the frit after being filtered by 0.2 µm filter. The SFC separation was carried out using L-column3 C18. The obtained peak areas were plotted in Figure 6.8, and the concentration of ARA in human pool serum was estimated as 0.76 µmol · L^{-1}. The major FFAs simultaneously detected were summarized in Table 6.4.

6.4 Conclusion

By using a split injection, a sample in $scCO_2$ by independent SFE hydraulics was introduced into SFC. Using a sub nanoliter (0.2 to 1.0 µL) sample, the LLOQs obtained were 0.5 to 0.8 fmol for phthalates, 1.18, 2.65, 13.3 and 34.5 fmol for ARA, C20:0, α-T and VK_1, respectively. The minimum chromatographic peak width was 1.8 s, although approximately 2 s of instrumental dispersion was observed in the PTR flow tube. By using a 1.0 mm ID × 30 mm length column, separation can be performed in 30 s, but the peak width for less than 10 s of retention time seems to be thresholded by instrumental dispersion. In contrast, the 2.1 mm ID × 100 mm length column shows a reasonable

Table 6.4: FFAs found in 0.1 µL of human pool serum by SFE/SFC-PTR MS. (RSD n=3 for ARA to exclude standard added samples, otherwise n=8.))

name	retention time (s)	Area (counts)	RSD(%) (n=6)	Ratio $Area/Area_{ARA}$
C12:0	50.3 ± 0.5	9797	8.5%	3.7
C14:0	56.1 ± 0.5	21 924	9.9%	8.2
C16:1	59.0 ± 0.6	28 424	8.8%	10.6
C20:5	63.1 ± 0.6	1219	10.7%	0.5
C16:0	63.2 ± 0.8	78 596	10.4%	29.4
C18:2	63.3 ± 0.8	23 361	12.2%	8.8
ARA	64.9 ± 0.8	2669	14.8%	(1.0)
C18:1	66.7 ± 0.7	51 856	2.3%	19.4
C22:6	67.6 ± 0.6	923	16.4%	0.3
C20:2	71.3 ± 0.6	1735	8.0%	0.6
C18:0	72.0 ± 0.9	46 191	9.9%	17.3
C22:4	72.9 ± 1.0	397	15.0%	0.1
C20:1	75.8 ± 0.8	3035	5.7%	1.1
C20:0	82.4 ± 0.9	2716	7.1%	1.0
C22:1	86.9 ± 1.0	932	10.6%	0.3
C24:0	108.7 ± 1.4	1963	45.9%	0.7

retention factor (k) and theoretical plate (N) relationship within a 2 min separation time, where all peak widths were larger than 2 s. The obtained LLOQ values with reported FFA amounts in the tissue suggest that the present method may be applicable to quantitate FFAs in a single cell. To improve the separation efficiency for achieving a short separation time, better sensitivity, and peak area reproducibility, an engineering design of the PTR flow tube and a split injection system will be investigated.

参考文献

[1] Gindlhuber, J.; Schinagl, M.; Liesinger, L.; Darnhofer, B.; Tomin, T.; Schittmayer, M.; Birner-Gruenberger, R. *IJMS* 2022, **23**, 3356.

[2] Falomir-Lockhart, L. J.; Cavazzutti, G. F.; Giménez, E.; Toscani, A. M. *Frontiers in Cellular Neuroscience* 2019, **13**.

[3] Sublette, M. E.; Russ, M. J.; Smith, G. S. *Bipolar Disorders* 2004, **6**, 95–105.

[4] Snaebjornsson, M. T.; Janaki-Raman, S.; Schulze, A. *Cell Metabolism* 2020, **31**, 62–76.

[5] Okugaki, T.; Kasuno, M.; Maeda, K.; Kihara, S. *Journal of Electroanalytical Chemistry* 2010, **639**, 67–76.

[6] Kim, H.-W.; Rapoport, S. I.; Rao, J. S. *Mol Psychiatry* 2011, **16**, 419–428.

[7] Chen, L.; Xie, B.; Li, L.; Jiang, W.; Zhang, Y.; Fu, J.; Guan, G.; Qiu, Y. *Chromatographia* 2014, **77**, 1241–1247.

[8] Veres, P.; Roberts, J. M.; Warneke, C.; Welsh-Bon, D.; Zahniser, M.; Herndon, S.; Fall, R.; de Gouw, J. *International Journal of Mass Spectrometry* 2008, **274**, 48–55.

[9] Gachet, M. S.; Rhyn, P.; Bosch, O. G.; Quednow, B. B.; Gertsch, J. *Journal of Chromatography B* 2015, **976-977**, 6–18.

[10] Yang, W.-C.; Adamec, J.; Regnier, F. E. *Anal. Chem.* 2007, **79**, 5150–5157.

[11] Moldovan, Z.; Jover, E.; Bayona, J. M. *Analytica Chimica Acta* 2002, 20.

[12] Kumar, A.; Prasad, A.; Pospíšil, P. *Sci Rep* 2020, **10**, 19646.

[13] Tang, C.; Tao, G.; Wang, Y.; Liu, Y.; Li, J. *J. Agric. Food Chem.* 2020, **68**, 669–677.

[14] Hondo, T.; Ota, C.; Miyake, Y.; Furutani, H.; Toyoda, M. *Anal. Chem.* 2021, **93**, 6589–6593.

[15] Lindinger, W.; Jordan, A. *Chem. Soc. Rev.* 1998, **27**, 347.

[16] Pan, Y.; Zhang, Q.; Zhou, W.; Zou, X.; Wang, H.; Huang, C.; Shen, C.; Chu, Y. *J. Am. Soc. Mass Spectrom.* 2017, **28**, 873–879.

[17] Ivanov, D.; Čolović, R.; Bera, O.; Lević, J.; Sredanović, S. *Eur Food Res Technol* 2011, **233**, 343–350.

[18] Sugiyama, K.; Saito, M.; Hondo, T.; Senda, M. *Journal of Chromatography A* 1985, **332**, 107–116.

[19] Jahn, K. R.; Wenclawiak, B. *Chromatographia* 1988, **26**, 345–350.

[20] Hofstetter, R.; Fassauer, G. M.; Link, A. *Journal of Chromatography B* 2018, **1076**, 77–83.

[21] Sakai, M.; Hayakawa, Y.; Funada, Y.; Ando, T.; Fukusaki, E.; Bamba, T. *Journal of Chromatography A* 2019, **1592**, 161–172.

[22] Giuffrida, D.; Donato, P.; Dugo, P.; Mondello, L. *J. Agric. Food Chem.* 2018, **66**, 3302–3307.

[23] Sánchez-Camargo, A. d. P.; Parada-Alonso, F.; Ibáñez, E.; Cifuentes, A. *Journal of Separation Science* 2019, **42**, 243–257.

[24] Liang, Y.; Zhou, T. *Journal of Separation Science* 2019, **42**, 226–242.

[25] Gere, D. R. *Science* 1983, **222**, 253–259.

[26] Kawai, Y.; Miyake, Y.; Hondo, T.; Lehmann, J.-L.; Terada, K.; Toyoda, M. *Anal. Chem.* 2020, **92**, 6579–6586.

第 7 章

Attempts to detect lipid metabolites from a single cell using proton-transfer-reaction mass spectrometry coupled with micro-scale supercritical fluid extraction: A preliminary study.

Proton-transfer-reaction (PTR) mass spectrometry (MS), a widely used method for detecting trace-levels of volatile organic compounds in gaseous samples, can also be used for the analysis of small non-volatile molecules by using supercritical fluid as a transporter for the molecules. Supercritical fluid extraction (SFE) is a method that permits lipophilic compounds to be rapidly and selectively extracted from complex matrices. The combination of the high sensitivity of PTR MS with the SFE is a potentially novel method for analyzing small molecules in a single cell, particularly for the analysis of lipophilic compounds. We preliminarily evaluated this method for analyzing the components of a single HeLa cell that is fixed on the stainless steel frit and is then directly introduces the SFE extracts into the PTR MS. A total of 200/90 ions were observed in positive/negative ion mode time-of-flight mass spectra, and the masses of 11/10 ions could be matched to chemical formulae obtained from the LipidMaps lipids structure database. Using various authentic lipophilic samples, the method could be used to detect free fatty acids in the sub-femtomole to femtomole order in the negative ion mode, the femtomole to sub-picomole order for fat-soluble vitamins, and the picomole order for poly aromatic hydrocarbons in both the positive and negative ion mode.

7.1 Introduction

Immortalized cells such as HeLa, HepG2, and Huh-7 cells have been widely used by researchers in the molecular biological sciences [1–8] because they are essentially identical cells that never change. The use of such cells has contributed to the study of tumor tissue formation at the molecular level. Because the enzymes and their substrates that are involved in the regulation of metabolic pathways for growing or suppressing tumors are present at trace levels, a collection of identical cells has long been essential for studies in this area. Pathological tumor tissue, however, is

Reprinted with permission from
T. Hondo, C. Ota, K. Nakatani, Y. Miyake, H. Furutani, T. Bamba, M. Toyoda *Mass Spectrometry* 2022, 11 (1), A0112. https://doi.org/10.5702/massspectrometry.A0112

comprised of a heterogeneous collection of cells. Because of this,, understanding the metabolism in a single cell and identifying the difference between cells and their population and cell-to-cell signaling systems is a crucial issue. Various lipid-soluble compounds, especially free fatty acids (FFAs), play significant roles in mammalian bodies and are involved in many diseases or disorders, such as cancers, fever, pain, and bipolar disorders[9–14]. However, their measurement in a single cell is not always easy due to the small amounts of these substances, the presence of isomers, and the complex sample preparation procedures.

Microscale supercritical fluid extraction is a potential candidate for preparing samples for the analysis of lipophilic molecules in a formed/structured entity such as a cell. The method permits the selective extraction of lipophilic compounds from a complex sample matrix by controlling the temperature and pressure with an entrainer, when necessary. Ivanov *et al.*[15] reported that SFE is a well-suited and recommended method for preparing samples for fatty acid analysis. Proton-transfer-reaction (PTR) ionization-mass spectrometry (MS) is a method that is well-suited for detecting molecules in a supercritical fluid without the need for sophisticated instrumentation[16]. In this method, a sample is applied on a stainless steel frit that is directly introduced into a PTR mass spectrometer by supercritical carbon dioxide ($scCO_2$) without further sample preparation. The PTR MS that we designed, essentially involves water positive/negative ion chemical ionization and has advanced detection sensitivity for both positive and negative ions, which are produced simultaneously[17]. It is tremendously advantageous for detecting FFAs with a high sensitivity and appears to show a better sensitivity in the negative ion mode.

7.2 Experimental

7.2.1 Apparatus

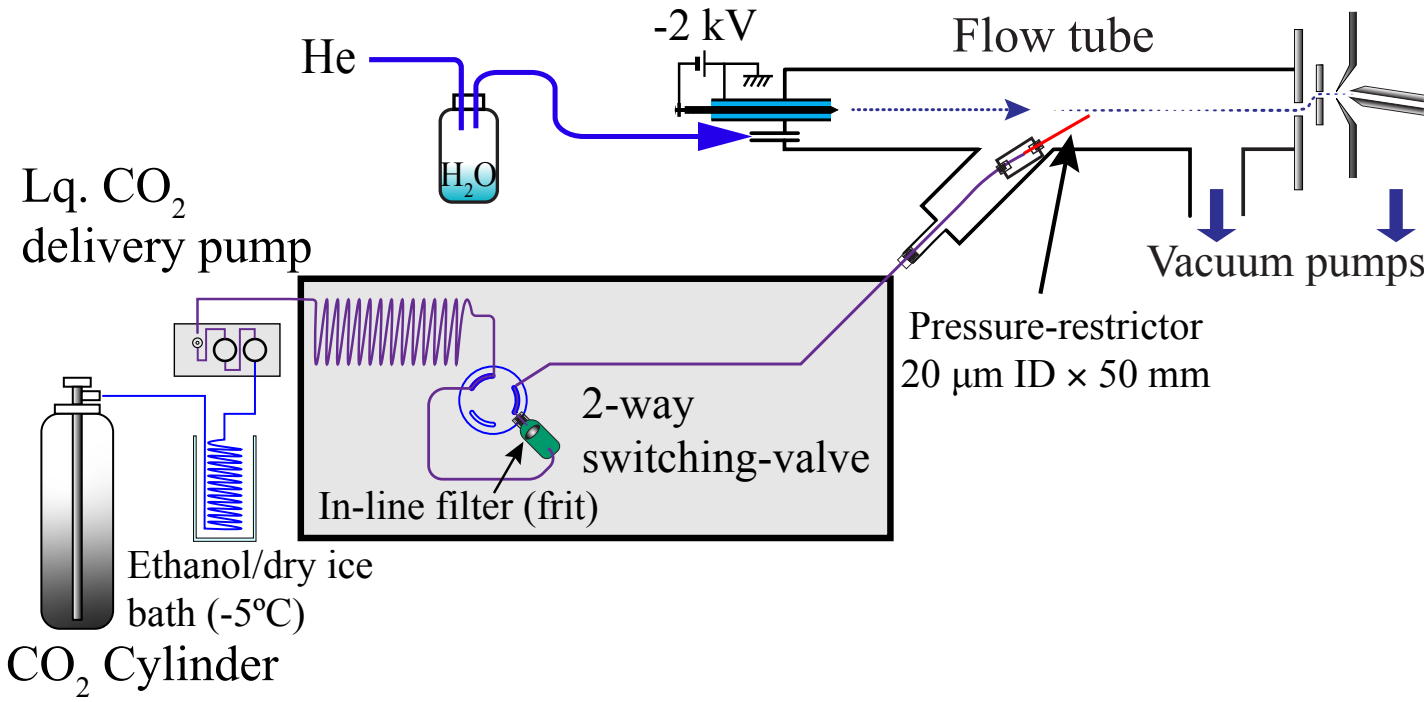

Figure 7.1: Block diagram of SFE-PTR MS

The apparatus used in this study was the same as previously reported[16] as the “Direct injection” (DI) method. The set up consists of a JMS-T100 LP (AccuTOF) time-of-flight (TOF) mass spectrometer (JEOL, Tokyo, Japan) with a altered data acquisition system using the Acqiris Model U5303A with QtPlatz (https://github.com/qtplatz/qtplatz) open source software. The data acquisition system simultaneously enables “peak detection” (PKD) and waveform averaging (AVG)[18,19]. Figure 7.1 illustrates a block diagram of the apparatus, which consists of an in-house constructed PTR flow tube, an SFE interface, and an AccuTOF interface. Liquid CO_2 from a cylinder (Iwatani Industrial Gases Corp,

Osaka, Japan) was precooled to −5 °C using an ethanol/dry ice bath and then pressurized up to 25 MPa at a rate of 500 µL/min by an LC Packings UltiMate Micropump (Thermo Scientific, MA, US). The pressurized carbon dioxide from the pump was connected to the Agilent 1100 Series Thermostatted Column Compartment (Agilent, CA, US) and a Rheodyne 7000 switching valve was connected through a microscale extraction vessel.

An inactivated fused silica capillary (GL Science, Tokyo, Japan) approximately 50 mm in length with a 20 µm inner-diameter (ID) inactivated fused silica capillary (GL Science, Tokyo, Japan) was used as a $scCO_2$ pressure restrictor, which holds up to 30 MPa at a liquid CO_2 flow rate set at 0.5 mL/min at the high-pressure end with the other end open to the PTR flow tube, which is at approximately 100 Pa.

General grade helium (Iwatani Industrial Gases Corp, Osaka, Japan) was connected to a flow tube after passing through a 250 mL volume of the solvent-reservoir bottle containing 10 mL of ultrapure water (Millipore, MA, US). The helium flow rate was set to 70 $mL \cdot min^{-1}$, which was controlled using a mass flow controller (MFC) (8500MC-0-1-2, KOFLOC Corp. Kyoto, Japan). The pressure of the flow tube was maintained in a range of 90 to 105 Pa by an AccuTOF vacuum system. The model PS350 high voltage power supply (Stanford Research Systems, Inc. Sunnyvale, CA, US) was used as a corona discharge power supply. The voltage for the discharge electrode was set to −2.0 kV, which resulted in 80 to 100 µA of current.

The pump head for CO_2 delivery was cooled to approximately 8 °C by the Peltier module (Hebei, TES1-12705, Hebei, China) prepared in-house.

An ACQUITY column in-line filter (Waters, MA, US) connected to a 2-way switching valve was used as the SFE vessel.

7.2.2 Chemicals

Hexamethoxyphosphazine (P321), Hexakis (2,2-Difluoroethoxy) phosphazene (P621), tetracosenoic acid, caffeine, pyrene, reserpine, oleic acid, vitamin K_1, and γ-oryzanol were purchased from FUJIFILM Wako Pure Chemicals Corporation, Osaka, Japan. Methanol, acetonitrile (LC/MS grade), and reagent-grade acetone (FUJIFILM Wako Pure Chemicals Corporation, Osaka, Japan) were used as a solvent for the above chemicals. Water was obtained from a Milli-Q Purification System (Merck, Germany). Cylinders of general grade helium and carbon dioxide (siphon type) (Iwatani Industrial Gases Corp, Osaka, Japan) were used in this study.

7.2.3 Mass calibration

Mass calibration was performed using sodium trifluoroacetate, an electrospray ionization (ESI) source for *m/z* between 159 and 703 using third-order polynomials. The PTR ion source was then attached by altering the ESI source.

7.2.4 HeLa cell sample preparation

HeLa cells were prepared as described in a previous report[20]. The cells (American Type Culture Collection) were cultured in 10 cm diameter dishes containing 10 mL of Dulbecco's modified Eagle's medium (DMEM, Thermo Fisher Scientific, Inc., Waltham, MA, USA) supplemented with 10 % (v/v) fetal bovine serum (FBS, Thermo Fisher Scientific, Inc.) and 1 % (v/v) Penicillin–Streptomycin Solution (Thermo Fisher Scientific, Inc.) as antibiotics. Cultivation dishes were incubated in a water-jacketed CO_2 incubator (WCI-165; ASTEC Co., Fukuoka, Japan) under an atmosphere of 5% CO_2 at 37 °C. When the cells reached 80% confluence, the medium in each dish was changed 1 h before cell sampling. The cultivated HeLa cells in 10 cm dishes were harvested at an 80% confluency by treatment with a Trypsin–EDTA solution for 3 min at 37 °C. After counting cell numbers using a cell counter (Moxi Z; ASONE Co., Osaka, Japan), the Trypsin–EDTA-treated HeLa cells were collected in a 15-mL tube by centrifugation with a swing type rotor at 250×*g* for 1 min at 20 °C. The resulting cell pellets were washed four times with 10mL PBS. The

PBS aliquot was then added to the cell pellets, and 1×10^{-4} cells $\cdot$ mL^{-1} cell suspension was prepared. Single HeLa cells were aspirated from the suspension in the fused-silica capillary (100 µm ID., 360 µm OD., 75 mm length). After microscopic confirmation of a single HeLa cell, the isolated cell was ejected on the frit and then dried.

Another batch of HeLa cell pellets was prepared with the same protocol described above. After adding 1 mL of methanol to the HeLa cell pellets, the samples were vigorously mixed by vortexing for 1 min, followed by sonication for 5 min. After centrifugation for 5 min at 16 000×g and 4 °C, 700 µL of the supernatant was transferred to a 2 mL Eppendorf tube. A portion of the supernatant was appropriately diluted with methanol to make 100 cells $\cdot$ µL^{-1}, and this was used as a methanol-extract of a cell.

7.2.5　SFE-PTR MS Analysis procedure

A portion of the lock-mass reference sample was applied to the frit that holds a single HeLa cell, asdescribed above. After the acetonitrile had evaporated, the frit was set to the Acquity In-Line filter and the SFE was started by changing the 2-way valve position. SFE-PTR MS spectra were acquired using simultaneous PKD and AVG waveforms for intervals of 0.15 s, and were stored as a function of time. An extracted ion profile of an ion should show a bell-shaped curve (broad peak), which can be found by the peak detection algorithm. In contrast, the ion peaks derived from reagent ions and the intensity of the common instrumental background ions are maintained at the beginning and then decrease when the sample-derived ions begin to arrive. By using a chromatographic peak detection algorithm, the ions that show peak-like shapes were highlighted in magenta[21], indicating that the magenta color-coded ions appear to be derived from the SFE sample. The color-coded HeLa cell spectrum was then compared with the spectrum obtained when the HeLa cell was not on the frit, which contains the PBS buffer and the lock-mass reference sample. The ion peaks that were common to both the HeLa cell spectrum and no HeLa cell spectrum within ±5 mDa are highlighted in gray. All the magenta color-coded ion peaks were then compared with the structures listed in the LipidMaps database.

7.3　Results and Discussion

7.3.1　Detection capability for authentic samples

We preliminarily tested the detection capability and sensitivity of the method using authentic samples. A list of compounds and the amounts needed to give an intensity (counts) of 100 are listed in Table 7.1. Each compound purchased from the supplier described in the Experimental section was dissolved in acetonitrile, and appropriately diluted samples were applied to the frit. After waiting a few minutes for the acetonitrile to evaporate, the frit was placed in the In-Line column filter, SFE was started so as to monitor the series of mass spectra as a function of time. Figure 7.2 illustrates the SFE profile for arachidonic acid as a typical cell component. The extracted ion profile of SFE for each ion was calculated, and the peak area was then obtained as the sum of ion counts within the half-height width region of the given extracted ion profile. The limit of quantitation was then calculated as the amount needed to produce 100 ion counts[19], which were calculated from the slope of the sample amount vs. the number of ion counts for at least 2 or more different amounts of sample. The quantitative error for 100 counts is 10% (square root of 100), assuming that the counting result closely follows a Poisson distribution. The repeatability of the counts was approximately 50% of the relative standard deviation (RSD) due to the SFE pressure restrictor that occasionally became unstable. Nevertheless, the method showed an excellent detection sensitivity at the femtomole order for most of the medium to long-chain FFAs in the negative ion mode that were tested.

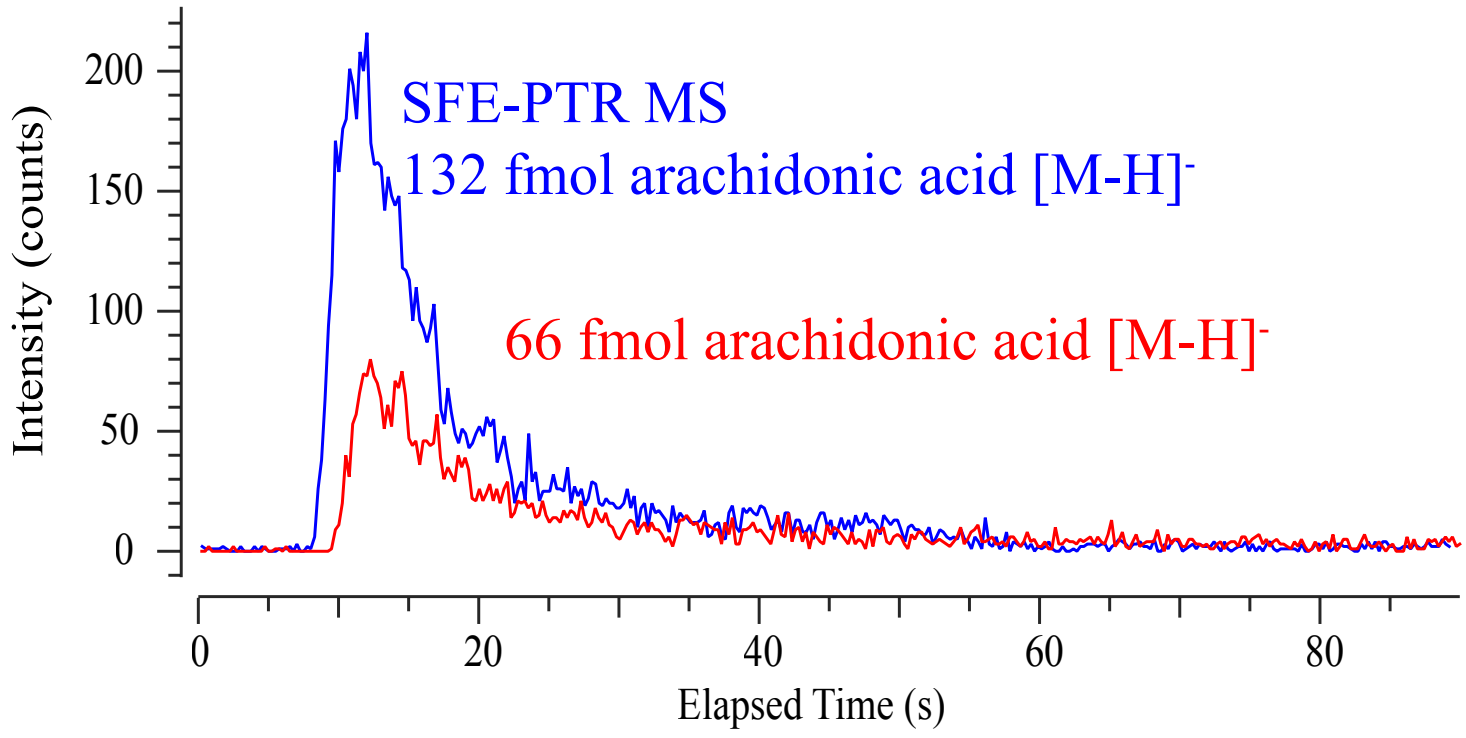

Figure 7.2: Extracted ion profiles of SFE-PTR MS for 66 fmol (red) and 132 fmol (blue) of arachidonic acid in negative ion mode.

Table 7.1: Detection capabilities for various authentic samples

Compound	mass	positive ion mode		negative ion mode	
Acetaminophen	151.063	4.9 fmol	$[M+H]^+$	274 fmol	$[M-H]^-$
Phenacetin	179.095	1.4 fmol	$[M+H]^+$	203 fmol	$[M-H]^-$
Caffeine	194.080	0.077 fmol	$[M+H]^+$	–	
Pyrene	202.078	9.5 fmol	$[M+H]^+$	–	
Oleic acid	282.256	–		0.048 fmol	$[M-H]^-$
Stearic acid	284.272	–		10 fmol	$[M-H]^-$
Linolic acid	280.240	–		0.20 fmol	$[M-H]^-$
Arachidic acid	312.303	–		27 fmol	$[M-H]^-$
Arachidonic acid	304.240	–		19 fmol	$[M-H]^-$
Tetracosanoic acid	368.365	–		17 fmol	$[M-H]^-$
α-Tocopherol	430.381	63 fmol	$[M+H]^+$	4 fmol	$[M-H]^-$
Vitamine K_1	450.350	406 fmol	$[M+H]^+$	41 fmol	$[M]^-$
γ-Oryzanol	602.434	–		1.6 fmol	$[M-H]^-$
Reserpine	608.273	8.3 fmol	$[M+H]^+$	8000 fmol	$[M-H]^-$
Ivermectin (B_{1a})	874.508	2.3 fmol	$[M+NH_4]^+$	–	

7.3.2 HeLa cell sample analysis

A total of 20 fmol of P321, P621 (positive ion mode), or 10 pmol tetracosenoic acid (negative ion mode) acetonitrile solution was added to the frit as the mass reference, which holds a single HeLa cell. After waiting a few minutes for the acetonitrile to evaporate, the frit was placed into the Acquity In-Line filter, and the ”2-way switching valve” position was then switched to start the SFE. Three cells for each of the positive and negative ion modes were measured.

Figures 7.3 and 7.4 are the co-added SFE-PTR mass spectra for a single HeLa cell SFE (top). The steps to obtain these spectra and the definition of the color code are described in section 7.2.5. The bottom spectra on both figures are the spectra for mass reference samples (P321, P621, or tetracosenoic acid) under the same conditions with the

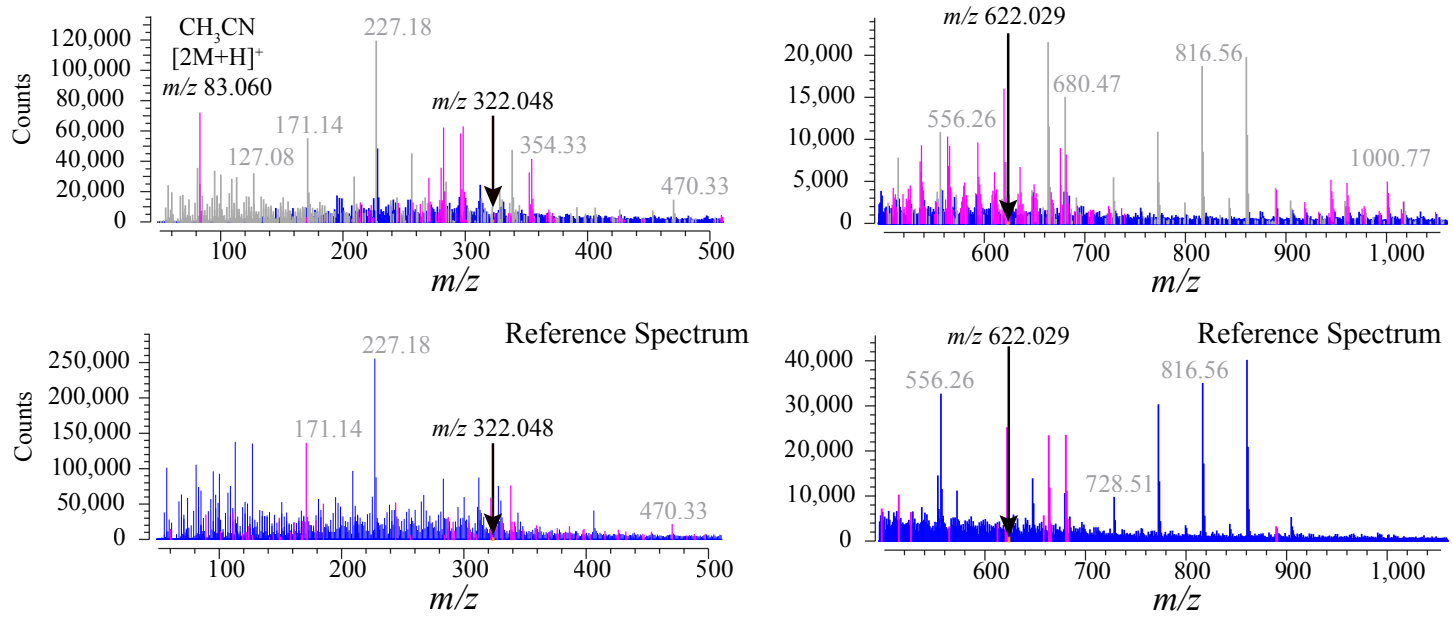

Figure 7.3: Positive ion mode SFE-PTR mass spectrum of a cell on the frit (top). SFE-PTR spectrum of lock mass references sample (bottom)

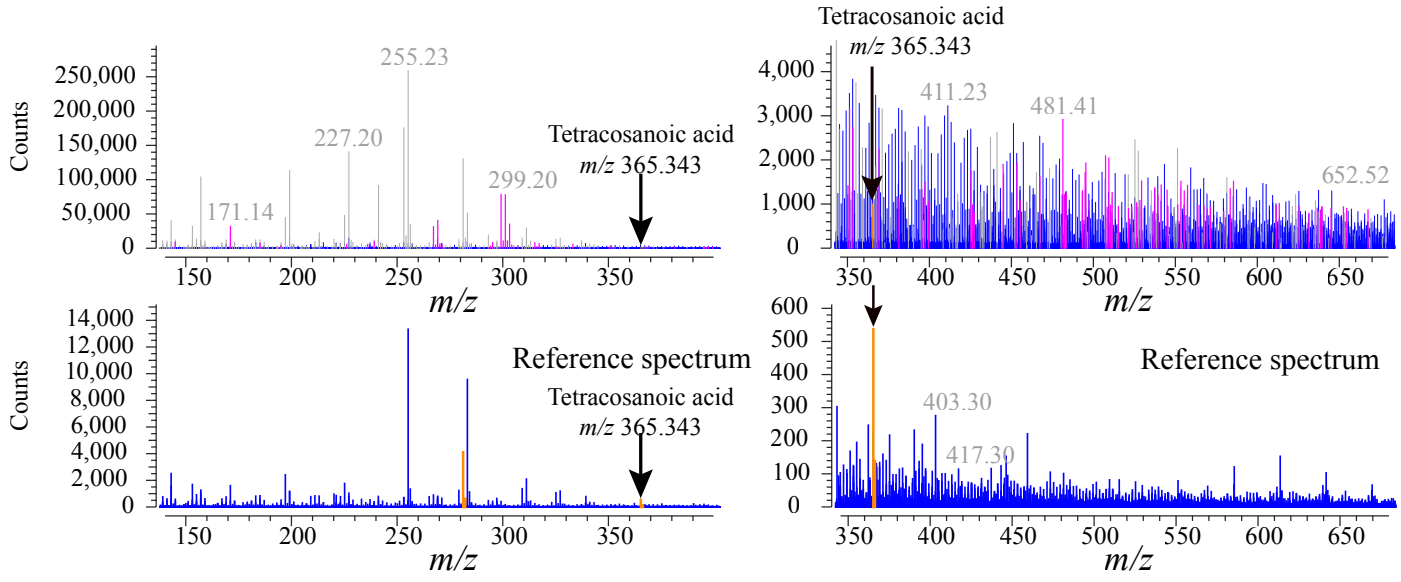

Figure 7.4: Negative ion mode SFE-PTR mass spectrum of a cell on the frit (top). SFE-PTR spectrum of lock mass reference sample (bottom) SFE-DI-PTR spectrum of lock mass reference sample (bottom)

single HeLa cell sample analysis as the blank spectra. All mass peaks on the spectra obtained from the HeLa cell were grayed out if the corresponding masses (±5 mDa width) are also shown in the reference spectrum at the bottom of each figure. All the extracted ion profiles for the masses on the HeLa cell spectra were then evaluated.

7.3.3 Methanol extracted HeLa cell sample analysis

Figures 7.5 and 7.6 are the co-added SFE-PTR mass spectra for 20 HeLa cell equivalent amounts of a methanol-extracted cell (top), and their background spectra in the bottom. Color codes are the same as for previous spectra. A total of 200 (91) and 50 (4) ions were observed from the SFE of a single HeLa cell and methanol extracts in the positive (negative) ion mode. Figure 7.7 shows a comparison of the observed ions obtained from the SFE directory from a single HeLa cell and the methanol-extracted cell. Table 2 shows a list of matched ions that appear in both

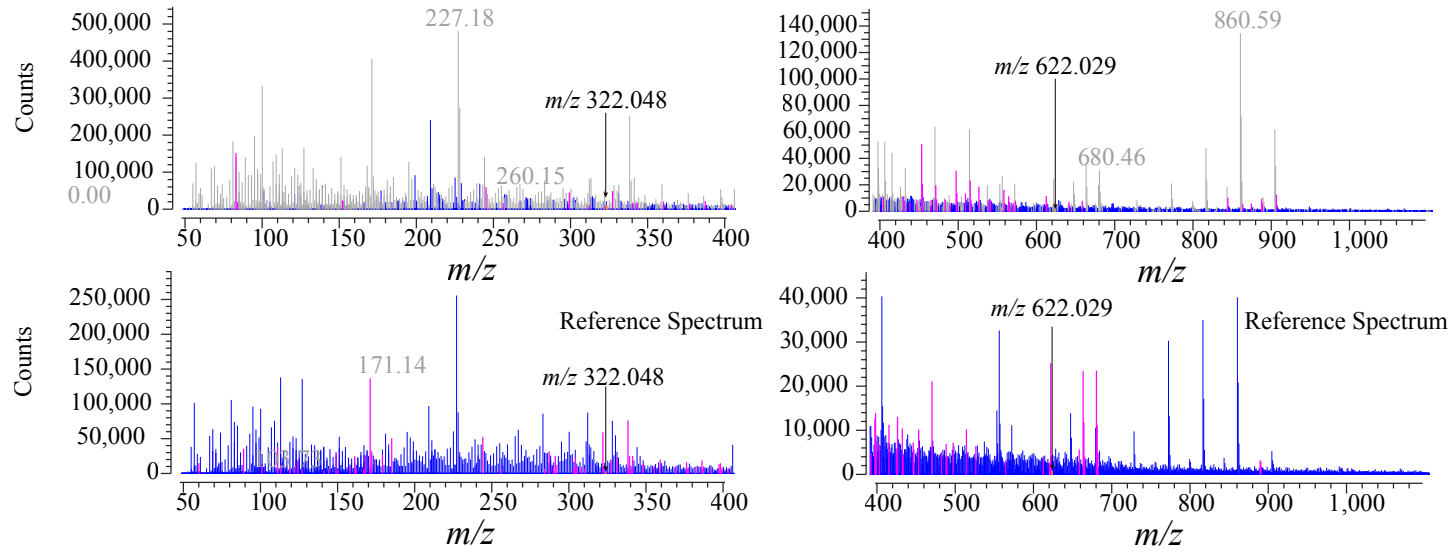

Figure 7.5: Positive ion mode SFE-PTR mass spectrum of 0.2 µL (20 cells equivalent) of the methanol-extract of a cell (top). SFE-PTR mass spectrum of lock mass reference sample (bottom)

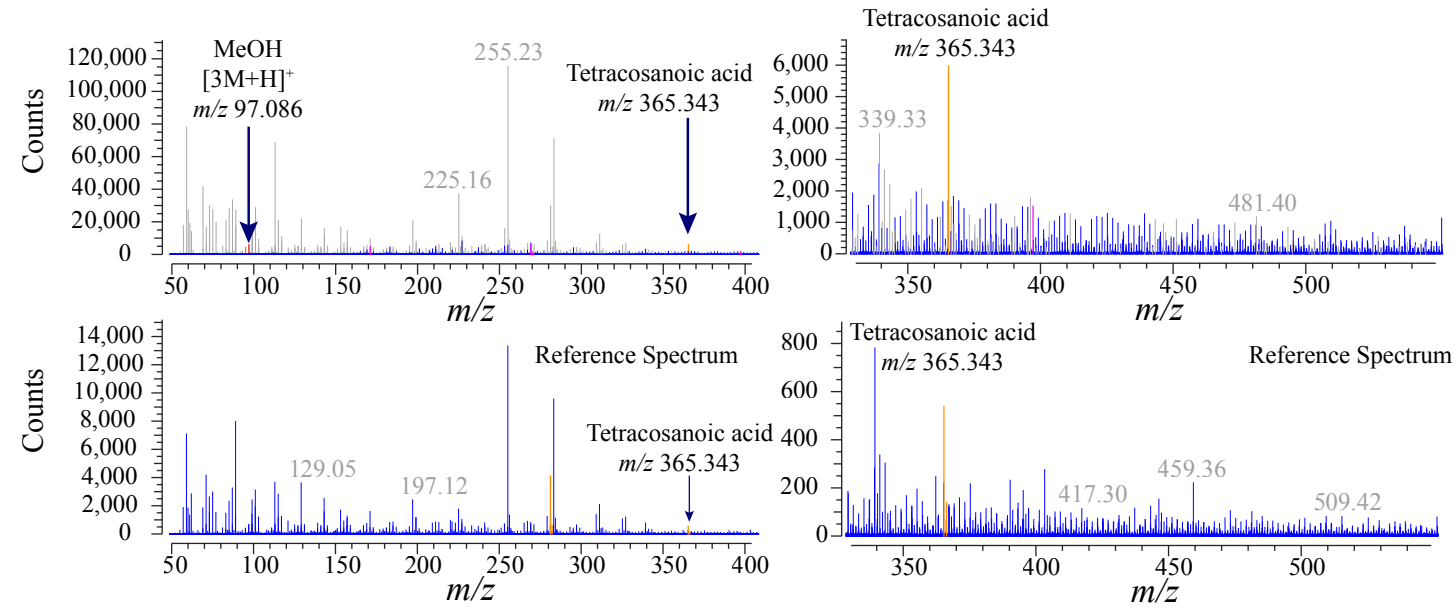

Figure 7.6: Negative ion mode SFE-PTR mass spectrum of a methanol-extract equivalent to 20 cells (top). SFE-PTR spectrum of lock mass reference sample (bottom)

Table 7.2: List of ions observed in both SFE of a single HeLa cell and the methanol-extracted cell

MeOH extracts		SFE of single cell		δm (mDa)
positive ion mode				
m/z	intensity	*m/z*	intensity	
526.422	18011	526.425	4440	-2.75
negative ion mode				
m/z	intensity	*m/z*	intensity	
171.137	4602.5	171.139	31818	-1.87
269.242	5924	269.245	40638	-2.82

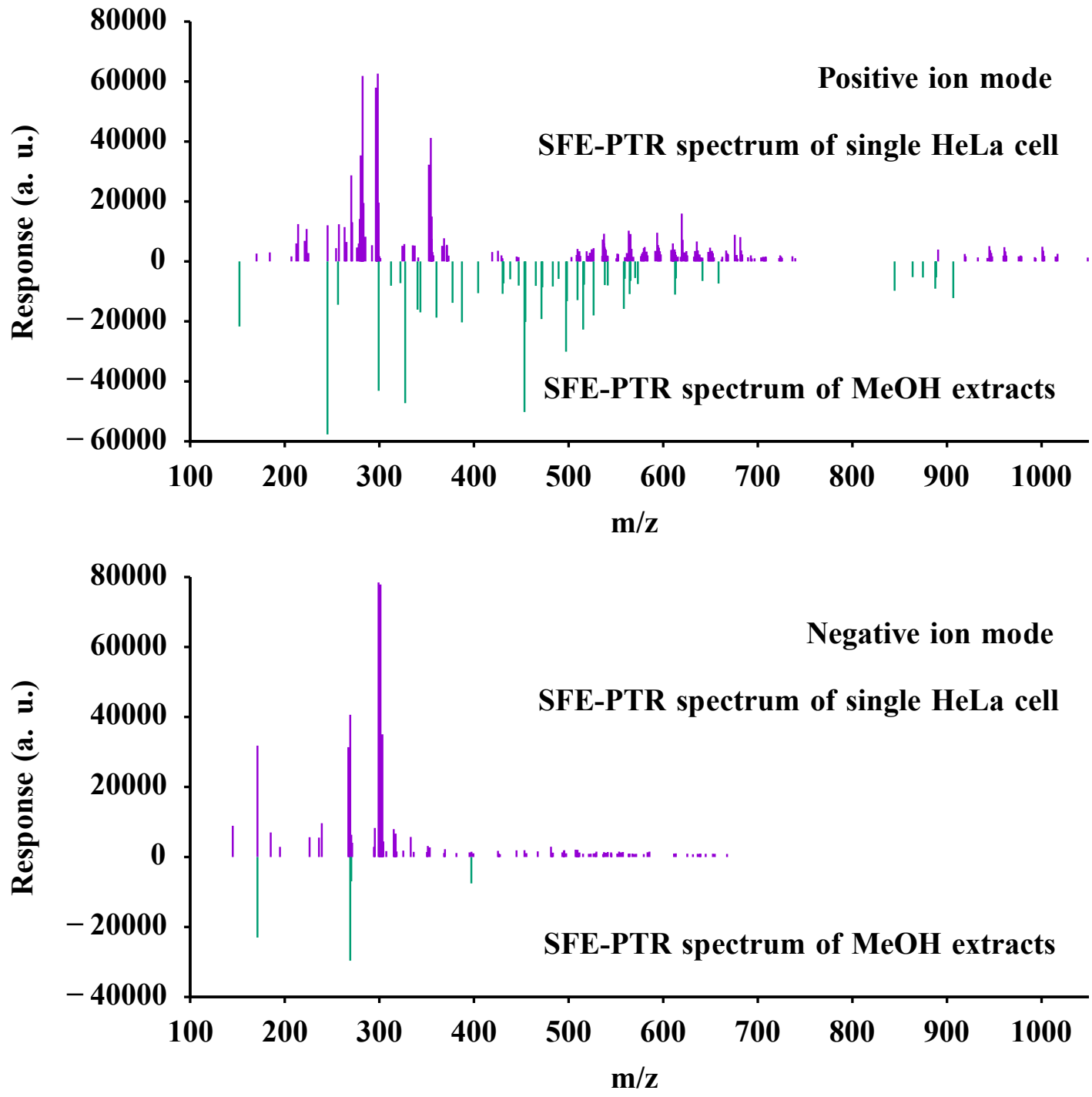

Figure 7.7: Comparison of direct SFE from a cell and methanol extracts (20 cells equivalent). Spectra were plotted for the selected ion peaks where it does not appear on the lock-mass reference spectrum in addition to the removal of background ions.

extraction methods. It is unlikely that most ions observed in SFE from a single HeLa cell were not present in the methanol-extracted cell. Recently, lipidomics researchers, Höring *et al.*[22] reported that the extraction efficiency of lipids varies greatly depending on the polarity of the solvent being used. The present results suggest an extraction bias for lipids between intact cells and their methanol extracts. We currently do not have sufficient evidence for whether the detected ions originate from a cell or are contaminants from the environment, such as plasticizers from the vials used in the experiments.

One of the advantages of PTR ionization combined with SFE without a modifier is that it produces simple ions, such as protonated and deprotonated ions, with an occasional loss of water or hydrogen. Unlike liquid chromatography with electrospray ionization (ESI), no complex adducts, such as sodium, ammonium, acetonitrile, etc., are produced. Therefore, the list of all possible ion formulae for a list of lipid structures can easily be synthesized *in silico*. A list of structure data (LMSD Database) obtained from https://www.lipidmaps.org/ was used after desalting and substituting

Table 7.3: Assigned peaks for positive ion mode obtained from the SFE of a single HeLa cell
A number followed by a '+' sign represents the additional number of structures that match the formula listed in LipidMaps database.

m/z (error (σ mDa))	Abundance	RSD	Formula		+isomers	Exact *m/z*
221.102 (±1.2)	2135	19 %	$C_9H_{16}O_6$	$[M + H]^+$		221.102
263.236 (±2.7)	39 475	41 %	$C_{18}H_{30}O$	$[M + H]^+$	+1	263.237
282.279 (±0.4)	248 297	14 %	$C_{18}H_{35}NO$	$[M + H]^+$	+1	282.279
296.258 (±1.1)	169 561	91 %	$C_{18}H_{33}NO_2$	$[M + H]^+$	+1	296.258
297.084 (±3.0)	1418	33 %	$C_{15}H_{21}BrO$	$[M + H]^+$	+1	297.085
298.273 (±2.6)	130 455	99 %	$C_{18}H_{35}NO_2$	$[M + H]^+$	+1	298.274
300.063 (±2.7)	407	1 %	$C_{16}H_{12}O_6$	$[M]^+$	+63	300.063
593.575 (±2.1)	31 613	39 %	$C_{38}H_{75}NO_3$	$[M]^+$	+2	593.574
613.176 (±2.9)	621	13 %	$C_{27}H_{32}O_{16}$	$[M + H]^+$	+3	613.176
890.612 (±1.8)	709	10 %	$C_{47}H_{88}NO_{12}P$	$[M + H]^+$	+1	890.612
1000.766 (±0.4)	22 547	73 %	$C_{56}H_{105}NO_{13}$	$[M + H]^+$	+2	1000.766
P321	4255	14 %	$C_6H_{18}N_3O_6P_3$	$[M + H]^+$	–	322.048
P621	2868	38 %	$C_{12}H_{18}F_{12}N_3O_6P_3$	$[M + H]^+$	–	622.029

isotope-specified atoms by using KNIME 4.6.1 with RDKit Node. The normalized structure data was saved as an SDF file, which contains 39883 unique structures for masses 1200. A list of possible ions was generated by adding a combination of formulae $+H^+$, $-e$, and $-OH^-$ for positive ions, $-H^+$, $+e$, and $+OH^-$ for negative ions. The ions matched within a standard deviation of 3 mDa errors (n=3) are listed in Tables 7.3 and 7.4. Eleven ions in the positive ion mode could be assigned to chemical formulae as listed in Table 7.3. Most of the assigned ions do not match uniquely to the structure, even limited to LipidMaps listed structures. The ion assigned to *m/z* 282.279 ($[C_{18}H_{35}NO + H]^+$) is possibly a protonated oleamide, which is a common background derived from laboratory ware[23]; however, the corresponding SFE profile was not found in the reference spectrum and, therefore, it remains listed. A total of 10 ions in the negative ion mode were assigned to a formula as listed in Table 4. One of the ions that appeared at *m/z* 303.233 matches FFA C20:4, the protonated form of $C_{20}H_{32}O_2$, off by -0.16 mDa. Its formula matches 41 molecular structures (isomers) listed in the database, thus, whether it is a single molecule or multiple co-eluting molecules is unknown. The number of counts for each sample run in triplicate experiments was 22589, 1352, and 2568 for *m/z* 303.233 ion, which roughly corresponds to 3.8 pmol, 230 fmol, and 440 fmol of arachidonic acid. The repeatability of the present study was around 10 to 76% RSD for the other ions but the ions for *m/z* 299.202, 301.217, and 303.233 are specifically large (123-135%). Although it is too early to evaluate the quantitative results in this preliminary study, it still holds the potential to permit the cell-to-cell variance to be determined, which cannot be discovered by the analysis of a whole cell homogenate. Even though the SFE is capable of selective extraction from the sample matrix, many compounds are simultaneously co-eluted and enter the analyzer, which may suppress ionization. Adding supercritical fluid chromatography (SFC) following the SFE may improve detection sensitivity and the accuracy of identification of molecules. Several configurations of online SFE coupled with SFC have been reported in the past four decades and have been shown to have a tremendous advantage in terms of enhancing analytical sensitivity and accuracy due to the fact that there is less chance of producing contaminants, rapid sample preparation, and the fact that no sample handling before SFE is needed. To establish an SFC-PTR MS interface, a study of peak dispersion in the PTR flow tube is mandatory[17,24].

Table 7.4: Assigned peaks for negative ion mode obtained from the SFE of a single HeLa cell A number followed by a '+' sign represents the additional number of structures that match the formula listed in the LipidMaps database.

m/z (error (σ mDa))	Abundance	RSD	Formula		+isomers	Exact *m/z*
171.139 (±0.3)	52 787	51 %	$C_{10}H_{20}O_2$	$[M-H]^-$	+1	171.139
194.994 (±2.0)	1561	76 %	$C_9H_8OS_2$	$[M-H]^-$	+1	194.994
239.201 (±1.4)	6906	52 %	$C_{15}H_{28}O_2$	$[M-H]^-$	+1	239.202
294.183 (±1.5)	3139	15 %	$C_{17}H_{26}O_4$	$[M]^-$		294.184
299.201 (±2.2)	20 520	123 %	$C_{20}H_{28}O_2$	$[M-H]^-$	+1	299.202
301.217 (±0.7)	19 337	135 %	$C_{20}H_{30}O_2$	$[M-H]-$	+1	301.217
303.233 (±0.5)	8836	135 %	$C_{20}H_{32}O_2$	$[M-H]^-$	+42	303.233
381.374 (±1.6)	279	9 %	$C_{25}H_{50}O_2$	$[M-H]^-$	+8	381.374
425.340 (±1.1)	1659	20 %	$C_{27}H_{43}N_3O$	$[M]^-$		425.341
455.390 (±1.6)	1110	54 %	$C_{31}H_{52}O_2$	$[M-H]^-$	+1	455.389
Tetracosenoic acid	10 299	40 %	$C_{24}H_{46}O_2$	$[M-H]^-$	–	455.389

7.4 Conclusions

We report on an evaluation of SFE-PTR MS for analyzing small lipophilic molecules contained in a single HeLa cell. About 200/90 ions were the observed in positive/negative ion mode mass spectra. In contrast, fewer ions were observed from methanol extracts of HeLa cells, and most of the ions observed in both SFE and methanol extracts did not match, although we have not yet addressed those differences. The ions of 11/10 (positive/negative) match the chemical formula obtained from the lipids database, which contains 39883 unique structures. Each of the assigned ions has a range of about 1000 to 60 000 ion counts, which demonstrates that the method described here has great potential for detecting small molecules in a single cell. Adding SFC separation following the SFE would be expected to improve molecular identification performance since SFC has a high column efficiency. Although, more improvement in the instrumentation for an SFC-PTR ion source is needed to allow for a narrow peak to be visualized in the SFC chromatogram, which is typically less than 0.5 s.

Furthermore, the process used in this study does not fully resolve the issue of false positive results by unidentified contaminants derived from laboratory ware used in the sample processing. The present method shows, however, the potential of the method for use in the analysis of metabolites from a single-cell.

参考文献

[1] Cabodevilla, A. G.; Sánchez-Caballero, L.; Nintou, E.; Boiadjieva, V. G.; Picatoste, F.; Gubern, A.; Claro, E. *Journal of Biological Chemistry* 2013, **288**, 27777–27788.

[2] Yu, Y.; Vidalino, L.; Anesi, A.; Macchi, P.; Guella, G. *Mol. BioSyst.* 2014, **10**, 878–890.

[3] Rosa, A.; Murgia, S.; Putzu, D.; Meli, V.; Falchi, A. M. *Chemistry and Physics of Lipids* 2015, **191**, 96–105.

[4] Levchenko, S. M.; Qu, J. *Biosensors* 2018, **8**, 123.

[5] Rysman, E.; Brusselmans, K.; Scheys, K.; Timmermans, L.; Derua, R.; Munck, S.; Van Veldhoven, P. P.; Waltregny, D.; Daniëls, V. W.; Machiels, J.; Vanderhoydonc, F.; Smans, K.; Waelkens, E.; Verhoeven, G.;

Swinnen, J. V. *Cancer Res* 2010, **70**, 8117–8126.

[6] Xu, D. et al. *Nature* 2020, **580**, 530–535.

[7] Braghini, M. R.; Lo Re, O.; Romito, I.; Fernandez-Barrena, M. G.; Barbaro, B.; Pomella, S.; Rota, R.; Vinciguerra, M.; Avila, M. A.; Alisi, A. *Journal of Experimental & Clinical Cancer Research* 2022, **41**, 107.

[8] Rivas Serna, I. M.; Romito, I.; Maugeri, A.; Lo Re, O.; Giallongo, S.; Mazzoccoli, G.; Oben, J. A.; Li Volti, G.; Mazza, T.; Alisi, A.; Vinciguerra, M. *International Journal of Molecular Sciences* 2020, **21**, 8452.

[9] Chen, L.; Xie, B.; Li, L.; Jiang, W.; Zhang, Y.; Fu, J.; Guan, G.; Qiu, Y. *Chromatographia* 2014, **77**, 1241–1247.

[10] Kim, H.-W.; Rapoport, S. I.; Rao, J. S. *Mol Psychiatry* 2011, **16**, 419–428.

[11] Snaebjornsson, M. T.; Janaki-Raman, S.; Schulze, A. *Cell Metabolism* 2020, **31**, 62–76.

[12] Sublette, M. E.; Russ, M. J.; Smith, G. S. *Bipolar Disorders* 2004, **6**, 95–105.

[13] Gindlhuber, J.; Schinagl, M.; Liesinger, L.; Darnhofer, B.; Tomin, T.; Schittmayer, M.; Birner-Gruenberger, R. *IJMS* 2022, **23**, 3356.

[14] Falomir-Lockhart, L. J.; Cavazzutti, G. F.; Giménez, E.; Toscani, A. M. *Frontiers in Cellular Neuroscience* 2019, **13**.

[15] Ivanov, D.; Čolović, R.; Bera, O.; Lević, J.; Sredanović, S. *Eur Food Res Technol* 2011, **233**, 343–350.

[16] Hondo, T.; Ota, C.; Miyake, Y.; Furutani, H.; Toyoda, M. *Anal. Chem.* 2021, **93**, 6589–6593.

[17] Hondo, T.; Ota, C.; Miyake, Y.; Furutani, H.; Toyoda, M. *Journal of Chromatography A* 2022, **1682**, 463495.

[18] Kawai, Y.; Hondo, T.; Jensen, K. R.; Toyoda, M.; Terada, K. *J. Am. Soc. Mass Spectrom.* 2018, **29**, 1403–1407.

[19] Kawai, Y.; Miyake, Y.; Hondo, T.; Lehmann, J.-L.; Terada, K.; Toyoda, M. *Anal. Chem.* 2020, **92**, 6579–6586.

[20] Nakatani, K.; Izumi, Y.; Hata, K.; Bamba, T. *Mass Spectrometry* 2020, **9**, A0080–A0080.

[21] Cloos, K. C.; Hondo, T. *Journal of Chromatography B* 2009, **877**, 4171–4174.

[22] Höring, M.; Stieglmeier, C.; Schnabel, K.; Hallmark, T.; Ekroos, K.; Burkhardt, R.; Liebisch, G. *Anal. Chem.* 2022,

[23] Jug, U.; Naumoska, K.; Metličar, V.; Schink, A.; Makuc, D.; Vovk, I.; Plavec, J.; Lucas, K. *Sci Rep* 2020, **10**, 2163.

[24] Ota, C.; Hondo, T.; Miyake, Y.; Furutani, H.; Toyoda, M. *Mass Spectrometry* 2022, **11**, A0108.

第 8 章

結論 (General Discussion and Conclusions)

8.1　緒言

超臨界流体抽出 (supercritical fluid extraction; SFE) ／超臨界流体クロマトグラフィー (supercritical fluid chromatography; SFC) と，中真空化学イオン化 (medium vacuum chemical ionization; MVCI) 質量分析法 (mass spectrometry; MS) を組み合わせる新しい超高感度脂質測定法を開発し，それについて検討を行った．MVCI と名付けたこのイオン化法は，約 100 Pa の加水した He 雰囲気で放電させることで生じる試薬イオン (H_3O^+ , OH^-) によって試料をプロトン付加分子，あるいは脱プロトン分子として質量分析を行う化学イオン化法である．このイオン化法の特徴は，SFC 移動相としてもっとも一般的に用いられる CO_2 をイオン化せず，有機物を高感度に検出可能なことである．

生体組織中で脂質は様々な疾病や組織形態形成に関連する．また，組織内の分布は組織全体の機能に深くかかわる．しかしながら，異性体が多いこと，存在量が微量であること，細胞破砕時の自己消化などの理由から，直接細胞内濃度を測定することが困難であった．そのため，細胞毎の脂質量の違いは，RNA 量などから推定されてきた．SFE は，組織から脂質を効率よく抽出でき，溶媒抽出より脂質定量に適することが報告されている．また，SFC はカラム効率が高く，異性体を短時間で分離可能である．さらに，超臨界流体は臨界温度以上では減圧過程で亜臨界状態のまま相変化なく 100 Pa に到達し，中真空中に溶質が開放され，効率よく化学イオン化できると考えられる．

本論文では，この分析法を，中真空化学イオン化 (medium vacuum chemical ionization; MVCI) とする．但し，一部，すでに論文掲載された内容については “PTR MS” と記述している．

8.2　イオン源への試料導入方法の検討

SFE/SFC と MVCI MS を組み合わせた本手法は，前例がないことから，どのような化合物が測定可能であるか，また，どのような試料導入方法が適切であるか，などについて 2章で検討を行った．

はじめに，測定試料をメタノールやヘキサンなどの液体に溶解し，それを HPLC 用インジェクターバルブを用いて超臨界流体流路上にフローインジェクション (FI) として試料導入する FI-PTR (FI-MVCI) について検討した．次に，HPLC 用インラインフィルターに試料をのせ，有機溶媒を揮発させた後，フィルター上の試料を SFE によりイオン源に導入する Direct Injection (DI)-PTR (DI-MVCI) について検討した．その結果，DI-MVCI を用いたカフェインの測定で得られたイオンカウント数は，12 941 counts $\cdot$ $fmol^{-1}$ ，定量下限 (LLOQ) 8 amol が得られ，FI-MVCI に比べて約 800 倍低い検出下限が得られることがわかった．この試料導入による感度の違いとして考えられる点は，FI-MVCI では，1 µL の有機溶媒が測定対象分子と共にイオン源に導入される点である．試料導入に用いられる有機溶媒は，カフェインの溶出過程から計算すると，流量 1 µL $\cdot$ s^{-1} と推定され，得られたピーク幅は 1.8 s であった．すなわち，1 µL の有機溶媒が圧力リストリクターを通過する際，平均有機溶媒濃度は 44 % 程度に達すると推定される．この高濃度の有機溶媒の存在により，見かけ上の臨界温度が急激に上昇し，実験で用いた 40 °C 条件では圧力リストリクター内に凝集を生じ，分析対象分子の円滑な中真空空間への開放が妨げられた

ことが要因と考えられる．勿論，有機溶媒が試薬イオンを消費することによるイオン化阻害は考えられるが，プロトン親和性が水より低いヘキサンを用いた場合でも大きく感度の損失があったことから，単純に有機溶媒による試薬イオンの枯渇の影響による感度損失とは考えていない．この点は，将来，リストリクター部を数百度の温度に加熱し，用いる有機溶媒の臨界温度よりも高く保てる実験装置が考案されれば明確になるのではないかと考える．

8.3　SFE-MVCI MS の検出限界

SFE-MVCI MS を用いたネガティブイオン検出では，遊離脂肪酸 (FFA) について 48 amol から 27 fmol という定量下限を達成できることを明らかにした．これは，文献に示されている FFA 定量下限に比べ 3 桁低い値である．また，アセトアミノフェン，フェナセチン，α-トコフェロール，ビタミン K_1，γ-オリザノール，およびレセルピンについてそれぞれ，274, 203, 4, 41, 1.6, 800 fmol の定量下限が得られた．

ポジティブイオン検出では，アセトアミノフェン，フェナセチン，カフェイン，ピレン，α-トコフェロール，ビタミン K_1，およびレセルピンについてそれぞれ，4.9, 1.4, 0.077, 9.5, 63, 406, および 8.3 fmol の定量下限が得られた．

アセトアミノフェン，フェナセチン，α-トコフェロール，ビタミン K_1, およびレセルピンは，ポジティブイオン，ネガティブイオンいずれも検出可能であった．

8.4　α-T イオン化反応及びその酸化生成物の検出

4章では植物の光合成において，細胞の自己防衛に重要な機能を果たすとされている α-T について液体クロマトグラフィー (LC)-エレクトロスプレーイオン化 (ESI) MS と SFE-MVCI MS で得られた質量スペクトルの比較を行った．この章では，ESI と MVCI の異なるイオン化法で質量スペクトルを測定し比較を行った．その結果，ESI の場合，最大強度は α-T ラジカルカチオン ($M^{+\bullet}$) であった．また，同時に $[M-H]^+$ (m/z 429.4)，ならびに 5-f-γ-T が検出され，いずれも同一保持時間に溶出が認められることから，これらのイオンは，α-T の ESI 過程で生成したと考えられる．MVCI MS による α-T 測定の結果，プロトン付加分子が最大強度として得られ，ラジカルカチオン ($M^{+\bullet}$, m/z 430.4) も確認されたが，ESI と異なり，5-f-γ-T は認められなかった．

α-T の MVCI MS 測定の結果得られるイオン種の強度比は，調整後の保管方法や期間によって大きく変化することが判明した．その理由の 1 つは，α-T が保管環境によっては速やかに酸化されること，およびその酸化の過程が複雑で様々な酸化生成物（異性体）を生じることが原因と考えられる．

5章では α-T とその酸化物を SFE/SFC-MVCI MS を用い酸化生成物同定を可能にする手法について述べた．α-T は古くから知られた抗酸化作用をもつ物質であるが，極性が極めて低いため イオン化されにくく，かつ LC 分離も困難な化合物である．α-T による植物細胞の防衛反応は非酵素的反応であることから，いわゆる酵素動力学的なメカニズム解析を用いることが出来ず，α-T が一重項酸素や脂肪酸ラジカルなどとどのような反応を行うかは直接反応生成物を測定することが必要である．しかしながら，ほとんどの α-T 抗酸化作用による生成物は異性体であり，反応が早く，迅速な試料前処理と十分なクロマトグラフィーでのピーク分離 (resolution) が求められる．本研究で用いた split injection による SFE/SFC-MVCI MS では，試料をフリットに展開後 120 s の測定時間で，8 種類の酸化生成物について分離度 (Rs) 1.1 以上を達成することができた．

8.5　SFE/SFC-MVCI MS の開発

6章では SFE-MVCI MS に分離カラムを導入したときのピーク幅や保持時間について検討を行い，定量下限について述べた．内径 2.1 mm× 長さ 100 mm のカラムを用いることで，α-T について保持時間 87.7 s，保持係数 1.87, 理論段数 3300 を達成した．また定量下限はフタル酸が 0.5 から 0.8 fmol，アラキドン酸が 1.18 fmol，α-T が 13.3 fmol, VK_1 が 34.5 fmol であった．いずれも，SFC を用いない SFE-MVCI MS で測定した場合に比べ，お

よそ一桁低い定量下限が得られた．

SFE/SFC split injection を用いたフタル酸エステルの保持係数 (k) に対する理論段数の詳細な検討の結果，MVCI イオン源内部で，およそ 2.5 s のピークの広がりを生じていることを示唆する結果が得られた．SFC はカラム効率が高く，かつ分離が高速であることから，ピーク幅 0.5 s 以下の検出応答速度が要求される．そのため，SFC での分析に応用するためには，さらなる改良が必要である．

8.6　シングルセル分析への応用可能性

7 章では実際に，SFE-MVCI MS を用いて HeLa 単一細胞からの脂質代謝物の検出の可能性について調べた．SFE-MVCI MS では，ポジティブイオンモードで 200 イオン，ネガティブイオンモードで 91 イオンを細胞由来の分子として検出できた．

本研究を通じて様々な化合物について MVCI によるイオンを調べた結果，測定対象分子 M に対して，得られるイオンは，ポジティブイオン: $[M + H]^+$, $[M - H + H]^+$, $[M - H_2O + H]^+$，ネガティブイオン: $[M - H]^+$, $[M + H - H]^+$, $[M + OH]^-$ のいずれかであった．この結果に基づいて，LipidMaps LMSD データベースに登録されている化合物中，質量 1200 以下の 45932 構造に対して，可能性のあるイオン式を *in silico* 合成し，HeLa 細胞から得られたイオンの *m/z* と比較した結果，ポジティブイオン 11 種，ネガティブイオン 10 種について化学組成を決定することができた．しかしながら，ほぼすべての組成に対して複数の異性体がリストされており，分子同定には至っていない．分子同定を行うには，SFC をもちいた異性体分離と保持予測アルゴリズムを併用する方法，ならびにタンデム質量分析法を併用するなどが必要である．

8.7　結言

本研究では超臨界二酸化炭素と MVCI を組み合わせた新しい質量分析法について議論を行った．本研究で作製した SFE/SFC-MVCI MS を用いることで不揮発性有機物や植物の光合成に不可欠な物質である α-T，細胞壁に存在し重要な役割を持つアラキドン酸などを測定することができた．また HeLa 単一細胞から数多くの低分子化合物が検出でき，そのうちポジティブイオン・ネガティブイオン合わせて 21 イオンについて化学組成を明らかにすることができた．このように超臨界二酸化炭素と MVCI を組み合わせることで，食品や医薬品分野の様々な分析の高感度化，ハイスループット化に貢献できる可能性があると考える．

謝辞

本論文を結ぶにあたり，終始ご懇切なる御指導頂きました大阪大学大学院理学研究科附属フォアフロント研究センターの豊田岐聡教授，兼松泰男教授，本堂敏信博士，科学機器リノベーション・工作支援センターの古谷浩志准教授には深く感謝いたします。また，大阪大学大学院理学研究科附属フォアフロント研究センター特任研究員である三宅ゆみ博士には，質量分析装置の基礎からご指導，助言頂き，大阪大学大学院理学研究科附属フォアフロント研究センターの青木順助教，市原敏雄さんには装置の開発等ご協力いただき，深く感謝いたします．

九州大学生体防御医学研究所附属高深度オミクスサイエンスセンターの馬場健史教授，中谷航太学術研究員には HeLa 細胞をご提供いただき，深く感謝申し上げます．

関西大学化学生命工学部青田浩幸教授，郭昊軒助教には研究の発表等たくさんの助言をいただきました．深く感謝いたします．質量分析グループの方々，光高分子化学研究室の方々には，研究に関することだけでなく心休まる時間をつくっていただきました．心から深く感謝し，厚く御礼申し上げます．

2023 年 2 月 15 日

Table of octanol-water partion coefficieent and dissociation constant

			pKa		
Compound	mass	log *P*	acidic	basic	data source
Acetaminophen	151.063	2.0	9.46	-4.4	ChemAxon http://www.t3db.ca/toxins/T3D2571
Phenacetin	179.095	2.0	14.98	-4.2	*ibid.*
Caffeine	194.080	-1.0	–	-0.92	*ibid.*
Pyrene	202.078	4.6	–	–	*ibid.*
Oleic acid	282.256	6.1	4.99	–	*ibid.*
Stearic acid	284.272	6.3	4.95	–	*ibid.*
Linolic acid	280.240	5.9	4.99	–	*ibid.*
Arachidic acid	312.303	7.1	–		
Arachidonic acid	304.240	6.2	4.82	–	https://go.drugbank.com/drugs/DB04557
Tetracosenoic acid	368.365	8.7	–		
α-T	430.381	8.8	10.8	-4.9	ChemAxon http://www.t3db.ca/toxins/T3D2571
VK_1	450.350	9.2	–		
γ-Oryzanol	602.434	10.2	–		
Reserpine	608.273	4.2	16.29	7.39	https://go.drugbank.com/drugs/DB04557

Table of acquired (raw) data id used in this thesis.

Figure number	acquisition date	run#	
2-3	2020-12-18	0010	PTR_130bar_Caffine_RF=200_0010
2-4	2021-02-25	0010	sfe_pos_caffeine_5fmol_0010
2-5	2021-10-29	0002	oleic_acid_7fmol_0002
3-1	2021-06-30	0010	toco_neg_0010
3-2	2021-02-19	0007	sfe_neg_oryzanol_400pg_0007
3-3	2021-02-19	0007	ibid.
3-4	2021-06-30	0015	tocooleVKreseoryza_neg_0015
4-1	2021-06-14	0010	Tocopherol_2pmol_0010
4-2	2021-06-14	0010	Tocopherol_2pmol_0010
	2021-06-15	0008	Tocopherol_2pmol_pos_0008
4-3	2021-07-15	0006	UPLC95_50uM_1uL_toco_0006
4-5	2021-07-15	0006	UPLC95_50uM_1uL_toco_0006
5-5	2022-04-15	0014	SFEDISFCGLC18-1,0mL-a-T_2pmol-0415_0014
	2022-04-15	0007	SFEDISFCGLC18-1,0mL-a-T_2pmol-0414_0007
	2022-04-15	0008	SFEDISFCGLC18-1,0mL-a-T_2pmol-0404_0008
5-6	2022-05-20	0002	*-1,0mL_pos_vk1+toco+pthalate_x100_1uL_0002
5-7	2022-05-26	0027	*_1,0mL_pos_pthalate-x100_toco,VK-10uM-1,0uL_0027
5-8	2022-08-18	0024	SFE20s10uLSFC_pos_10uM_aT-08-18_1uL_0024
	2022-08-18	0030	SFE20s10uLSFC_pos_10uM_aT-07-28_1uL_0030
5-9	2022-08-18	0024	SFE20s10uLSFC_pos_10uM_aT-08-18_1uL_0024
	2022-08-18	0030	SFE20s10uLSFC_pos_10uM_aT-07-28_1uL_0030
6-3	2022-05-26	0007	*pos_pthalate-x100_toco,VK-10uM-0,2uL_0007
6-4	2022-05-26	0046	*pos_pthalate-x100_toco,VK-10uM-1,0uL-70sccm_0046
7-2	2021-11-25	2003,2010	Arachidonic_66fmol_neg_2003
7-3	2021-10-15	0005,0004	
7-4	2021-10-15	0008,0001	
7-5	2021-10-15	0013,0004	
7-6	2021-10-15	0012,0001	

LaTeX processed on 2023/02/08 at 18:13:36